Mineralogical and geophysical monitoring of naturally occurring radioactive elements in selected Wisconsin aquifers. [DNR-051] 1990

Taylor, Robert (Associate Professor); Mursky, Gregory
Madison, Wisconsin: Wisconsin Department of Natural Resources, 1990

https://digital.library.wisc.edu/1711.dl/YYPDZBJFHSMD28C

Wisconsin Groundwater Management Practice Monitoring Project

No. 46

GROUNDWATER
Wisconsin's
buried treasure

Wisconsin Department of Natural Resources

FINAL REPORT

MINERALOGICAL AND GEOPHYSICAL MONITORING OF NATURALLY OCCURRING RADIOACTIVE ELEMENTS IN SELECTED WISCONSIN AQUIFERS

by

Robert W. Taylor, Department of Geosciences
University of Wisconsin-Milwaukee
Milwaukee, WI 53201

and

Gregory Mursky, Department of Geosciences
University of Wisconsin-Milwaukee
Milwaukee, WI 53201

June 12, 1990

FINAL REPORT

MINERALOGICAL AND GEOPHYSICAL MONITORING OF NATURALLY OCCURRING RADIOACTIVE ELEMENTS IN SELECTED WISCONSIN AQUIFERS

by

Robert W. Taylor, Department of Geosciences
University of Wisconsin-Milwaukee
Milwaukee, WI 53201

and

Gregory Mursky, Department of Geosciences
University of Wisconsin-Milwaukee
Milwaukee, WI 53201

June 12, 1990

ABSTRACT

The total radium content of water produced from the Cambrian, Ordovician sandstone aquifer of southeast Wisconsin is not related to the structure, thickness, or shale content of the formations associated with this aquifer. The total radium content of produced water is also unrelated to the radiometric content of the lower sandstone units within the aquifer.

On the basis of six wells for which complete geophysical logs were available, it was possible to establish a very strong relationship between the radium-228 levels in water from these wells and the thorium-232 content and thickness of the Ordovician dolomite section of the aquifer, Galena-Platteville formations. The correlation coefficient associated with this relationship is 0.97. Using the same six wells it is also possible to establish a very strong correlation, 0.93, between the radium-226 content of produced water and the uranium-238 content and thickness of the upper aquifer sandstone, St. Peter formation. For these six wells, the total radium content of produced water is entirely determined by the dolomite section and the St. Peter sandstone and is completely independent of all other units within the aquifer. In view of the spatial distribution and water quality variations associated with the six study wells, generalization of the results to all of southeastern Wisconsin appears to be reasonable.

The results of this study would not have been possible without the availability of modern geophysical logs and the spectral-gamma log is particularly critical.

TABLE OF CONTENT

PAGE

LIST OF FIGURES

PAGE

PAGE

PAGE

PAGE

LIST OF TABLES

INTRODUCTION

BACKGROUND

The presence of radium-226 and radium-228 in community water systems presents a potential health hazard resulting from the affinity of radium to substitute for calcium in skeletal material. The excessive ingestion of radium leads to the accumulation of radium within bone material with a resulting increase in the risk of osteogenic sarcomas and carcinomas. To minimize these health hazards the U.S. Environmental Protection Agency (EPA), as part of the drinking water standards, has established an acceptable limit of 5pCi/l for combined radium-226 and radium-228. There is, however, some belief that the standard may be raised to 5pCi/l for each isotope yielding a total radium content of 10pCi/l.

Radium-226 is the seventh element in the uranium-238 decay series; this series is presented for completeness in Table 1. Radium-228 is the first daughter in thorium-232 decay series; this series is presented for completeness in Table 2.

RADIUM IN WISCONSIN GROUND WATER

Routine sampling of community water systems in Wisconsin has revealed, at least, 44 wells which exceed the 5pCi/l drinking water standard (Hahn, 1984) for combined radium-226 and radium-228. The locations of these wells within the state are presented in Figure 1. While it is not known to what extent the wells in confirmed violation represent population density or some other sampling bias, they are almost entirely associated with the 14

TABLE I

Radioactive decay properties of the Uranium-238 series.

		Major radiation energies (MeV)		
Nucleide	Half-life	alpha	beta	gamma
^{238}U	4.5x10^{9} yr.	4.15 4.20	-	-
^{234}Th	24.1 d.	-	0.10 0.19	0.06 0.09
^{234}Pa	1.17 min.	-	2.29	0.77
^{234}Pa	6.75 hrs.		0.53 1.13	0.10 0.70 0.90
^{234}U	2.5x10^{5} yr.	4.72 4.77	-	0.05
^{230}Th	8.0x10^{4} yr.	4.62 4.68	-	0.07 0.10
^{226}Ra	1602 yr.	4.60 4.78	-	0.19
^{222}Rn	3.82 d.	5.49	-	0.07
^{216}Po	3.05 min.	6.00	0.33	-
^{214}Pb	26.8 min.	-	0.65 0.71 0.98	0.30 0.35
^{218}At	2 sec.	6.65 6.70	?	-
^{214}Bi	19.7 min.	5.45 5.51	1.00 1.50 3.26	0.61 1.12 1.18
^{214}Po	164 microsec.	7.69	-	0.80
^{210}Tl	1.3 min.	-	1.30 1.90 2.30	0.30 0.80 1.30
^{210}Pb	21 yr.	3.72	.016 .061	0.50
^{210}Bi	5.01 d.	4.65	1.61	-
^{210}Po	138.4 d.	5.31	-	0.80
^{206}Tl	4.19 min.	-	5.71	-
^{206}Pb	stable	-	-	-

(Gableman 1977)

TABLE II

Radioactive decay properties of the Thorium-232 series.

Nucleide	Half-life	Major radiation energies (MeV)		
		alpha	beta	gamma
^{232}Th	1.41×10^{9} yr.	3.95 4.01	-	-
^{228}Ra	5.8 yr.	-	.055	-
^{228}Ac	6.13 h.	-	1.18 1.75 2.09	0.34 0.91 0.96
^{228}Th	1.91 yr.	5.34 5.43	-	0.08 0.21
^{224}Ra	3.64 d.	5.45 5.68	-	0.24
^{202}Rn	55 sec.	6.29	-	0.6
^{216}Po	0.15 sec.	6.78	-	-
^{212}Pb	10.6 h.	-	.346 .586	0.24 0.30
^{212}Bi	60.6 min.	6.05 6.09	1.55 2.26	0.04 1.62
^{212}Po	304 nanosec.	8.87	-	-
^{208}Tl	3.10 min.	-	1.28 1.52 1.80	0.51 0.58 2.60
^{208}Pb	stable	-	-	-

Radioactive decay properties of the Potassium-40 series

^{40}K	1.26x10 y.	-	1.32	1.46
^{40}Ar ^{40}Ca	stable			

(Gableman 1977)

FIGURE 1

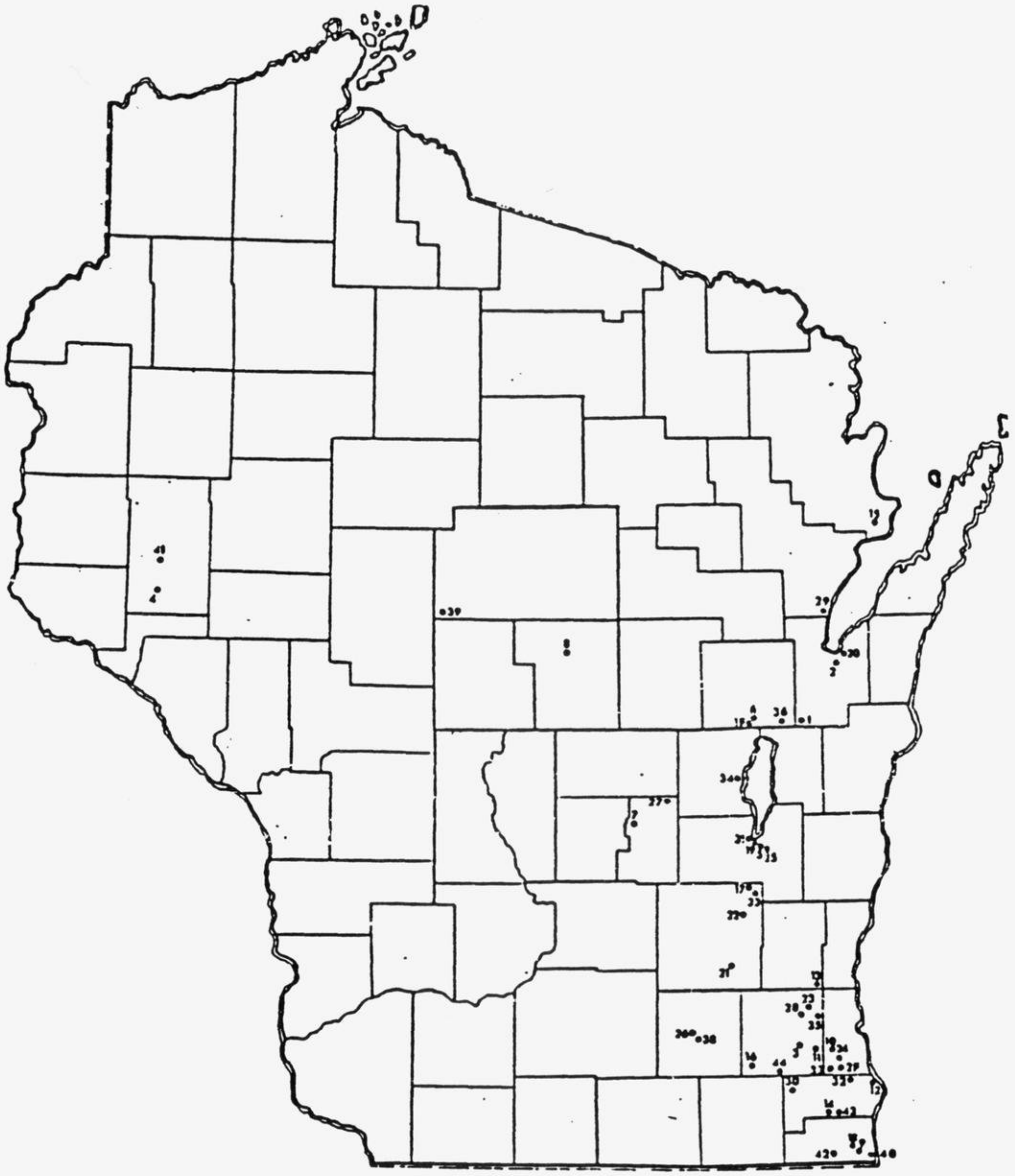

DNR MAP OF WELLS IN
VIOLATION OF RADIUM STANDARD

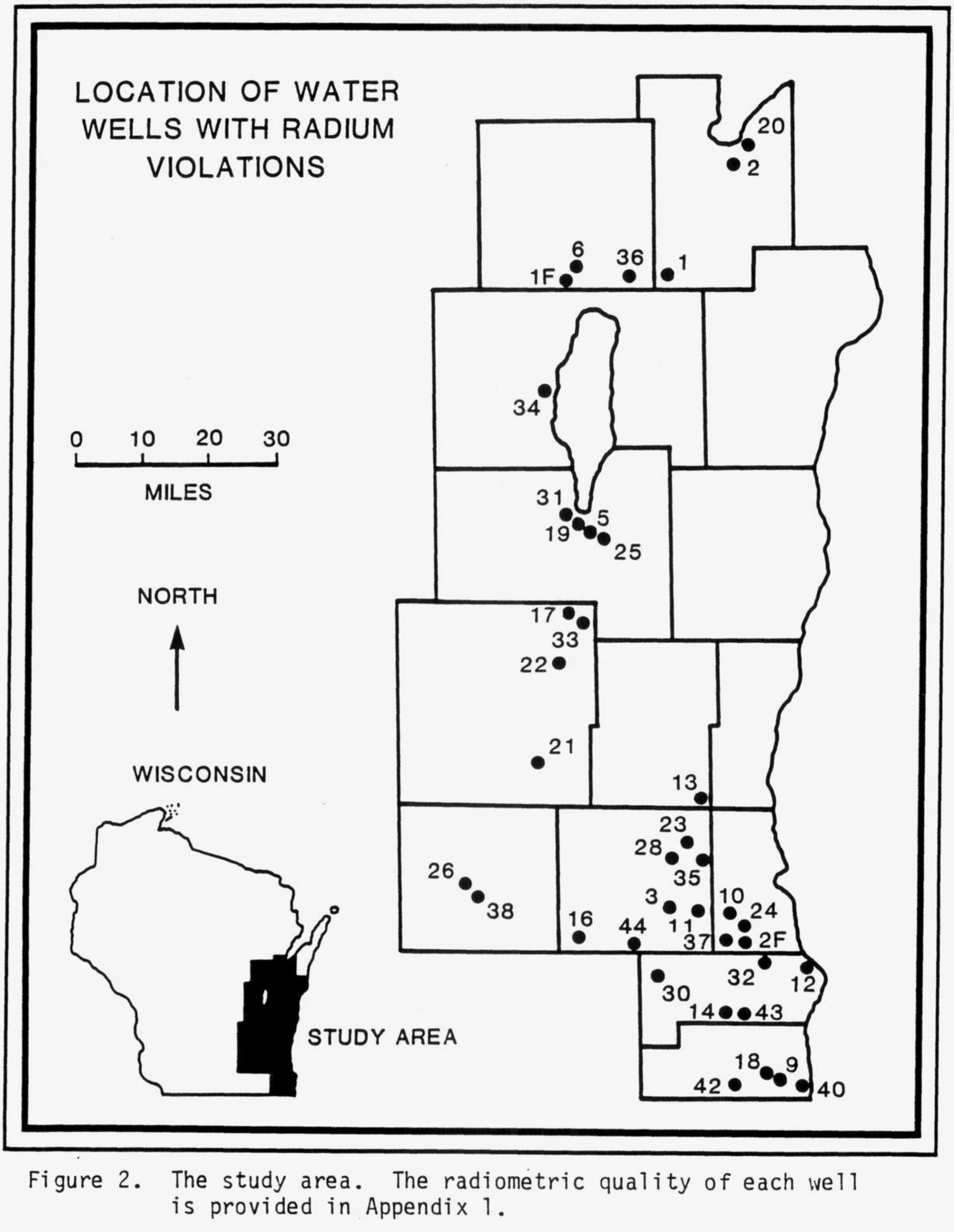

Figure 2. The study area. The radiometric quality of each well is provided in Appendix 1.

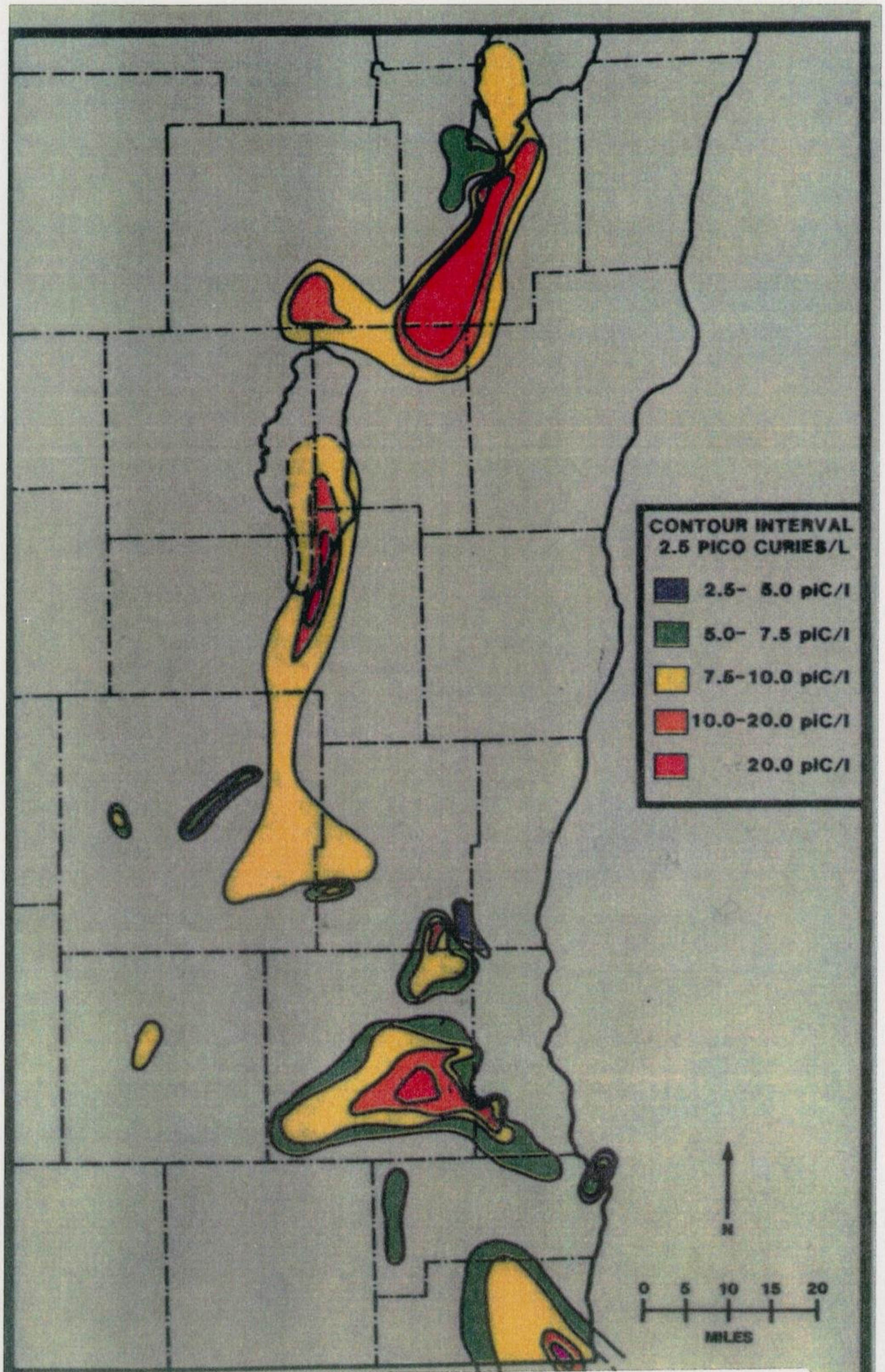

Figure 3. Contoured radium concentrations.

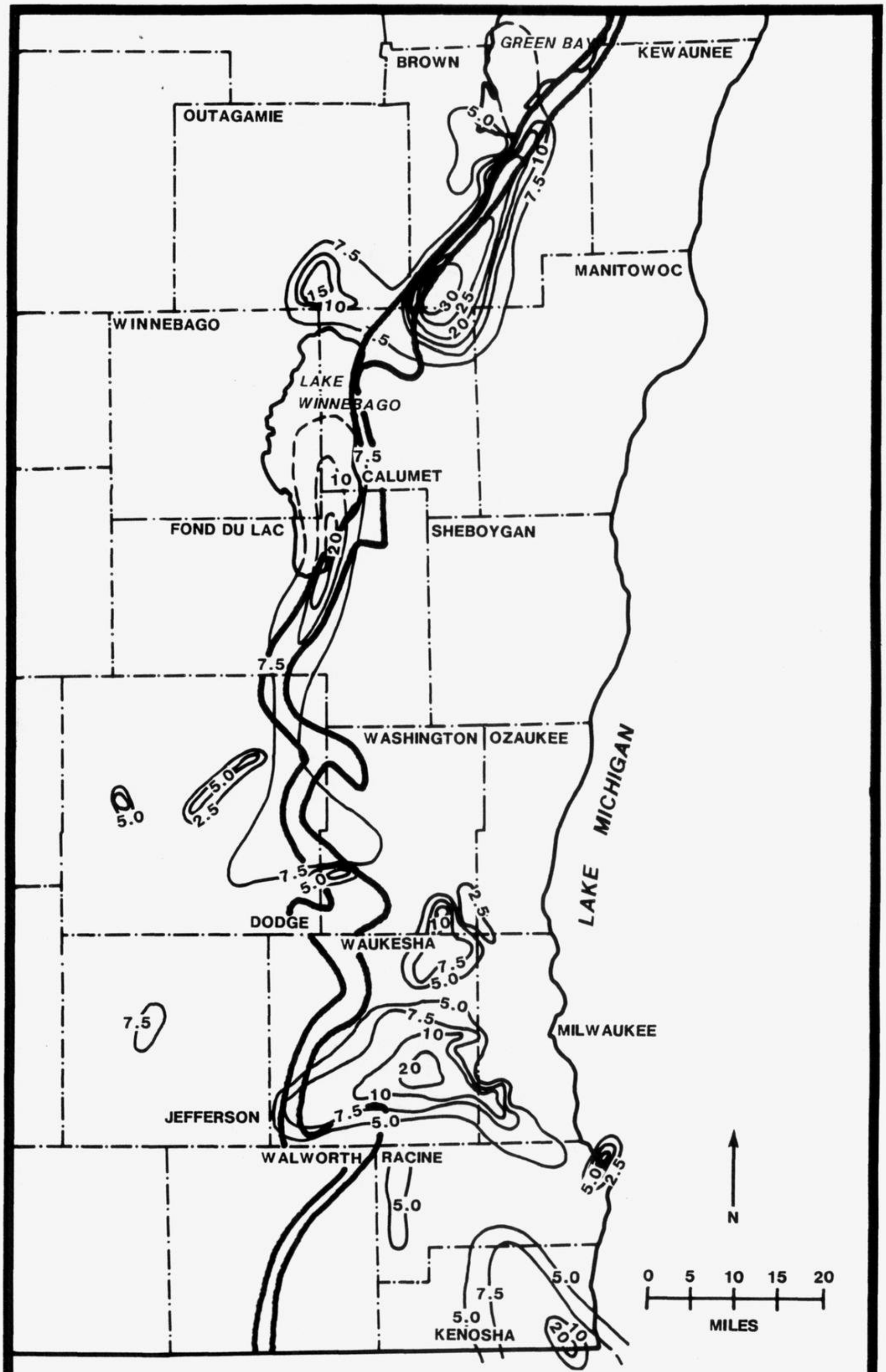

Figure 4. The spatial relationship of radium concentrations to the Maquoketa formation outcrop.

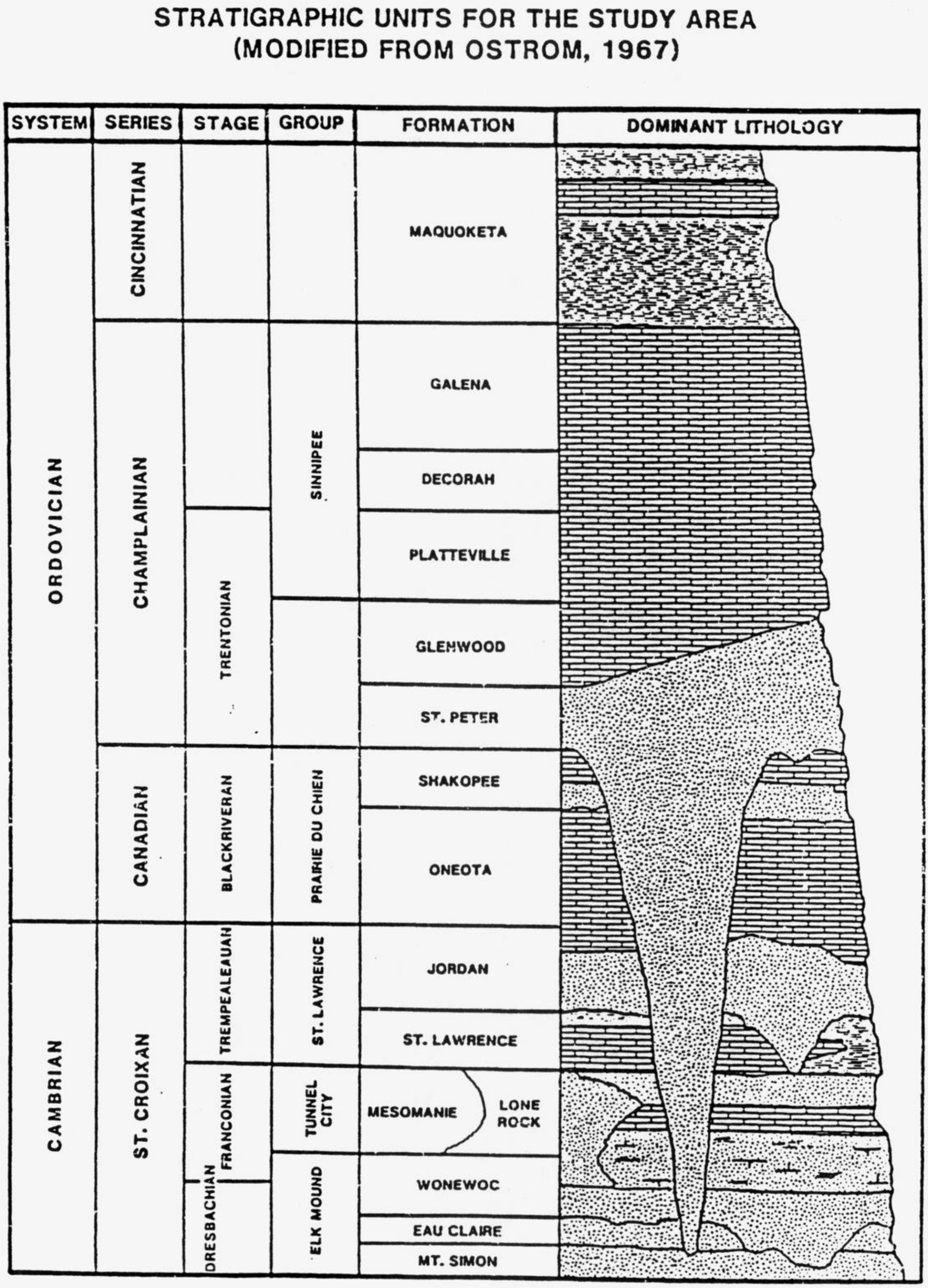

Figure 5. Stratigraphic units of interest within the study area.

county area defined in Figure 2. This study is limited to these 14 counties because they essentially account for all known violations.

The 44 wells are all producing from the Cambrian, Ordovician sandstone aquifer and the observed total radium levels within the wells define a series of systematically trending highs. This systematic distribution of radium highs is color displayed in Figure 3. It is interesting to note that the radium highs appear to nearly coincide with the outcropping of Maquoketa shale within the state. This spatial coincidence is demonstrated in Figure 4. It must be noted, however, that there is no established, or even suggested, reason why the radium levels in water produced from Cambrian and Ordovician sandstones would be related to the presence of the Maquoketa shale outcrop.

GENERAL GEOLOGIC SETTING

The study area consists of 14 counties along the eastern third of the state which extends north form Kenosha County at the Illinois-Wisconsin border up to and including Brown County on the southern shore of Green Bay (Figure 2). A generalized stratigraphic column shown in Figure 5, modified from Ostrom (1967), outlines the lithology and nomenclature of the area. Absent from the sequence are the recent glacial deposits and the units that comprise the unconfined aquifer which, for the purposes of this study, are not significant.

The primary water producing zone, for the wells of interest, is the Lower Paleozoic sandstone aquifer which includes three formations known to produce water with total radium concentration (RA-226 and Ra-228) greater than 5pCi/1 (Emrich and Lucas, 1963). These formations, the Mr. Simon, Eau

Claire, and St. Peter (Figure 5) were deposited during cyclic transgression-regression of epeiric seas which covered the North American Mid-continent during the Lower Paleozoic Era. Periodic tectonic uplifts and downdrops of the Wisconsin Arch throughout the lower Paleozoic Era caused fluctuations in sea level, and sequential changes in the near-shore depositional environment.

The Lower Cambrian Mt. Simon Formation lies unconformably on Precambrian quartzites and granites. It is a well-sorted, friable, medium to fine-grained sandstone. The Mount Simon Formation can contain up to 20 percent feldspar, and commonly has a heavy mineral fraction consisting of zircon, tourmaline and garnet. The upper 20 to 30 feet is often marked by interbeds of poorly-sorted strata of shale and arenaceous carbonate which occur in the generally thick-bedded, sandstone. The interbedded strata contain ferrugineous cement, and glauconite, pyrite, shale, or dolomite, in addition to the previously listed feldspar and heavy minerals. The average thickness of this formation in the study area in 485 feet.

The Lower Cambrian Eau Claire Formation overlies the Mount Simon Formation throughout the study area. It represents the argillaceous sandstone and/or shale which is typical of the depositional shelf environment. The Eau Claire Formation is generally thin-bedded, shaly to silty sandstone cemented with carbonate. Garnet is the dominant heavy mineral in this sequence,but zircon and tourmaline have also been identified.

Compositional variation in the Eau Claire Formation is generally a function of the sediment supply during the time of deposition, causing variations in the sand to shale ratio, and locally, to carbonate content. Fine sand, silt and glauconite are common matrix minerals. The average thickness of the Eau Claire Formation in the study area is 130 feet.

The Middle Ordovician St. Peter Formation, is a well-sorted, friable, medium to fine-grained quartz sandstone. A notable heavy mineral fraction including zircon, tourmaline, and granite fragments is commonly identified. The dominant mineralogy is quartz, which typically occurs as etched and/or frosted, well-rounded grains. In the study area, the St. Peter averages 130 feet in thickness.

STUDY OBJECTIVES

The primary objectives of this study are as follows:

1. To determine if structural control is influencing the observed spatial distribution and magnitude of radium levels.
2. To determine if the observed radium distribution and levels are stratigraphically controlled.
3. To investigate the utility and accuracy of available spectral gamma logs in identifying radioactively enriched zones within the aquifer.
4. To determine the mineralogy and geochemistry of radioactively enriched zones within the aquifer.
5. To determine the chemical form of uranium-238 and thorium-232, the lithological association of these radionuclides, and the availability of parents, uranium-238 and thorium-232, and daughters, radium-226 and radium-228 to the groundwater system.
6. To suggest remedies for minimizing the concentration of radium in produced water.

GEOCHEMISTRY OF URANIUM, THORIUM, AND RADIUM

BACKGROUND

Radium-226 and radium-228 are daughter products of uranium-238 and thorium-232 respectively so that the availability of the two parents also controls the concentration of radium. For this reason the behavior of the parents and daughters is briefly discussed in order to properly understand the complexity of their occurrence, distribution and mobility in ground water systems.

Uranium and thorium, as minor constituents in the lithosphere, are present in trace amounts in almost all geological materials. The average concentration of Uranium in the earth crust amounts to 1.8 ppm (parts per million) and that of thorium 7.2 ppm. Uranium and thorium may occur in several ways in the rocks:

1) in the radioactive accessory minerals such as uraninite, thorite, monazite, zircon, and allanite.
2) as isomorphic substitutions in the crystal lattice of such minerals as sphene, apatite, niobates, tantalites, and titanites.
3) as molecular or ionic disseminations in, or associated with, the major rock-forming minerals.
4) as entrapments in lattice imperfections, along fractures and cleavage planes, along grain boundaries, or as fluid inclusions.

URANIUM

Uranium with atomic number 92 and weight 238 has an ion size of 1.05 _ and six valence electrons. Quadrivalent and sexivalent occurrences are common in nature. The ionic radius is very close to that of calcium (1.06 _) and trivalent rare earth (yttrium, 1.06 _), so uranium is preferentially captured by minerals of these elements. Sexivalent uranium compounds, because of their greater ionic potential, are chemically more mobile than quadrivalent uranium, thus uranium can be moved much more readily after oxidation to the uranyl state. Virtually all uranyl compounds except phosphates, vanadates, and to some extent, arsenates are readily soluble at low temperatures. Fixation usually is accomplished most readily by reduction with organic matter.

Fractional mobilization of uranium must be considered according to its chemical stability in minerals, the complexity of the minerals, the stability of uranium - complexing elements in the minerals and grain size of the minerals as well as their distribution in the rock, and the relative ease of access to the uranium by oxygen, water, or other oxidizing agents. Uranium oxidizability (and mobility) decreases from the simplest pitchblende through the simple silicates, complex silicates, multiple oxides and phosphates, largely because of difficult access by agents as well as decreasing Eh.

Once uranium is oxidized, its dissolution, and therefore, its mobility depend on the relative solubility of oxidation products. The type of oxidized minerals formed is, in turn controlled greatly by the lithology of the enclosing rocks. Thus, uranyl halides and nitrates are so soluble that they are rare in nature. Carbonates and sulfates are easily soluble and are uncommon, but silicates, phosphates, and vanadates are relatively insoluble and are common. If oxidized uranium encounters strongly reducing environment such as organic material, it is quickly reduced and immobilized.

Uranium is not equally distributed in different types of sedimentary rocks, but is persistent in all types to the extent that some of it can be selectively mobilized either by direct solution of uranyl ions or by oxidation and solution during geologic processes. In a stack of different sedimentary rocks uranium would be most easily mobilized from sandstone, less easily from a limestone, and hardly at all from a carbonaceous shale. The rocks from which uranium can be dissolved most easily are also those which offer the greatest porosity and permeability to leaching fluids.

Once uranium is in the groundwater system, the relative distribution of uriniferous water is unpredictable. Some is involved in active hydrodynamic subsurface cycles, some reaches stagnant sinks, some is absorbed into crystal lattices. The fact that most migrating groundwater remains relatively fresh suggests little areal retention of uranium, or cleaning action by filtering through aquifer material.

Because uranium is dispersed in most rock types in some abundance, the dominant potential source for mobilization is the rock which has both the greatest uranium abundance and the greatest volume. Uranium bound in refractory heavy minerals rarely becomes available for mobilization, except for the portion which occurs as interstitial oxide or cryptocrystalline aggregate.

There are, therefore, a number factors which can influence the uranium dissolved in ground water and they are:

1) The uranium content in source rocks and its leachability.
2) The proximity of the water to uranium-bearing rocks or minerals.
3) The degree of hydraulic isolation of the water from dilution by fresher water.

4) The pH and Eh of the water.
5) Concentration of carbonate, phosphate, vanadate, fluoride, sulfate, silicate, calcium, potassium, and other species which can form uranium complexes.
6) The presence of highly sorptive materials such as organic mater, ferric, manganese, and titanium oxyhydroxides, and clays.

THORIUM

Thorium, of atomic number 90 and weight 232 is a quadrivalent element with an ionic radius of 1.10 _. As with uranium, this ion size causes behavior similar to that of bivalent calcium, trivalent cerium (1.18 _), and the yttrium (0.99 to 1.11 _) group of minerals. Thorium resembles rare earths in the insolubility of its fluorides, carbonates, hydroxides, oxalates and phosphates, and is always associated with rare earths in nature. It forms complex ions in aqueous solutions of which halides are readily soluble in water. Therefore, thorium halides are probably fairly mobile in molecular or ionic form at moderate temperatures.

The similarity in most of their chemical characteristics causes uranium and thorium to remain together geologically except in regard to the oxidation valence state, which seems to be responsible for their eventual separation. Their large ionic size is incompatible with the molecular lattices formed by the common rock-forming minerals, therefore, they tend to concentrate with other large ions including the rare earths, titanium, niobium, and zirconium, with which they are chemically more compatible, to form such minerals as allanite, zircon, thorite, pyrochlore and monazite or uraninite. These minerals are generally stable and resistant to chemical breakdown.

The main reason for the fractionation of uranium and thorium is the oxidation of uranium to the uranyl valance state; thorium does not undergo such a reaction. Uranyl ions then can travel much further than thorium ions in the groundwater system, and would require special condition such as combination with phosphorous or vanadium to cause fixation in the uranyl state, and require reduction for fixation in the uranous state.

RADIUM

Radium is relatively immobile, however, some radium does go into solution adsorbing and desorbing continually onto mineral grains of the aquifer. Radium can occur in three forms, as radium-226, radium-228, and radium-224. Radium-226 is a long-lived daughter of the uranium-238 decay series (Table 1) whereas radium-228, and radium-224 are short-lived daughters of the thorium-232 decay series. (Table 2). Because of its short half-life (5.75 years), radium-228 can not migrate significant distances in aquifers from its site of generation. An important source of radium-228 is thought to be thorium-rich accessory minerals.

The mechanisms that control the occurrence of radium-226 in groundwater are more complex than for radium-228 because significant disequilibrium between the precursor nuclides to radium-226 may occur in groundwater flow systems due to differences in the chemical and radiologic properties of precursor nuclides (^{238}U, ^{234}Th, ^{234}Pa, ^{234}U, and ^{230}Th). Radium-226 may be placed in solution by alpha recoil or mobilized as a function of the ground water chemistry. There is a direct relation between the ionic strength of groundwater and the concentration of dissolved radium-226. Thus one would expect an increase of radium with depth due to increased salinity of deeper older water. Moreover, deep water usually contains a large amount of CO_2 which escapes when the water reaches atmospheric pressure. This causes Ca and Mg carbonates to precipitate, coprecipitating radium.

Several studies suggest that radium is rapidly adsorbed by aquifer materials, while others point out that adsorption of radium on quartz and kaolinite can be inhibited by low pH and elevated concentrations of Ca^{2+}

because of competition for adsorption sites. In addition, lack of Fe-oxides at the Eh-pH conditions in aquifer may also contribute to radium mobility, because the Fe-oxides commonly have large surface areas and are strong adsorbents of heavy metals. In a number of studies radium concentrations show a significant negative correlation with pH.

STRUCTURAL CONTROL OF RADIUM LEVELS

DATABASE

The sandstone units of primary concern, in descending order, are the St. Peter sandstone which is Ordovician in age and the Eau Claire and Mt. Simon sandstones which are both dated in the Cambrian. New structure and isopach maps were created because existing maps for the St. Peter and the Eau Claire had little detail and more subsurface control was needed than was available for some portions of the study area, particularly in the southern seven counties. Data for the updated structural maps was obtained from the Wisconsin Geologic and Natural History Survey, in the form of sample logs constructed by the Survey from wellbore cuttings obtained during the drilling of the wells.

RADIUM CONTROL BY ST. PETER SANDSTONE STRUCTURE

The structure map for the St. Peter generated from an analysis of the sample or well cutting logs is presented in Figure 6. Structurally, the Ordovician St. Peter sandstone is located in the easternmost limb of the Wisconsin Arch which is part of the larger Michigan Basin sedimentary sequence. The surface of the St. Peter sandstone is essentially linear, trending nearly parallel to the Lake Michigan coastline and gently dipping towards the east. In the western portion of the study area are many undulations observed in the upper surface of the St. Peter which can be attributed to continuous stream channel deposition and/or Karst topography in the pre-St. Peter depositional surface (Dott and others, 1985).

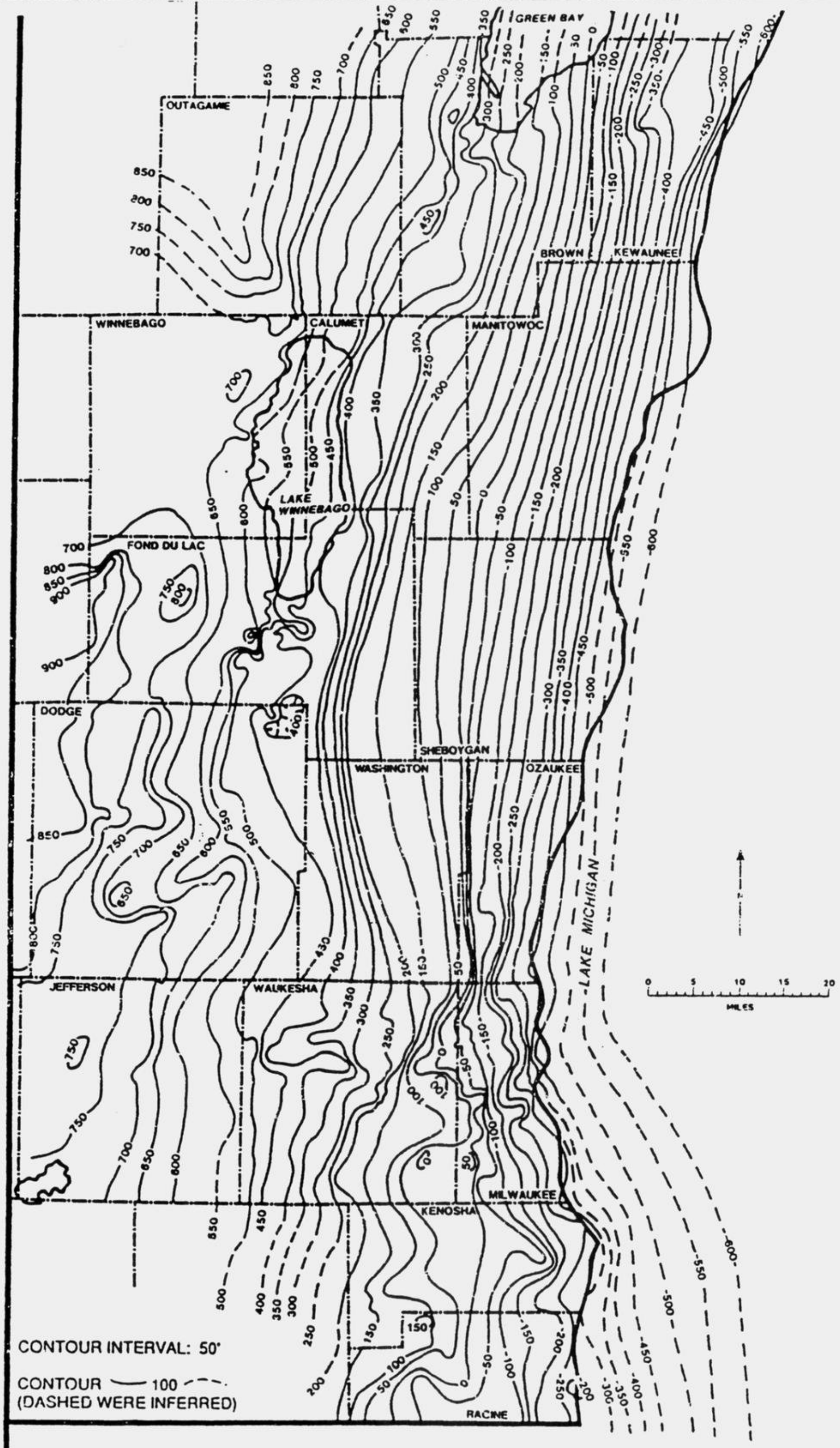

FIGURE 6
STRUCTURE OF ST. PETER SANDSTONE

To compare the groundwater radium concentration to the structure map of the st. Peter sandstone, the radium data map was superimposed on top of the St. Peter sandstone structure map and this comparison is presented in Plate II. Total radium isotope concentrations from the DNR water quality data in excess of 5.0 pCi/l can be observed over structural highs and lows as well as over thick and thin portions of the st. Peter sandstone. Concentration of 7.5 pCi/l and above can be observed on the structural high that runs from southeastern Dodge county trending NNE and terminating near Green Bay. High concentration of the radium isotopes can also be observed along the flank of the structural high in eastern Waukesha and western Milwaukee counties. Because high radium concentrations are seen on structural highs and on the flanks, there is no apparent relationship between the St. Peter structure and total radium concentrations.

An isopach of St. Peter sandstone thickness is presented in Figure 7. Plate III is a comparison of radium concentration with thickness of the st. Peter sandstone. High concentration of total radium-226 and radium-228 are seen in area where the St. Peter is thick and where it is thin. Therefore, there is no visible relationship between total radium isotope concentrations and thickness of the St. Peter sandstone.

RADIUM CONTROL BY EAU CLAIRE, WONEWOC SANDSTONE STRUCTURE

The Cambrian section within the study area consist of the Eau Claire, Wonewoc and Mt. Simon sandstones. The Eau Claire sandstone is present primarily in the southern portion of the study area and the structure associated with this unit is presented in Figure 8. The Wonewoc sandstone is present in

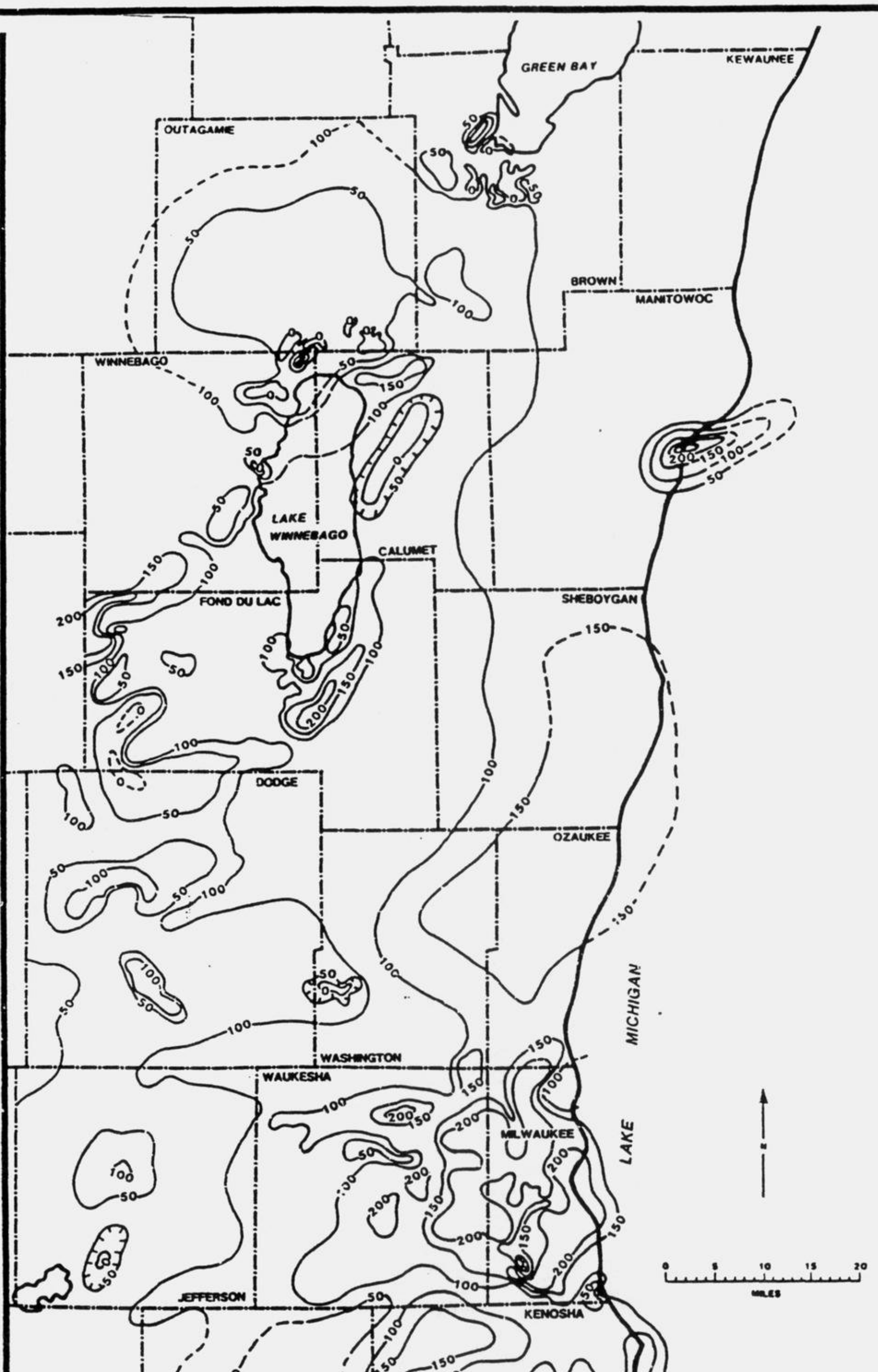

FIGURE 7
ISOPACH OF ST. PETER SANDSTONE

the north west portion of the study area and the structure generated for this unit is also presented in Figure 8. There are no major features associated with the structure of either sandstone. Plate IV is a comparison of radium concentration data with the Eau Claire structure map. Radium highs from the DNR water quality data are observed along structural highs and the flanks of the Cambrian structure map. Based on this comparison it is not possible to establish a relationship between the structure of the Eau Claire/Wonewoc horizons and any trend derived from the water quality data.

Insufficient data was available to generate any meaningful structure map of the Mt. Simon sandstone. Due to the insufficient data it was not possible to compare radium data to Cambrian thickness. However, the available comparison suggests this would not be a rewarding analysis.

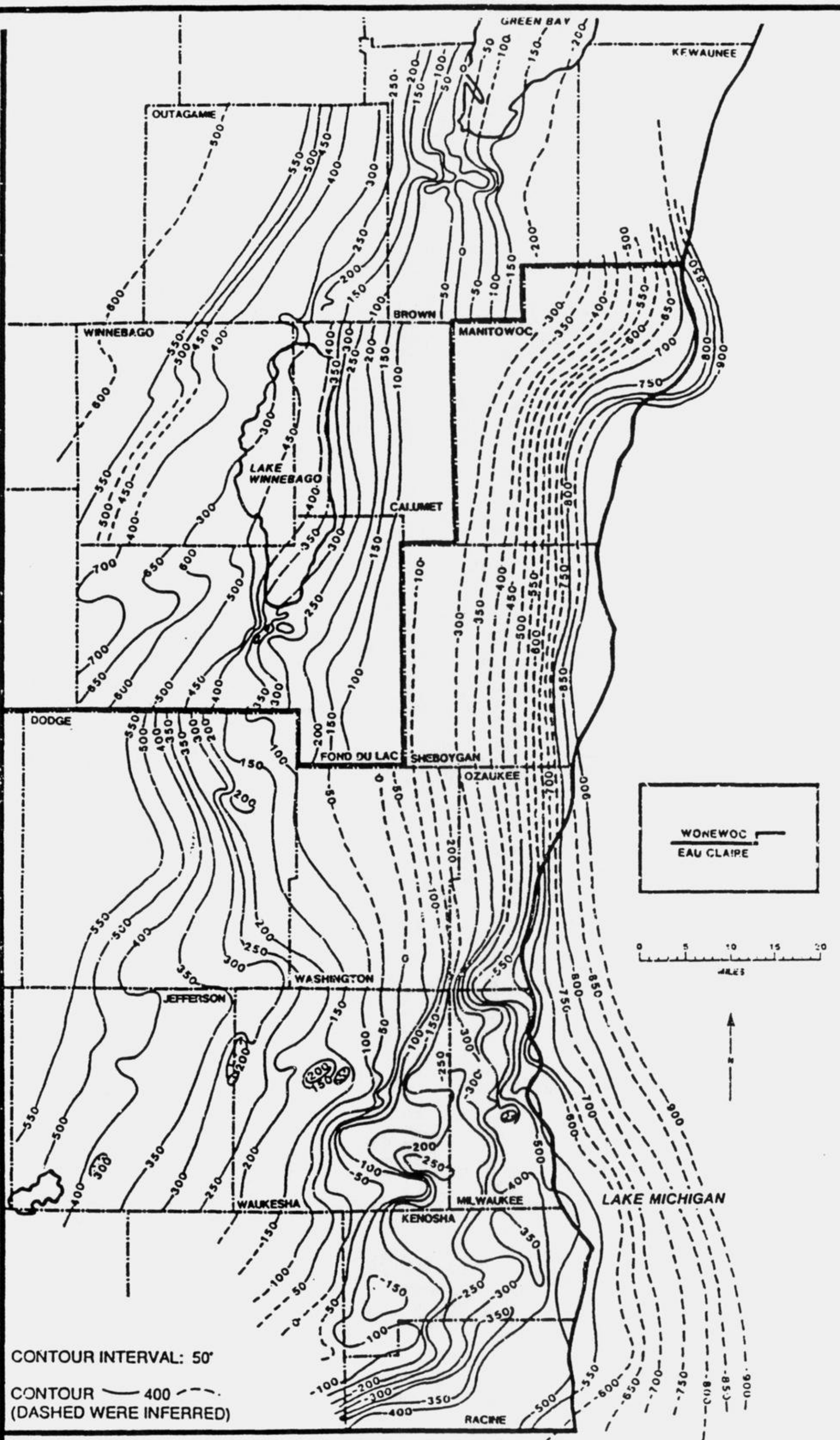

FIGURE 8
STRUCTURE OF EAU CLAIRE AND WONEWOC SANDSTONE

SHALE CONTROL OF RADIUM LEVELS

DATABASE

Natural gamma ray logs obtained form the Wisconsin Geologic and Natural History Survey provided the database used in generating percent shale maps for the study area. In calculating percent shale based on gamma ray response, a shale baseline and a sandstone baseline are defined on the log. The shale baseline is a smoothed estimate of the gamma ray response in a section of the borehole that is either known or assumed to be pure shale. Similarly, the sandstone baseline is a smoothed estimate of the gamma ray curve in a section of the borehole known or assumed to be clean sandstone. Figure 9 provides an example of these baselines. From these baseline parameters, the percent shale for any borehole interval can be linerally interpolated from:

$$V_{sh} = \frac{(V_{log} - V_{min})}{(V_{max} - V_{min})} \qquad (1)$$

where: V_{sh} = calculated volume of shale,

V_{log} = deflection of log at zone of interest,

V_{max} = shale base response

V_{min} = sand base response

A shale baseline was selected from the natural gamma ray response in the Maquoketa shale formation, however, the Maquoketa response was suppressed by steel casing. A correction chart (Gearhart Industries) yields values to compensate for various thicknesses of steel casing. The correction

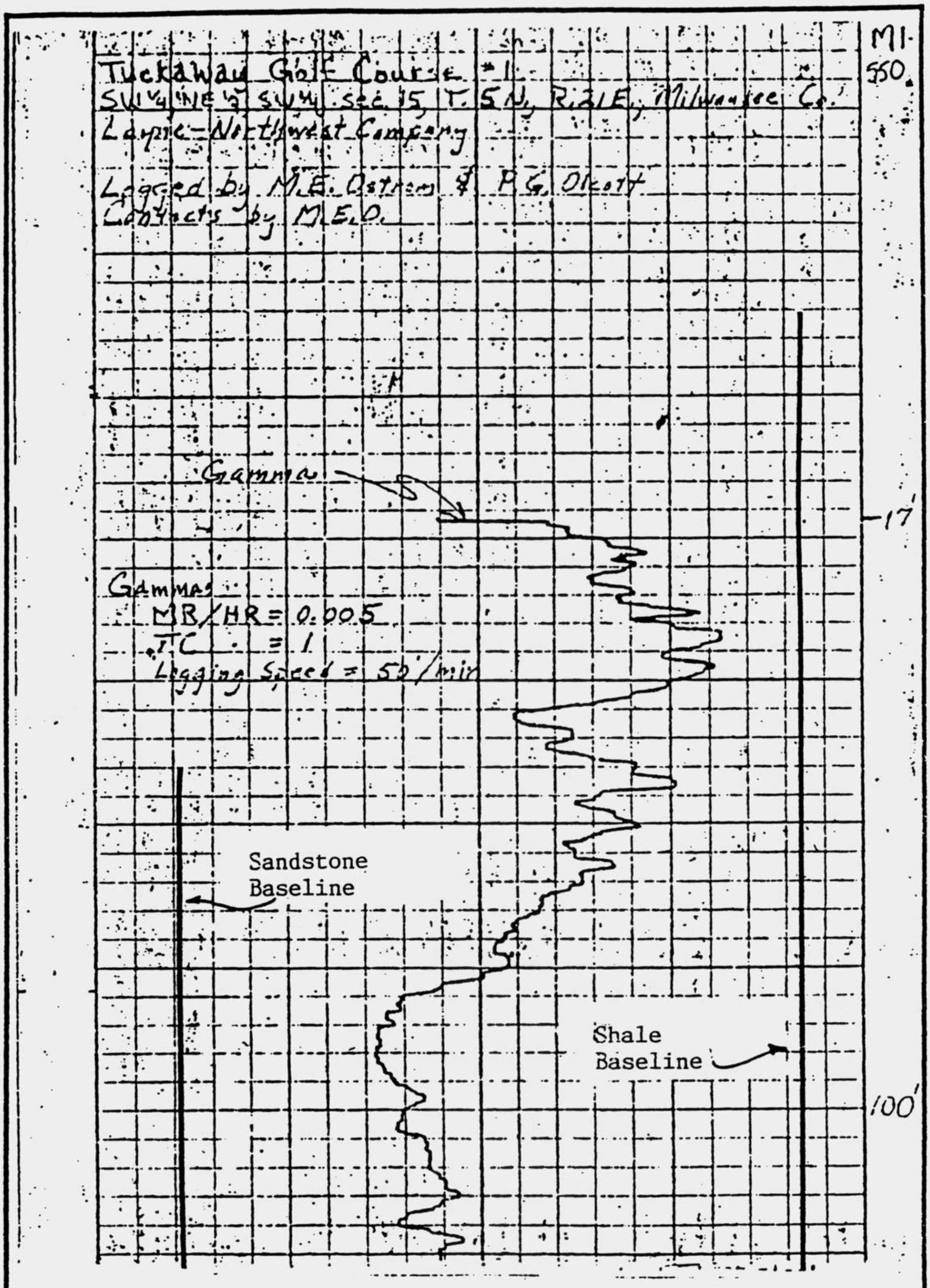

Figure 9. Example of a natural gamma ray log.

factor for 3/8 inch steel casing, which was used in all of the wells of the study area, is l.3. Log values in the cased interval of the Maquoketa shale were multiplied by this value. An average maximum value for the Maquoketa response was then calculated and used to create the percent shale maps. Vmin and Vlog values were selected separately for the St. Peter, the Eau Claire, and the Mt. Simon sandstones. The percent shale for each sandstone formation present at each well site was calculated from,

$$\% \text{ shale} = \frac{(V_{sh}\, h)}{H_{tot}}, \qquad (2)$$

where: V_{sh} = volume of shale calculated from equation 1

h = total thickness of shale seams within the sandstone formation,

H_{tot} = total sandstone formation thickness.

The gamma ray tool measures radioactive emissions and not grain size, hence, the term shale as used here is defined on the basis of radioactive minerals that are commonly associated with shales. The percent shale maps therefore are based solely on mineralogy rather than grain size parameters. The percent shale values for each formation were determined for every wellsite for which gamma ray logs were available.

RADIUM LEVELS AND SHALE CONTENT OF THE ST. PETER SANDSTONE

Figure 10 is a map of the percent shale calculated from equation 2 for the St. Peter sandstone. Most of Waukesha county and eastern Jefferson counties have some areas of closure based on the 5% shale contour line. Shale percentages in the St. Peter sandstone increase from the 5% area of closure out to 20%. The percent shale in the St. Peter sandstone for the

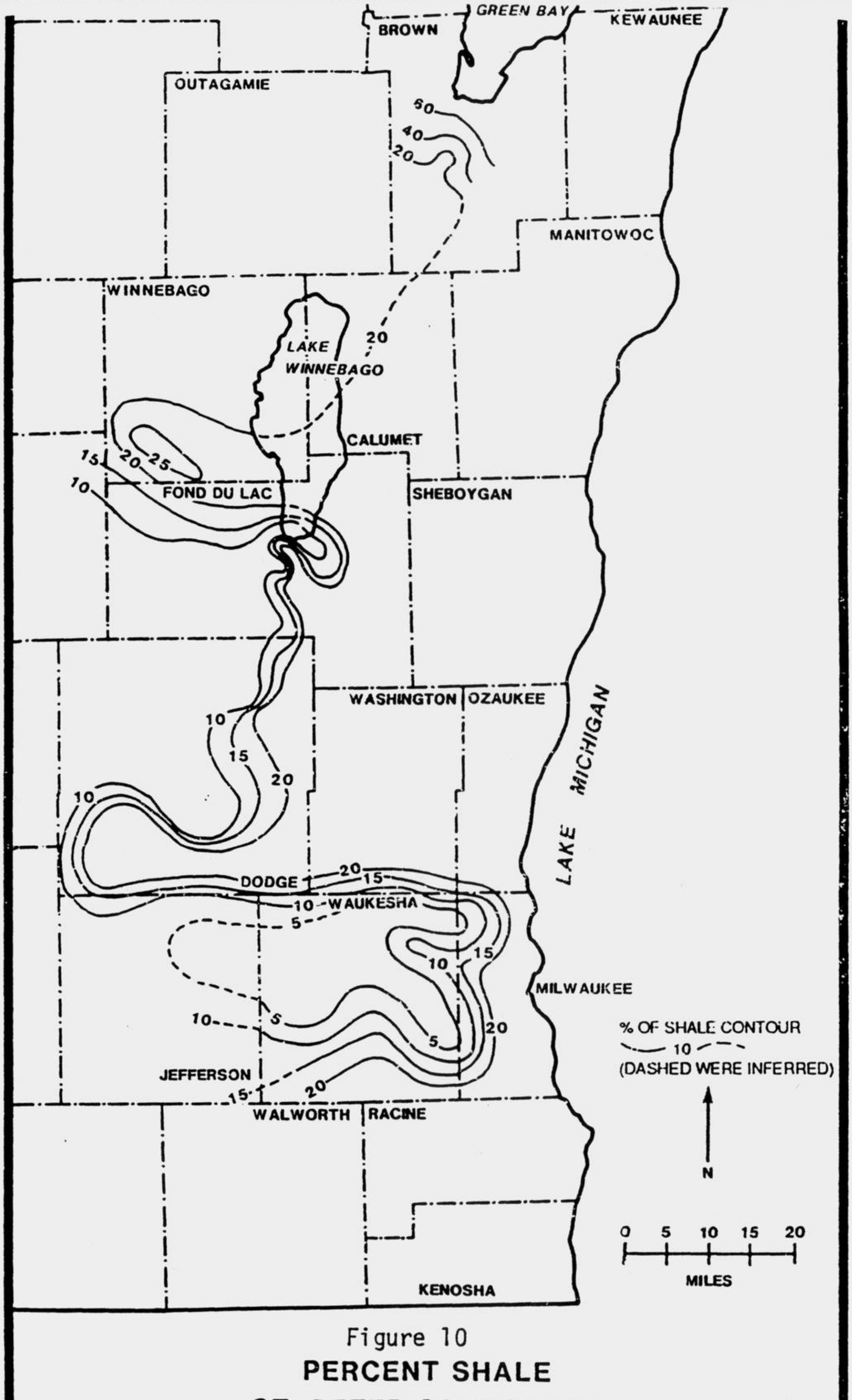

Figure 10

PERCENT SHALE

ST. PETER SANDSTONE

remainder of the study area trends N20E from the southwest corner of Dodge county up towards the southern tip of Lake Winnebago. From there, the shale belt trends approximately N60W towards the southwest corner of Winnebago county. The belt then curves southeast until it again resumes its N20E direction through the central portion of Lake Winnebago where it truncates near central Brown county.

The correlation of the radium concentration map with the St. Peter percent shale map is presented in Figure 11 where the radium concentration map is superimposed on top of the St. Peter percent shale map. There is some indication of a correlation between percent shale in the St. Peter sandstone and radium contamination of produced water for the northern portion of the study area. The concentration of total radium in the water samples appears to follow the belt of higher St. Peter shale content. In Fond du Lac and Dodge counties in particular there is an excellent correlation between total radium concentrations and percent shale in the St. Peter.

In Milwaukee and Waukesha counties, the relationship between shale percentage in the St. Peter and total radium in the water is less clear. High concentrations of total radium are found over the entire range of shale percentages within the St. Peter sandstone. The highest shale belt (15 to 20%) just skirts the easternmost limit of the radium water quality data. It is possible that the correlation is actually much better than it appears but has been visually degraded by the heavy pumping and resulting flow line diversions within these counties. However, there appears to be no way to confirm this other than through extensive ground water flow modeling.

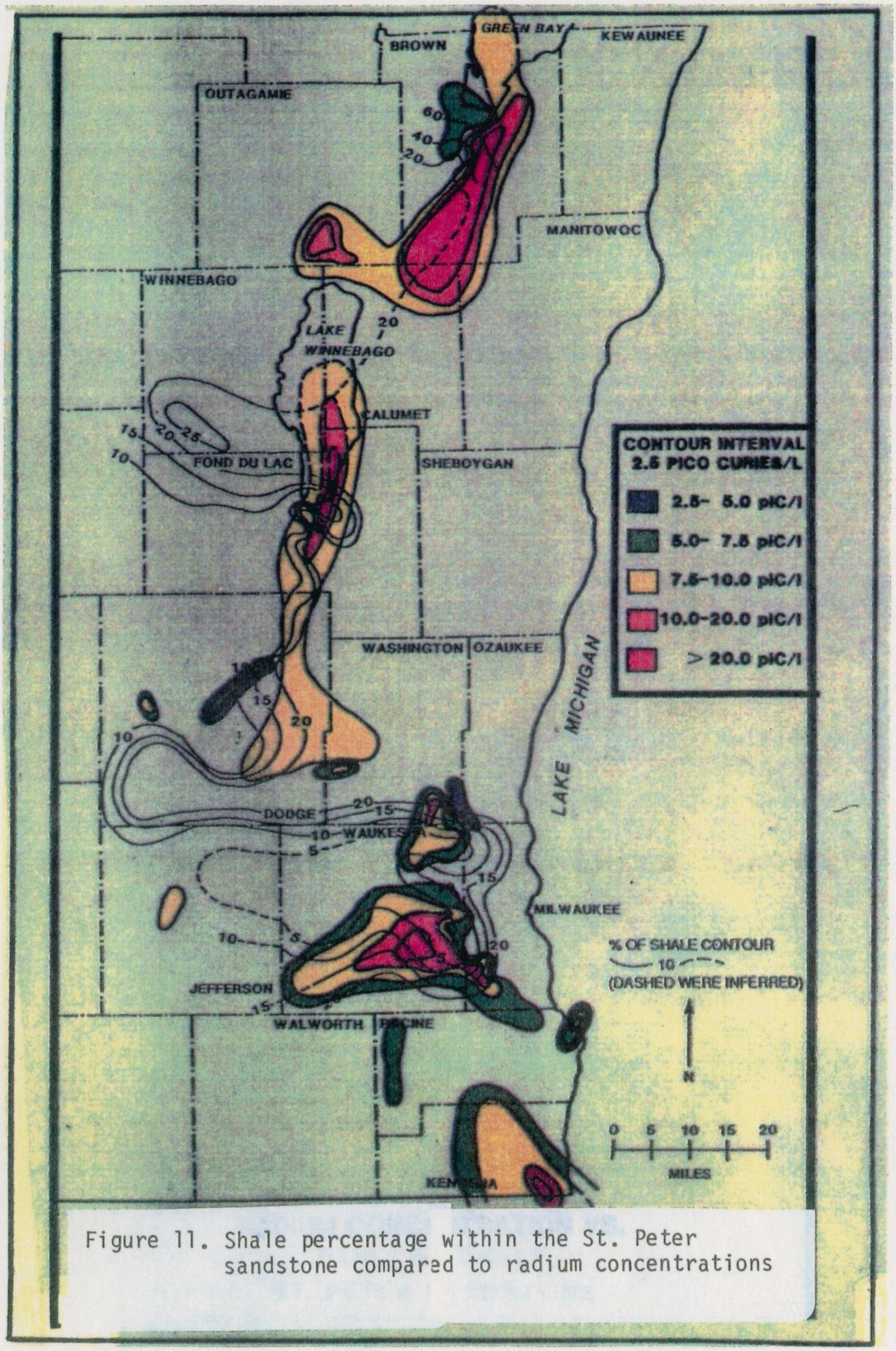

Figure 11. Shale percentage within the St. Peter sandstone compared to radium concentrations

RADIUM LEVELS AND SHALE CONTENT OF THE EAU CLAIRE SANDSTONE

Figure 12 is a map of the calculated shale percentages in the Eau Claire sandstone unit. It should be noted here that in the northern counties of the study area (Brown, Calumet, Fond du Lac, and Outagamie) the shale percentages are mapped based on the Elk Mound group. This stratigraphic group consists of Cambrian sandstones which include in descending order: the Wonewoc, the Eau Claire, and the Mt. Simon formations. The lumping of the three formations was accomplished at the time that the well cuttings were logged by state geologist. This combined group was the only geologic control available for the portion of the study area. For correlation purposes, the southeastern portion of the study area provides the best control.

Figure 13 is the radium concentration map superimposed on top of the Eau Claire sandstone horizon. There is a strong correlation between radium contamination found in the water samples and the 40 to 60 percent shale belt of the Eau Claire sandstone. In Waukesha county almost all of the water which tested in excess of the 5.0 pCi/l standard, falls within the 40 to 60 percent shale belt in the Eau Claire sandstone. In southwestern Milwaukee county where the shale belt extends in a southeasterly direction the water quality map also extends in this direction. This apparent correlation suggests that the shale lenses in the Eau Claire sandstone in the Waukesha and Milwaukee county areas may be a major source of radium-226 and radium-228 contamination.

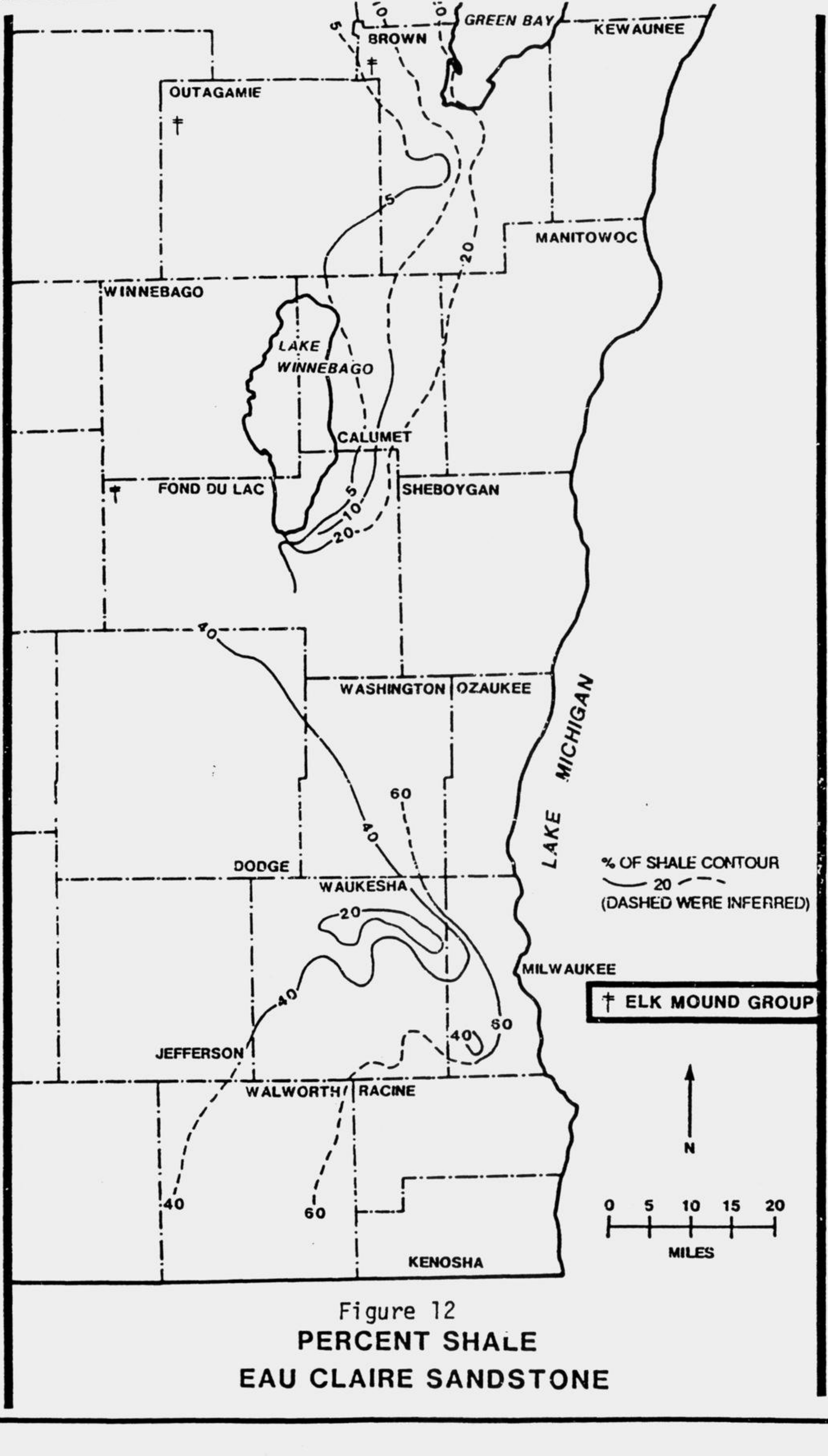

Figure 12

PERCENT SHALE

EAU CLAIRE SANDSTONE

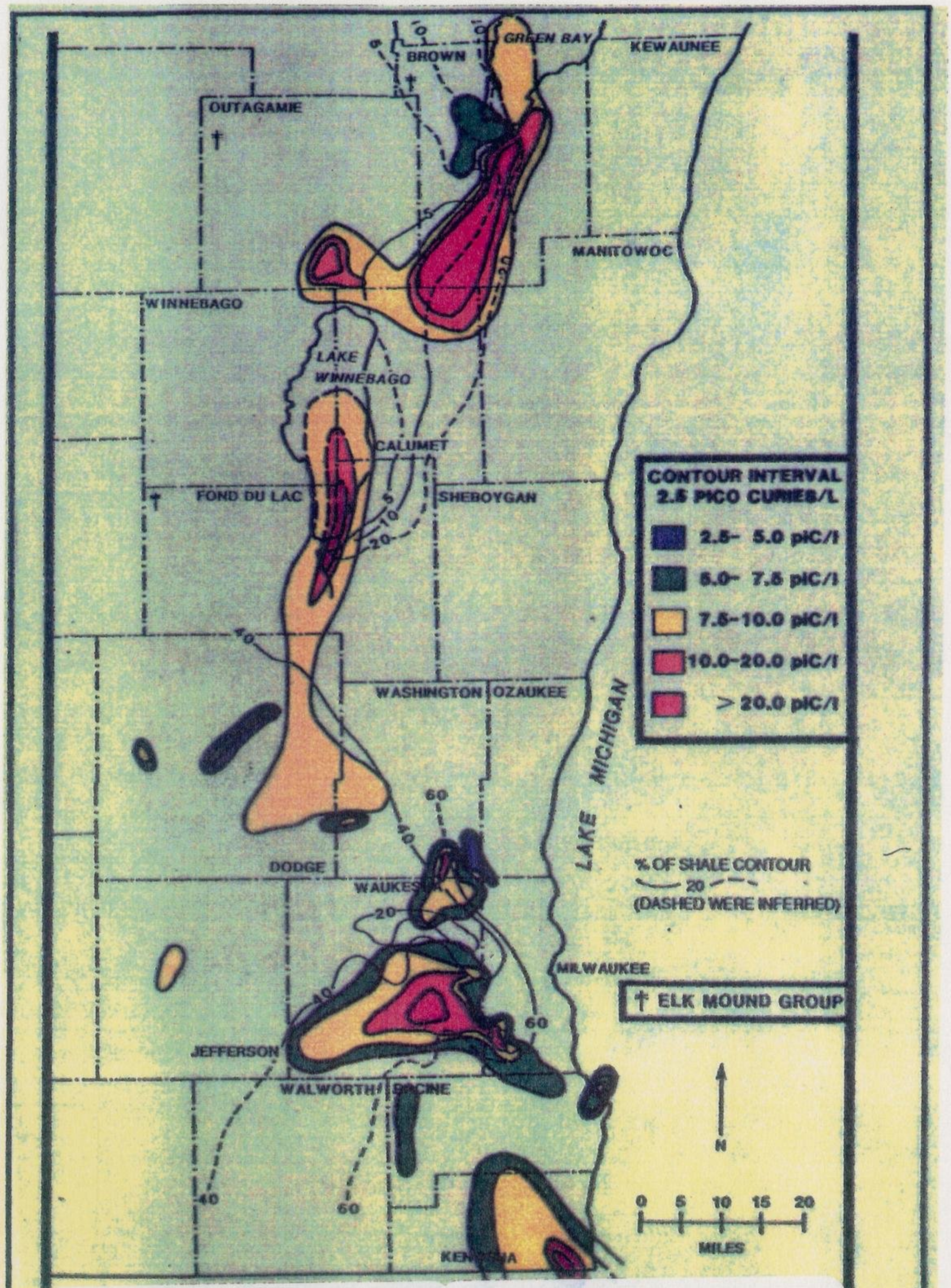

Figure 13. Shale percentage within the Eau Claire sandstone compared to radium concentrations.

RADIUM LEVELS AND SHALE CONTENT OF THE MT. SIMON SANDSTONE

The calculated shale content for drilled portions of the Mt. Simon sandstone is presented in Figure 14. While the drilled portions of this unit were generally shale free there is some indication of a closed 10 percent high centered in Waukesha County. Only one data point in Brown County was available for the northern section of the study area.

The radium concentration map is shown superimposed on the Mt. Simon percent shale map in Figure 15. In the area for which gamma ray logs for the Mt. Simon were available, basically Waukesha county, there is some indication of a correlation between water quality and the Mt. Simon shale content. The high radium levels are centered over high shale content and the radium levels and shale content appears similar in shape although the radium levels are somewhat offset to the east. As previously noted, the eastward offset may reflect heavy pumping in that direction.

THE INFLUENCE OF WELL PENETRATION

The potential affect of shale content within a given unit is modulated by the extent to which that unit contributes to total water production. The contribution to total production can be estimated to first order by considering the relation, expressed as a percentage, of Cambrian sandstone thickness to total Cambrian and Ordovician sandstone thickness. Using the sample logs this relation was calculated for all of the wells employed in this study. The resulting ratios are shown in color code in Figure 16. Figure 16 is color coded based on the Cambrian sandstone percentages. Blue dots on the map mean

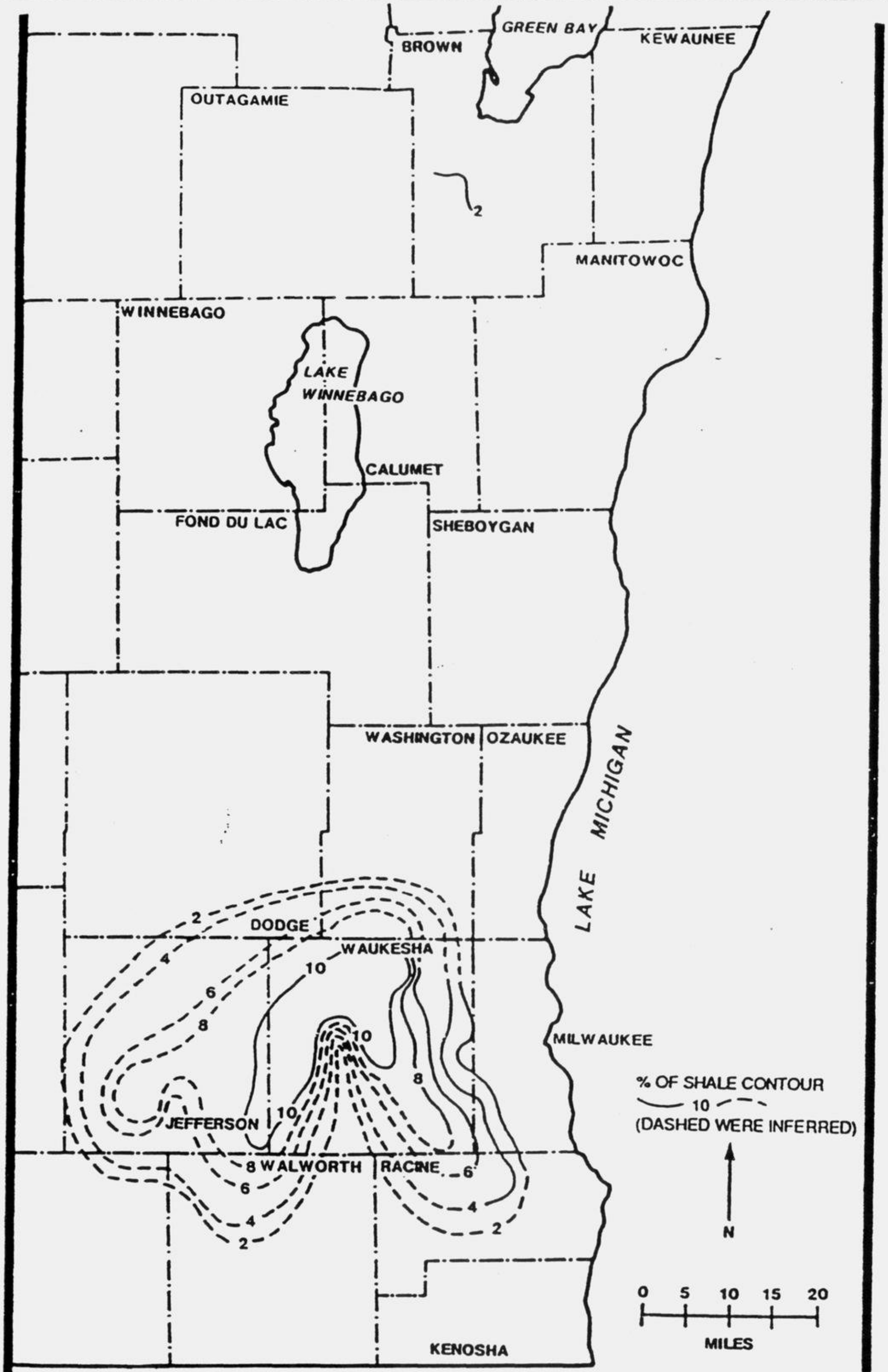

Figure 14
PERCENT SHALE
MT. SIMON SANDSTONE

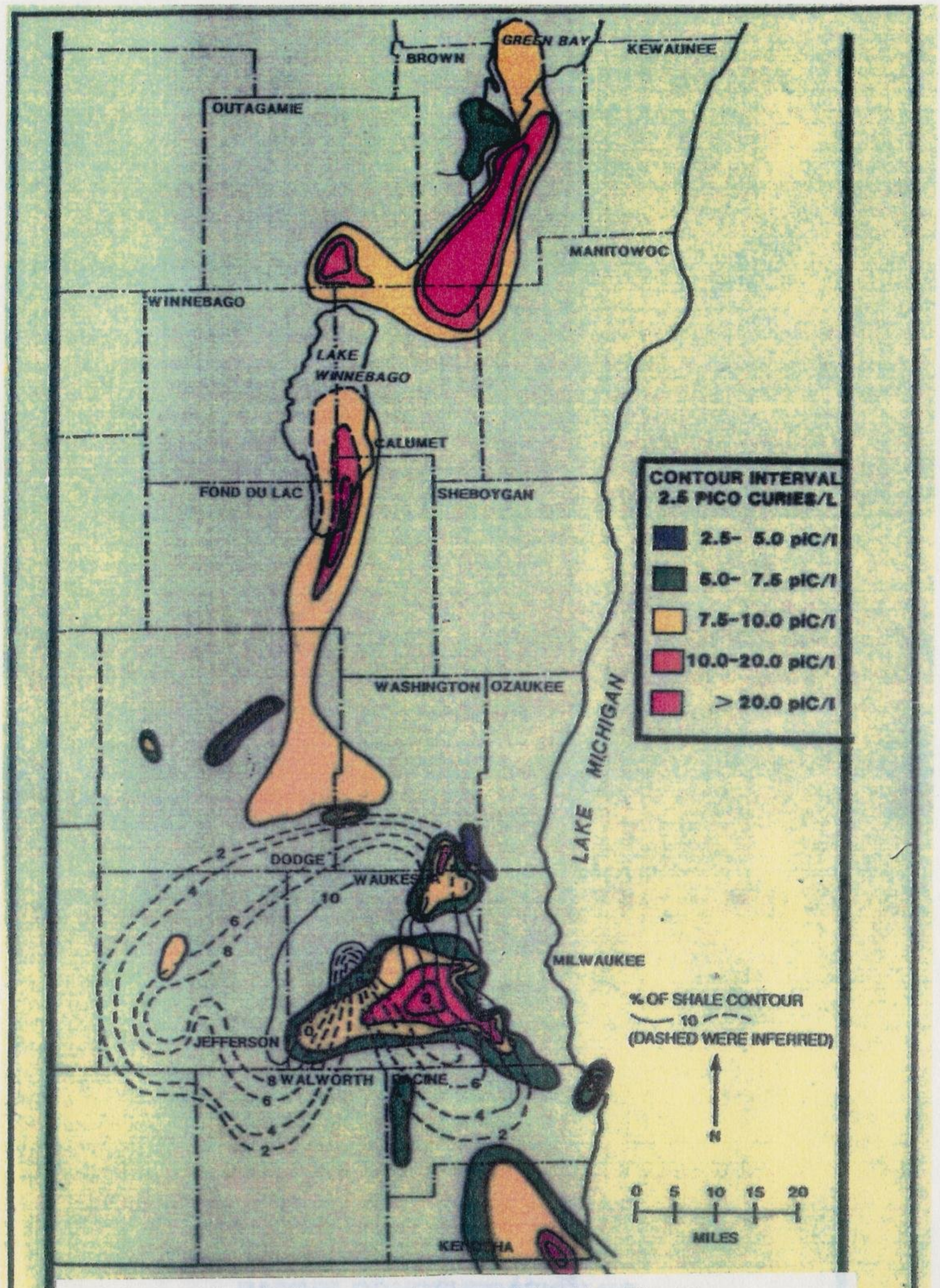

Figure 15. Shale percentage within the Mt. Simon sandstone compared to radium concentrations.

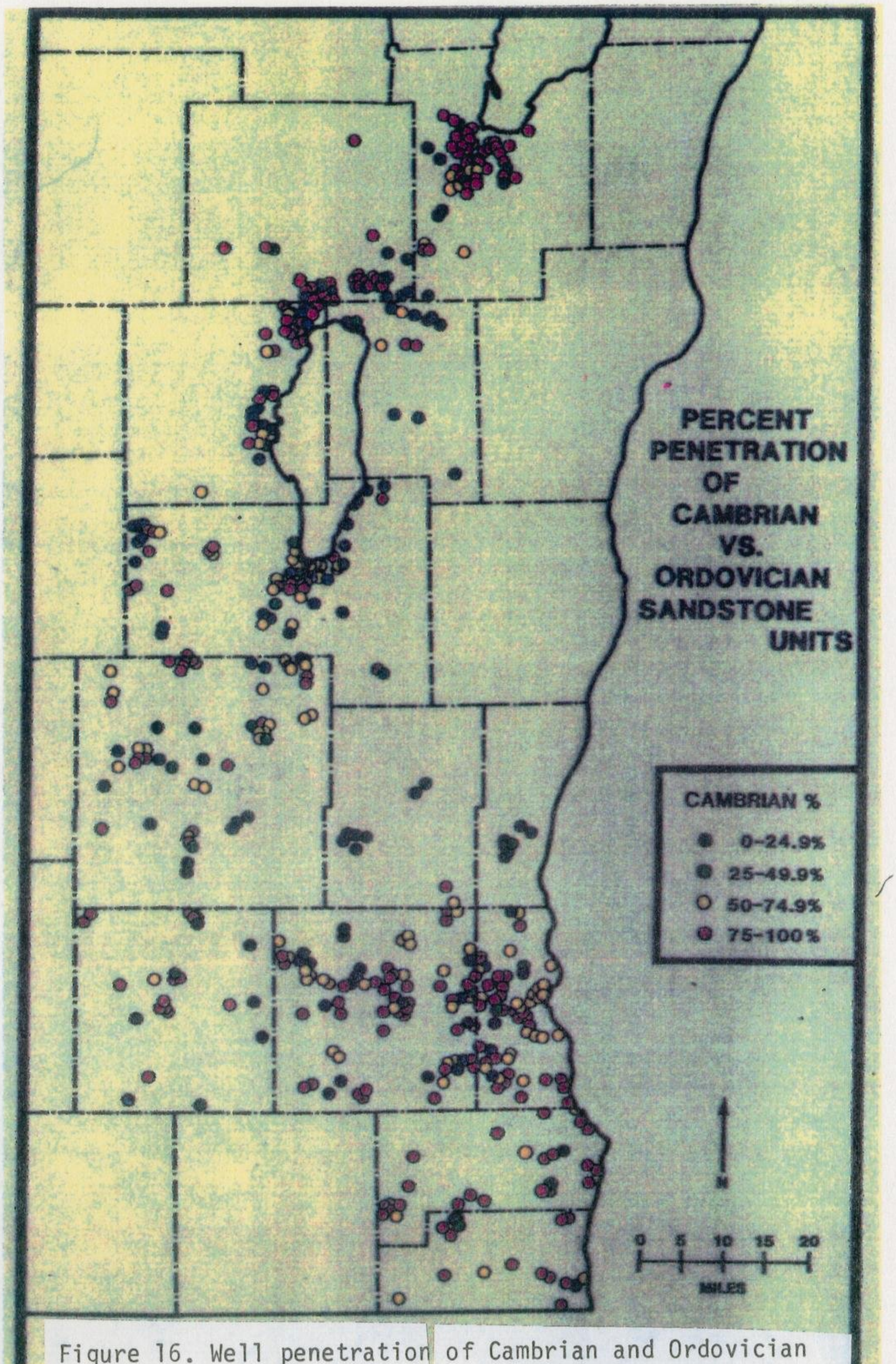

Figure 16. Well penetration of Cambrian and Ordovician sandstone

that the borehole cuts through anywhere from 0% to 24.9% Cambrian sandstone (or 75.1% to 100% Ordovician sandstone.) Green dots relate from 25% to 49.9% Cambrian sandstone (50.1% to 75% Ordovician sandstone) and so on. The lower the Cambrian sandstone percent thickness, the higher the Ordovician sandstone thickness and visa versa.

Figure 16 was used as an overlay in conjunction with the percent shale maps and the observed radium levels. This visual approach to accounting for the affects of wellbore penetration did not yield any clear correlations. However, in view of the size of the database and obvious significance of wellbore penetration, a more quantitative analysis is justified and should be conducted although it was not undertaken as part of this study.

QUANTITATIVE RELATION OF SHALE CONTENT TO RADIUM LEVELS

The preceding qualitative comparisons of shale content and observed radium levels suggest that the radium levels are somewhat related to the presence of shale. A confirmation of this relation should result from a direct comparison of shale content within a well with the radium levels observed in water from the well. Unfortunately, it is easier to propose this test than it is to accomplish it as only 13 wells could be found for which both measured radium levels and a gamma ray log were available.

A quantitative comparison of percent shale and total observed radium for these wells is presented in Figure 17. While there is a vague suggestion of an upward trend, the actual correlations coefficient is clearly too low to establish a meaningful relation between shale content and total radium in the product water.

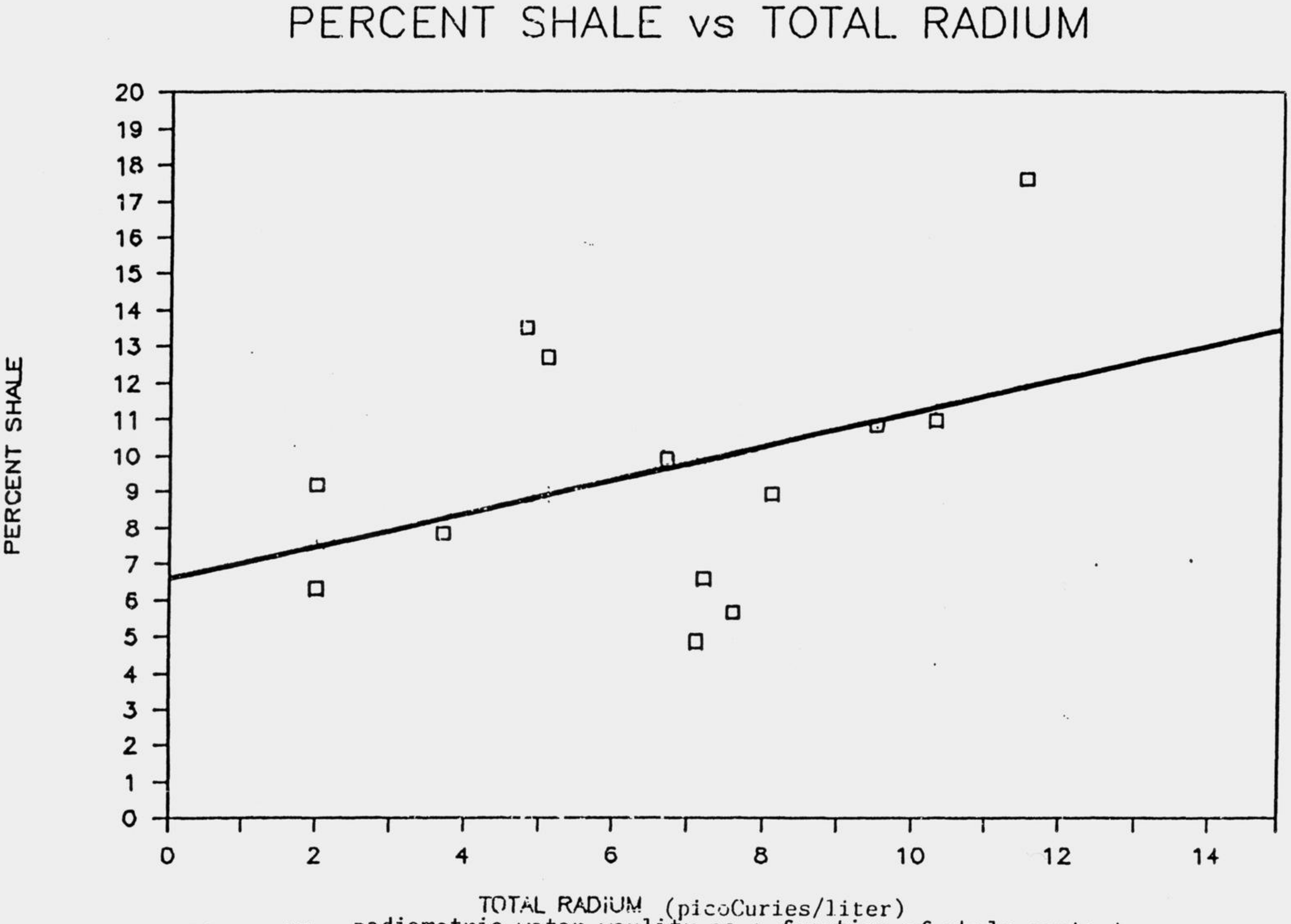

Figure 17. Radiometric water waulity as a function of shale content.

The relation of shale content to the radium-226 isotope in produced water is presented in Figure 18. The correlation coefficient for these data is 0.17 which is also too low to define any meaningful relationship. The relation of shale content to the radium-228 isotope in produced water is presented in Figure 19. The correlation coefficient of these data is less than 0.1.

Using the same 13 wells the relationship between radium-226 and radium-228 in the produced water is presented in Figure 20. The correlation coefficient of these data is 0.7 which indicates that the presence of either isotope in these wells is strongly coupled to the presence of the other. It also indicates that for these wells the ratio of radium-228 to radium-226 is nearly constant at a value of 0.65.

SUMMARY

A qualitative comparison of DNR water supply data with gamma ray log derived shale content appears to indicate a spatial correlation between the shale content of the producing sandstones and the observed radium levels. However, an attempt to quantify this relationship using 13 wells for which the necessary data was available proved totally negative. The 13 wells are a highly limited data set in comparison to the qualitative study so the number of involved wells should be greatly expanded prior to totally discounting the role of shale content. Nevertheless, on the basis of the available data, attempts to site low radium wells from shale content maps are not ensured of success.

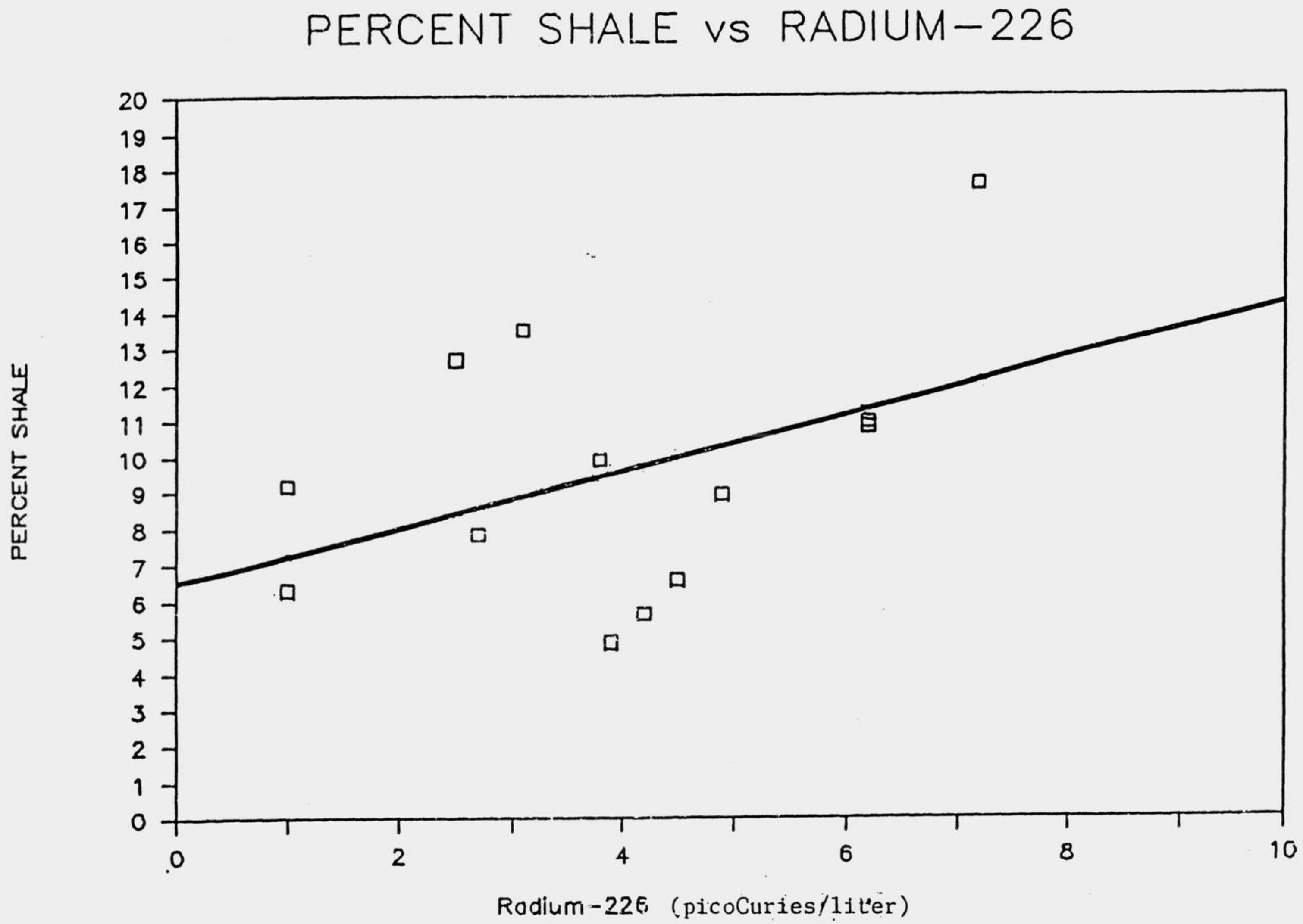

Figure 18. Radium-226 as a function of percent shale.

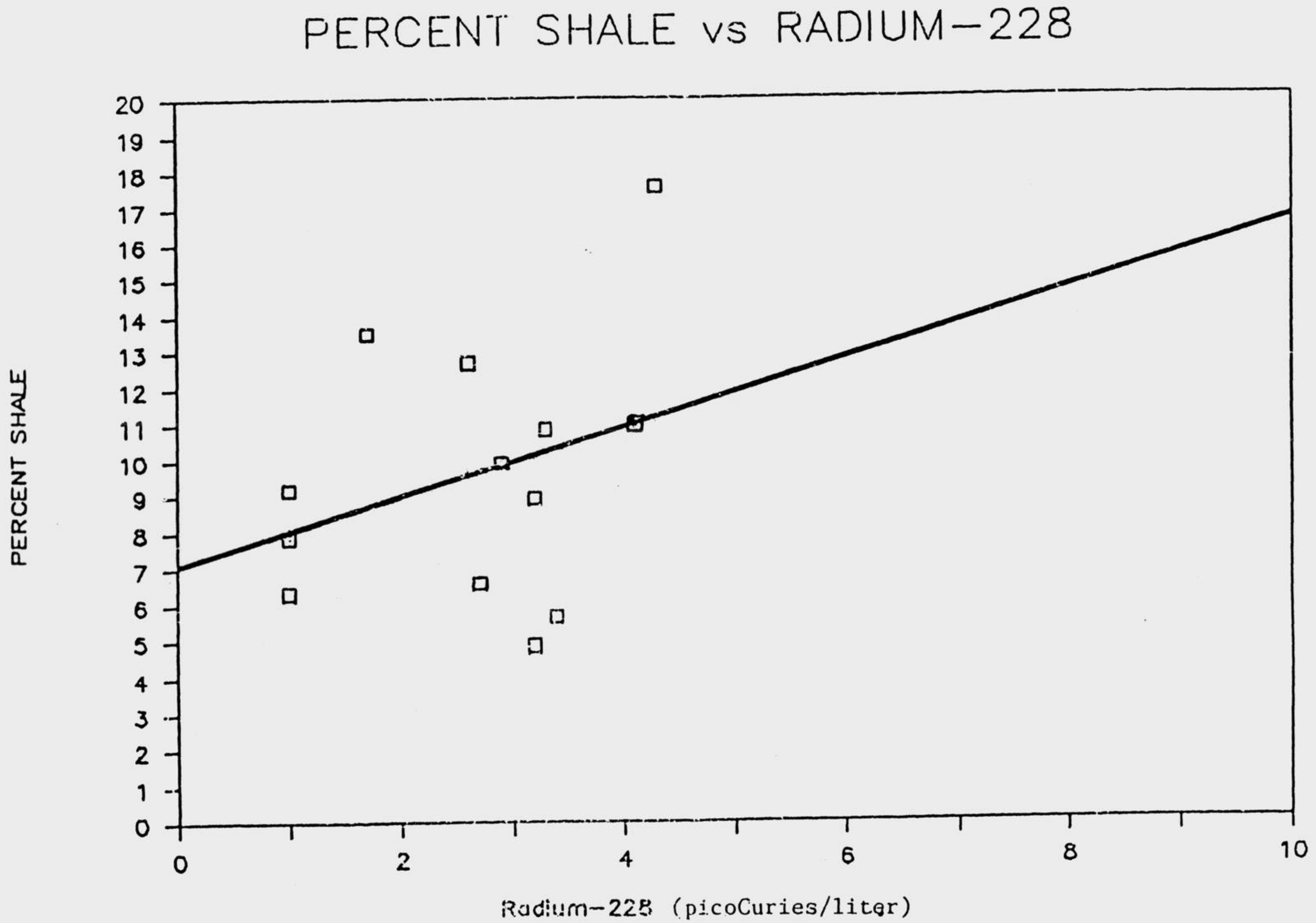

Figure 19. Radium-228 as a function of percent shale.

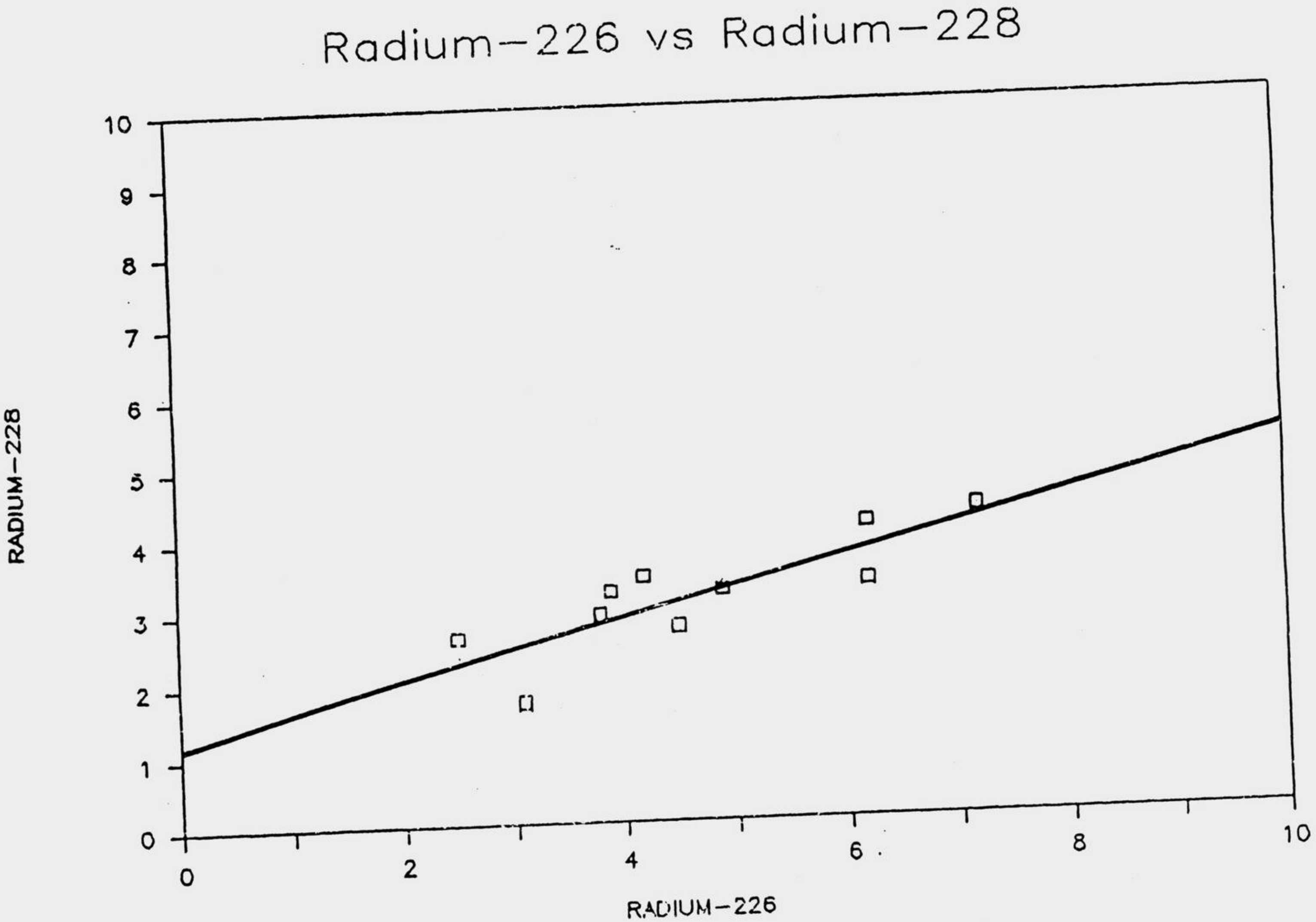

Figure 20. The relation of radium-226 to radium-228.

DETAILED WELL LOG ANALYSIS

DATABASE

The previous sections employed older natural gamma ray logs to determine the clay content of selected formations. While acceptable for this purpose, the availability of only a single curve, in presently unused units for natural gamma measurements, severely limits the potential for refined analysis. However, starting in late 1987 several water authorities approved the acquisition of full sets of modern logs for selected wells within their jurisdiction. Six of these complete log sets were available for this study. The locations of the six wells, North Fond du Lac (FDL), Mary Hill (MH), Imperial Estates (IE), Burleigh Road (BR), Park (PK), and Franklin (FR) are presented in Figure 21. The water quality and physical parameters of these wells are given in Table III.

Table III Radium isotope concentrations for wells with complete geophysical logs.

Well Site	Ra-226 (pCi/l)	Ra-228 (pCi/l)	Total	Well Depth(ft)	Casing Point(ft)
Mary Hill	4.0	4.0	8.0	910	275
North Fond du Lac	–	–	<1.0	750	160
Park Incorporated	4.1	2.6	6.8	1200	520
Imperial Estates	2.6	1.0	3.6	1740	590
Franklin No. #5	3.1	3.3	6.4	1605	530
Burleigh Road (before casing)	3.3	1.7	5.0	1600	570

Figure 21

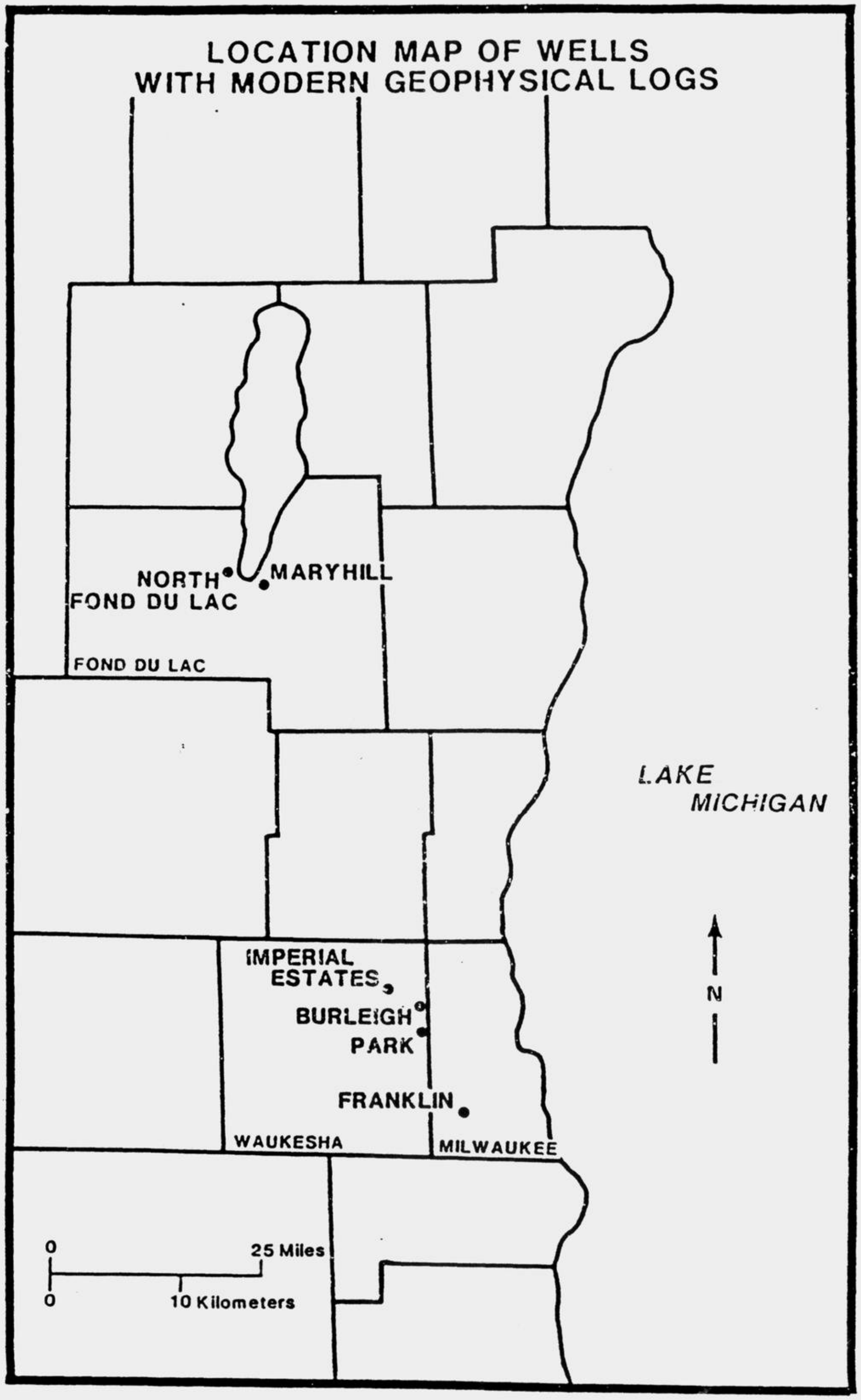
LOCATION MAP OF WELLS
WITH MODERN GEOPHYSICAL LOGS
NORTH
FOND DU LAC
MARYHILL
FOND DU LAC
LAKE
MICHIGAN
N
IMPERIAL
ESTATES
BURLEIGH
PARK
FRANKLIN
WAUKESHA
MILWAUKEE
0
25 Miles
0
10 Kilometers

For each of the wells defined in Figure 21 and Table III a dual indication log, density log, neutron log, and spectral gamma log were available. The dual indication log is a tool which measures formation resistivity. An example of the display associated with this log is provided in Figure 22. The density log uses an active source of gamma ray emission to determine bulk density. The neutron log employs an active source of neutrons to directly measure hydrogen density. The output of this tool is porosity calculated from the assumption that all hydrogen is associated with pore water. The density and neutron logs are normally run together and an example of this combined output is provided in Figure 23. The spectral gamma log utilized the measurement of natural gamma ray emission in discrete energy windows to determine the potassium, uranium and thorium content of rocks exposed within the borehole. An example of the display associated with this log is presented in Figure 24. The technology associated with the application and interpretation of these logs is discussed by Doveton (1986), Wylie (1984), Hallenburg (1984) and Hilchie (1982).

All of the log curves were hand digitized on a conventional digitizing table. The resulting digital data provided the data-base for this portion of the study. The six wells considered here did not result from a master plan but rather became available through an almost random selection. Despite this unplanned selection the six provide a unique data base which probably could not have been better selected.

The Park and Imperial Estates wells are both southern wells separated by about 6 miles. The Park well is in excess of the 5.0 pCi/l standard, while the Imperial Estates well is within compliance (Table III). Aside from variations in the thickness of sandstone layers within the formation, the logs are quite similar. Figure 25 compares the gamma ray response of the Eau

Figure 22

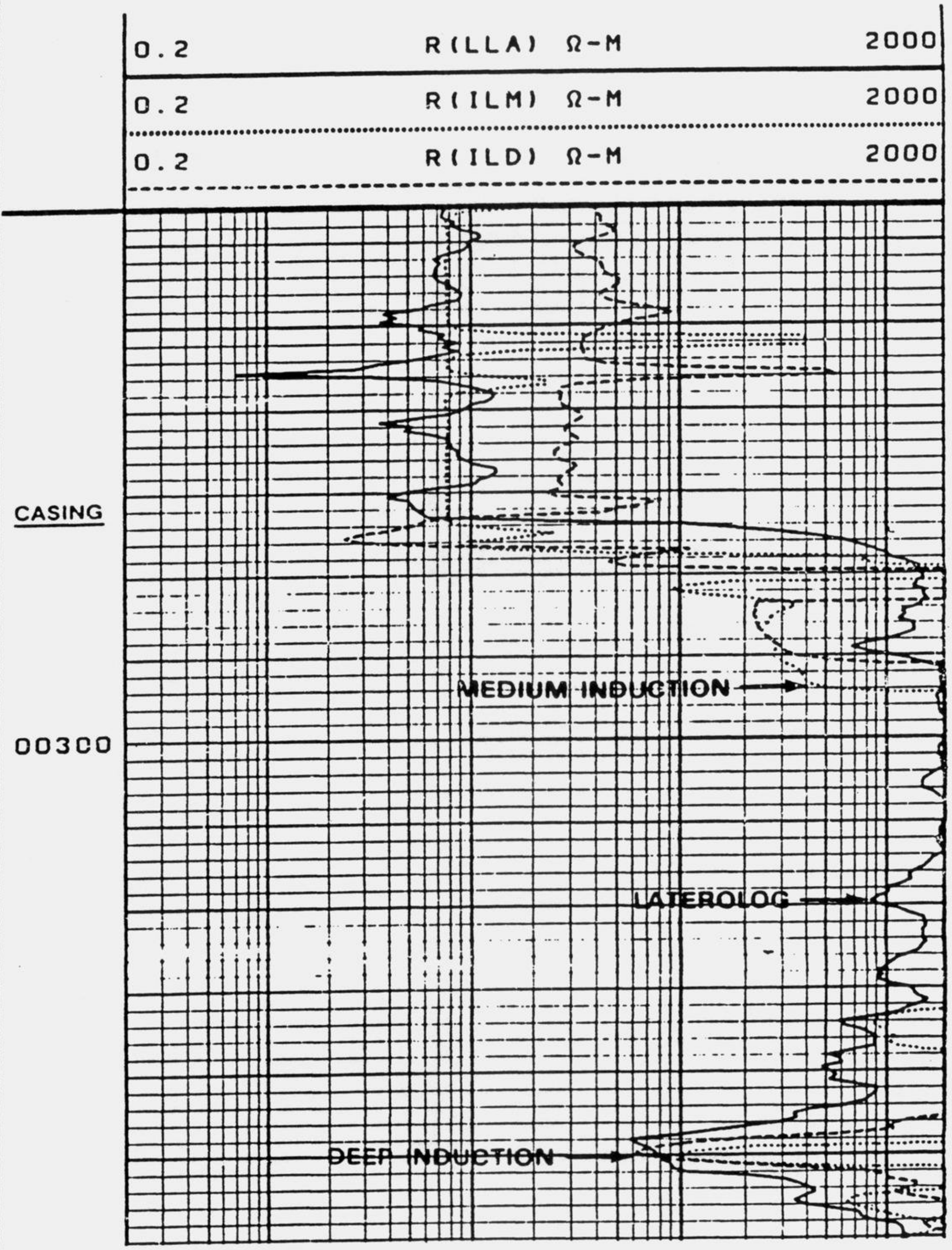

DUAL INDUCTION LATERLOG PRESENTATION

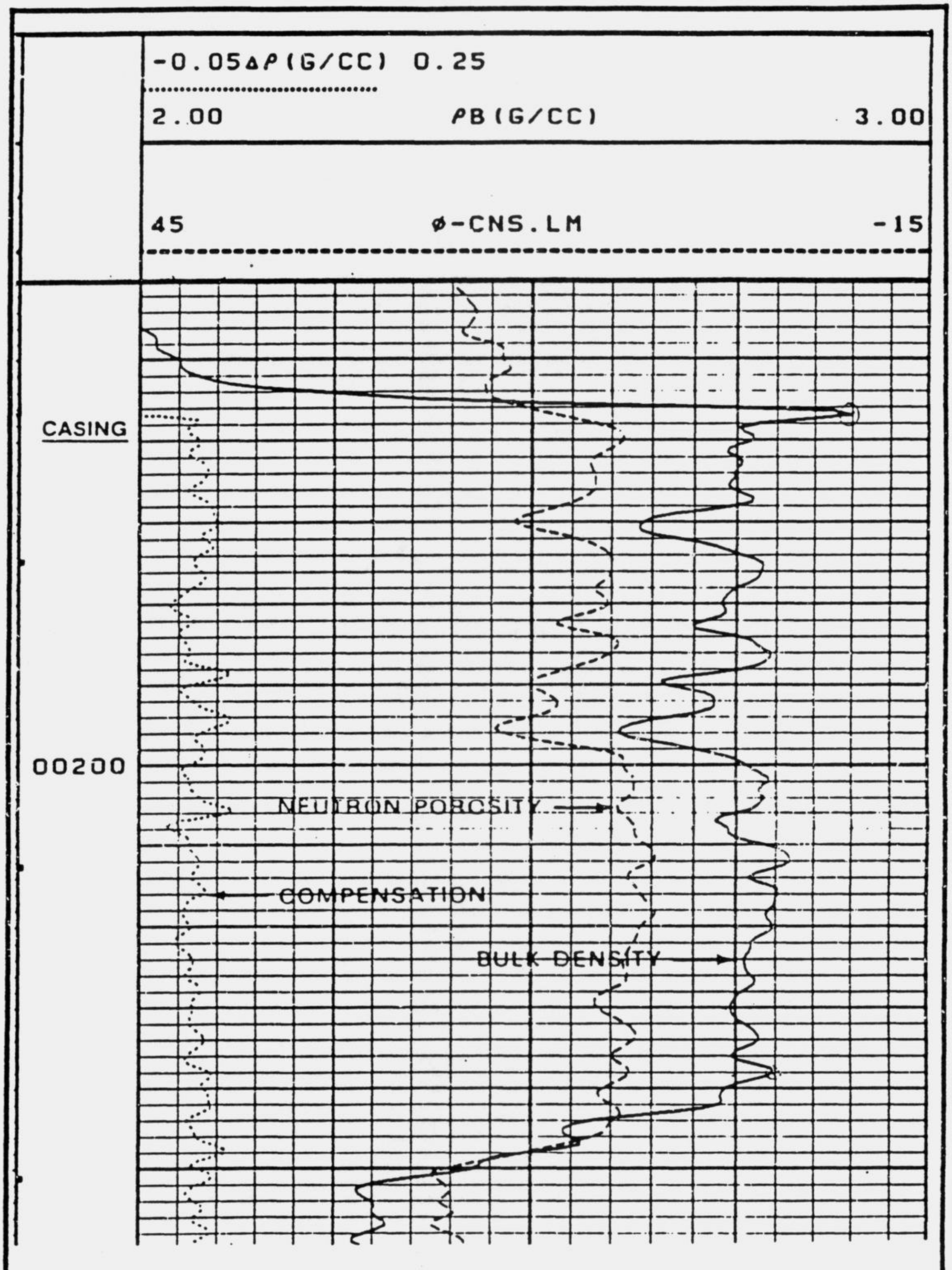

Figure 23

BULK DENSITY AND NEUTRON POROSITY LOG

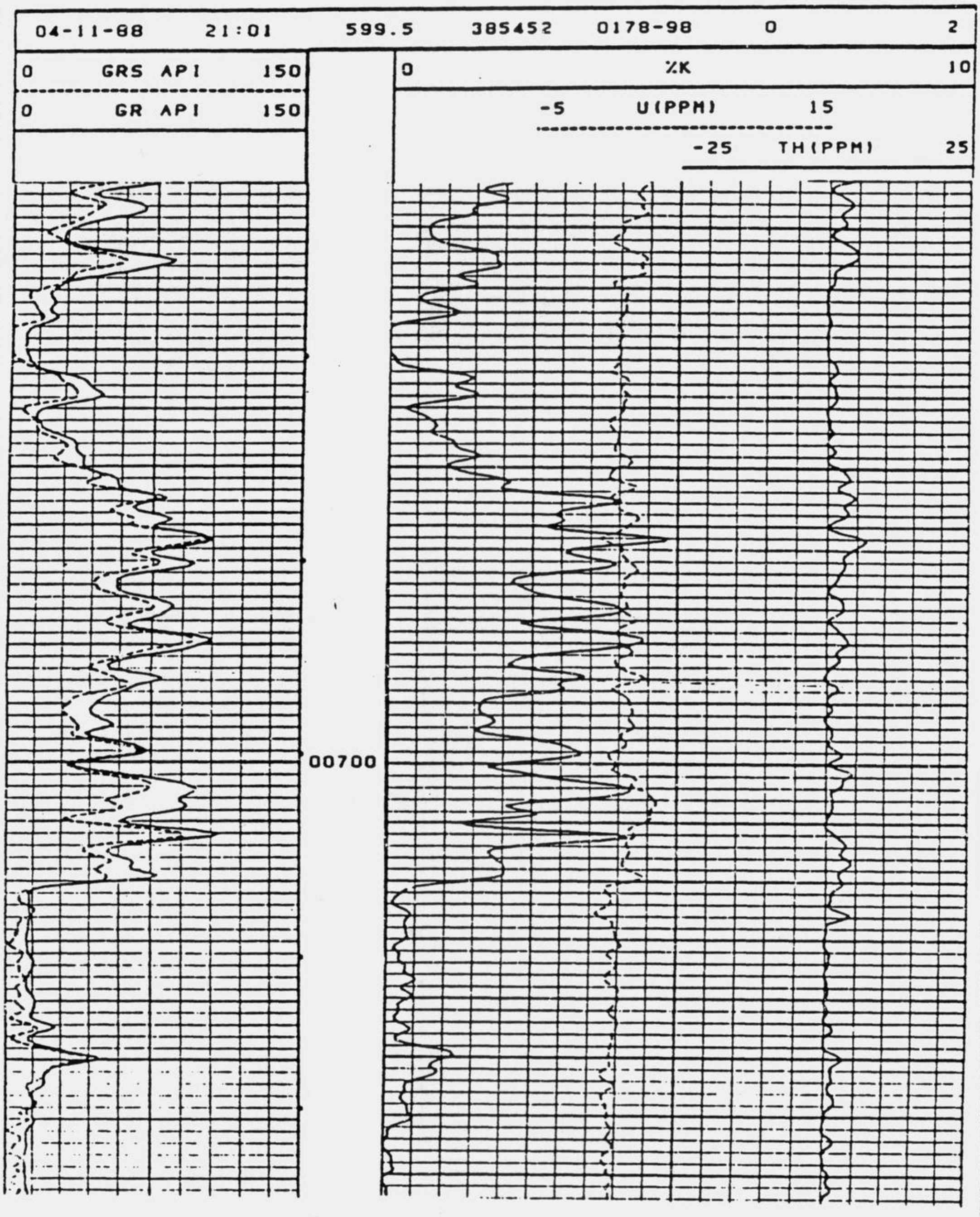

Figure 24

TYPICAL SPECTRAL GAMMA RAY LOG

Figure 25

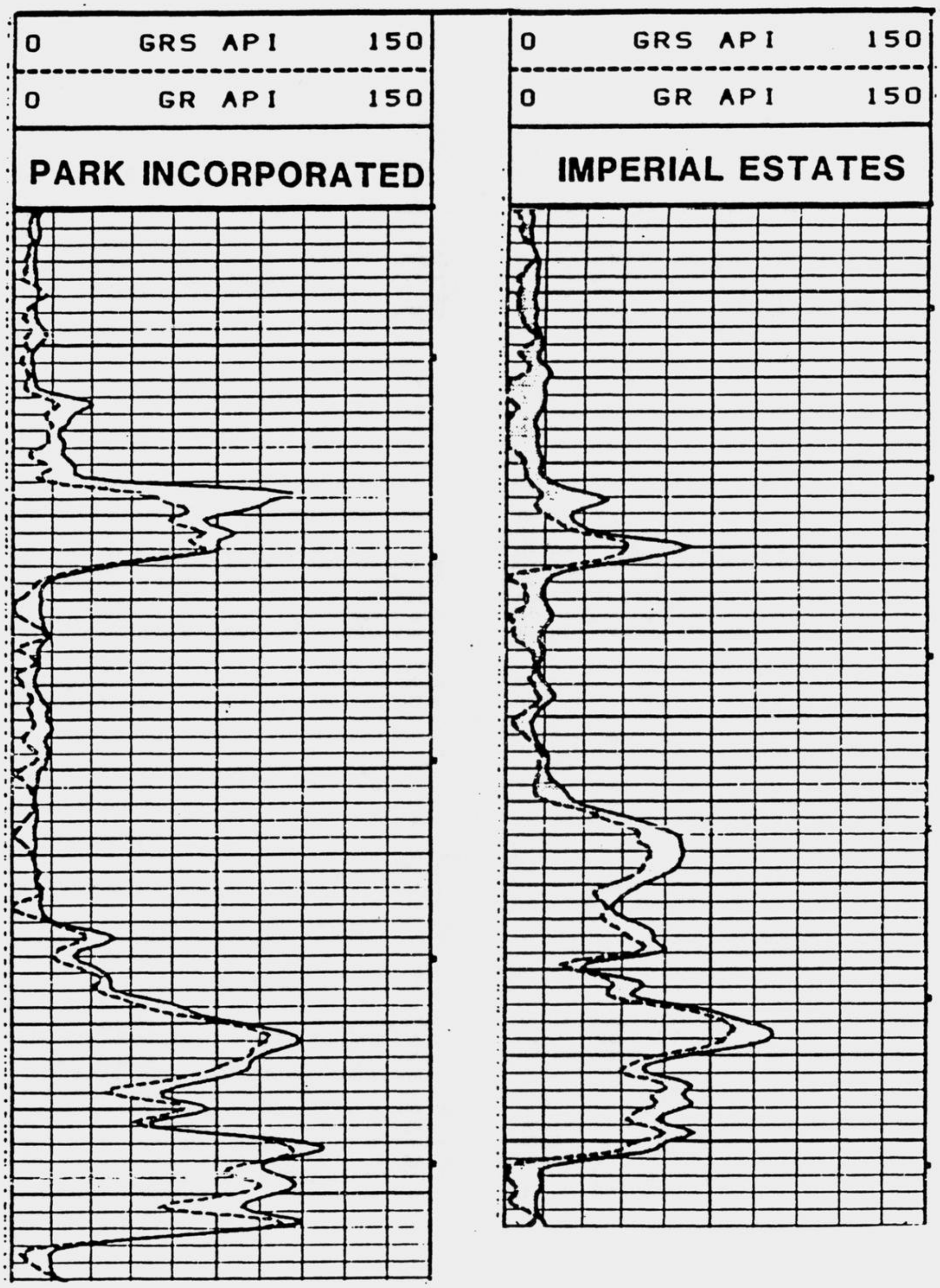

SPECTRAL GAMMA RAY LOG FOR
PARK AND IMPERIAL ESTATES
IN THE EAU CLAIRE SANDSTONE

Claire sandstone for these two wells. The Eau Claire was selected because of its distinguishable gamma response. There is an initial spike located at the top of the Eau Claire in each well. The magnitude of that peak at the Park well is 105 API units compared to 68 API units at Imperial Estates. This spike is followed down hole by a clean sand layer that is 50 feet thick at the Park well and 28 feet thick at the Imperial Estates well. This clean sand is then followed by a shaley sandstone unit that is 20 feet thick at the Park site and 40 feet thick at the Imperial Estates site.

Mary Hill and North Fond du Lac are northern wells separated by 5 miles. The Mary Hill water is above the standard while FDL is way below (Table III). Figure 26 compares the gamma ray responses in the Eau Claire sandstone. The uppermost portion of each site is interfingered with shale lenses or seams. This zone is about 28 feet thick at Mary Hill and has a maximum response of 112 API units. The North Fond du Lac upper section is about 45 feet thick with a maximum gamma response of 135 API units. Downhole from this shaley zone is a cleaner sandstone layer that is approximately 20 feet thick at both well sites. Continuing downhole, each wellsite has a shaley sandstone layer at the base of the Eau Claire formation. This layer is about 60 feet thick at Mary Hill with a maximum gamma response of 105 API units as compared to a 45 foot thick layer at North Fond du Lac with a maximum response of about 85 API units.

The Franklin and Burleigh Road wells, separated by a distance of 14 miles are an interesting and unique set. Figure 27A compares the gamma ray responses of the Eau Claire sandstone at each well Site. The uppermost portion of each log contains a shaley layer that is about 55 feet thick at both sites. The maximum response at Franklin is approximately 115 API units compared to 90 API units at Burleigh Road. Beneath this layer, the Eau Claire

Figure 26

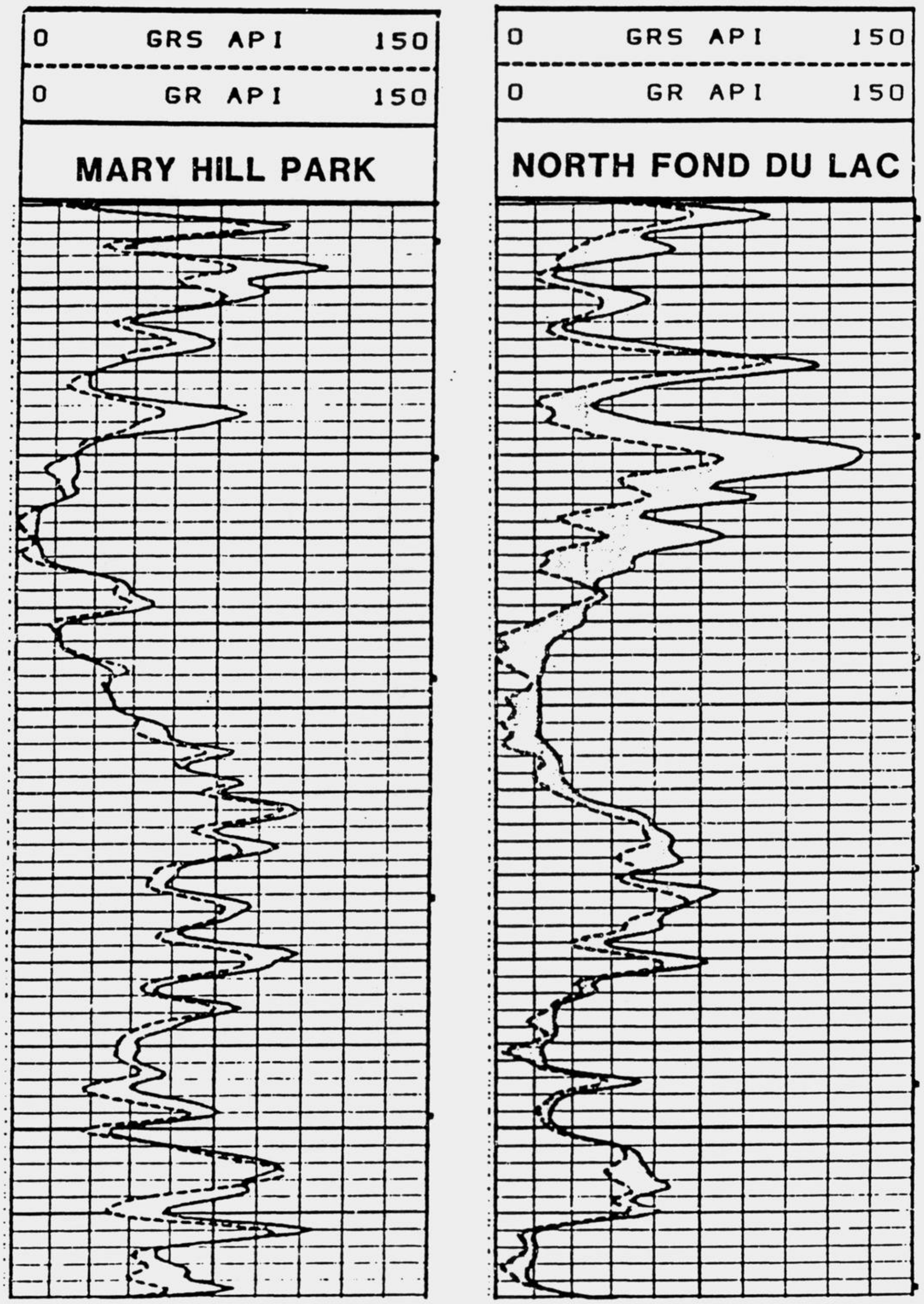

SPECTRAL GAMMA RAY LOG FOR
MARY HILL AND NORTH FOND DU LAC
IN THE EAU CLAIRE SANDSTONE

Figure 27A

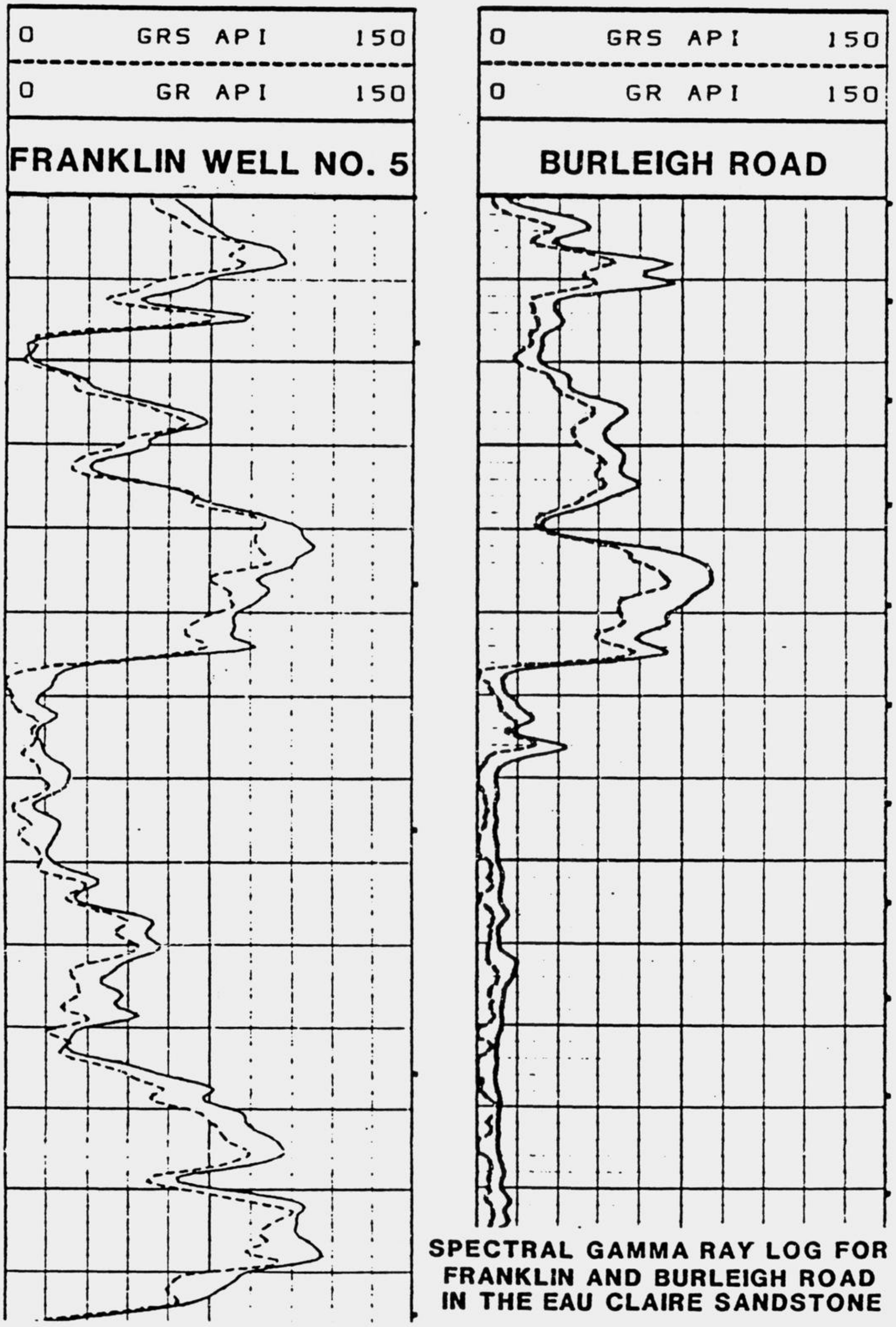

SPECTRAL GAMMA RAY LOG FOR FRANKLIN AND BURLEIGH ROAD IN THE EAU CLAIRE SANDSTONE

sandstone is clean at the Burleigh Road site. The Franklin well shows only 50 feet of clean sandstone until a second shaley layer is reached. Despite the obvious differences in the gamma ray responses for each well site, the total radium levels in produced water are remarkably similar. The uniqueness of these wells is that both were cased over the entire Eau Claire interval but the casing reduced the total radium concentration in only the Burleigh Road well.

The figures and discussions presented above have been limited to the Eau Claire section of each well. This limitation is necessary here because there is no way to present the full logs. Based on either the Eau Claire discussion presented here on the full log analysis, the six wells provide the following test cases:

1. Two northern wells, MH and FDL, with very similar lithology but totally different radium contents in the produced water.
2. Two southern wells, IE and BR, with nearly identical lithology but completely different radium content in the produced water.
3. Two southern wells, BR and FR, with somewhat different lithologies but nearly equivalent water.
4. Two wells, BR and FR, which were both selectively cased with apparently different degrees of success.

THE RADIUM CONTENT OF PRODUCED WATER AND BOREHOLE RADIONUCLIDES

Using the spectral gamma logs the average uranium and thorium content of each borehole was calculated. These results are presented in Table IV along with the radium content of the produced water.

Table IV Average uranium and thorium concentrations for wells with complete geophysical logs.

Well Site	U (ppm)	Th (ppm)	Ra-226 (pC/l)	Ra-228 (pC/l)
Mary Hill	2.0	1.6	4.0	4.0
North Fond du Lac	0.9	0.8	<1.3	<1.3
Park	0.8	0.9	4.1	2.7
Imperial	0.9	0.6	2.6	1.0
Franklin	1.3	0.7	3.1	3.3
Burleigh Rd.	0.8	0.9	3.3	1.7

Based on the data of Table IV there is no clear relationship between the radiometric water quality and the average radiometric content of the wellbore. However, there are correlations within the wellbore and within the waters.

A comparison of the average thorium and average uranium content of wellbore rocks is presented in Figure 27B. The correlation coefficient of these data is 0.91 indicating a very strong coupling of these two elements within the formations of the wellbore. However, it will be demonstrated that they are not strongly coupled at any particular depth. The thorium to uranium

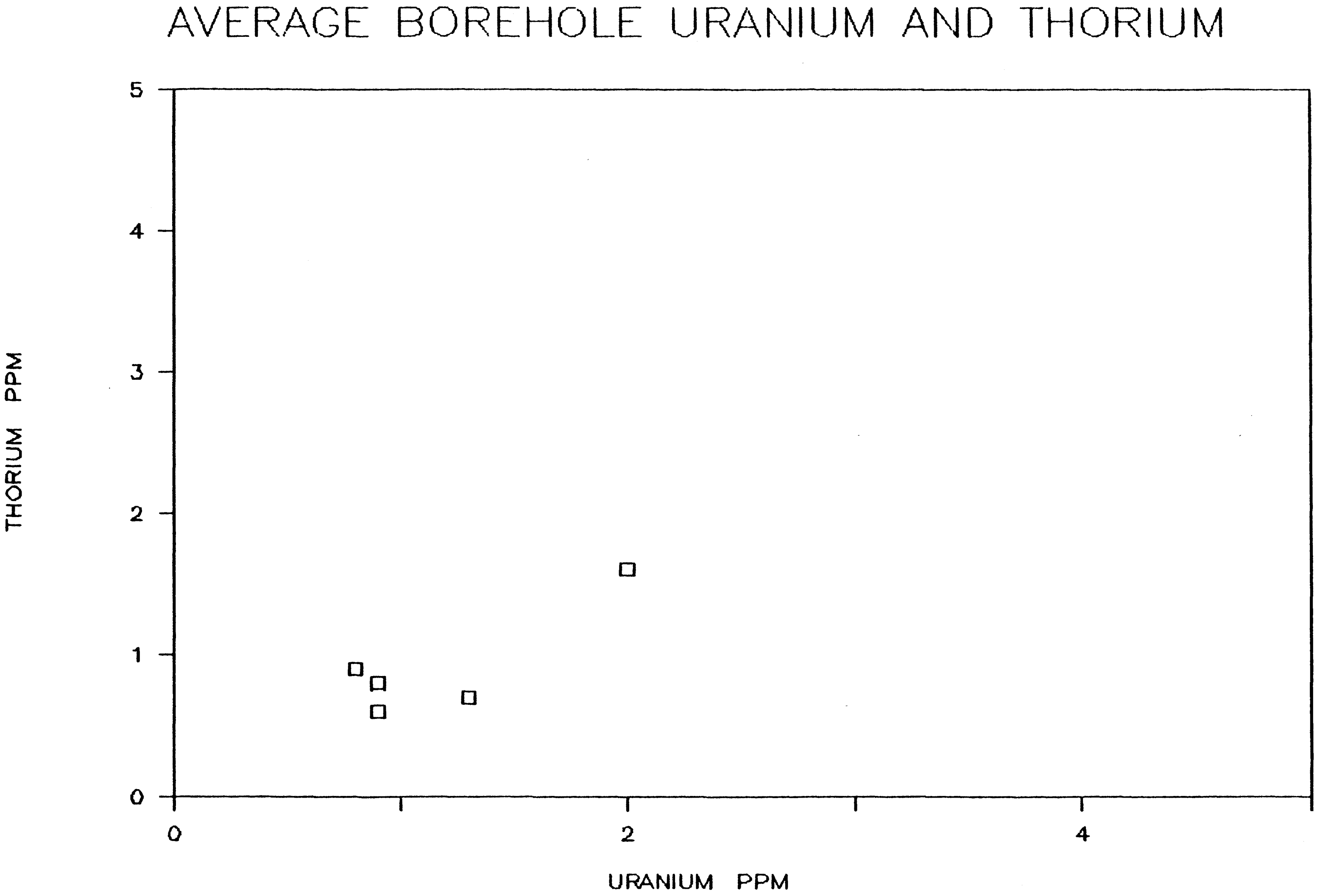

Figure 27B. Average borehole uranium and thorium.

ratio calculated from the average elemental values is 1.0 with a standard deviation of 0.2.

The observed levels of radium-226 and radium-228 in the produced water are not as strongly correlated as are the average borehole values of uranium and thorium. The levels of radium-228 and radium-226 observed in the produced water are compared in Figure 28. The correlation coefficient of these data is 0.77.

Thorium-232 is the immediate parent of radium-228 which has a half-life of 6 years (Table II). Given this short half-life the source of any radium-228 in the produced water must be very near with wellbore. Hence, the radium-228 content of water should be strongly determined by the thorium content of wellbore rocks. The validity of this physical argument is clearly demonstrated by Figure 29 which compares available thorium within the wellbore to radium 228 in the produced water. The correlation coefficient of these data is 0.93. Available thorium is defined as the average thorium level multiplied by the total length of open wellbore. This figure clearly demonstrates that the radium-228 content of produced water is entirely determined by the thorium content of wellbore formations. Thus, maps of formation thorium content could be used to site well with ensured low-levels of radium-228 in the produced water. Unfortunately, the creation of such maps would require a greatly expanded database of spectral gamma logs.

The half-life of radium-226 is 1600 years, Table I, and with a half-life this long migration away from the parent element uranium 235 is entirely possible. Thus, it cannot be argued that the source for the radium-226 must be near the wellbore. Figure 30 compares available source uranium, previously defined, with the radium-226 content of produced waters. The correlation coefficient of these data is 0.37 which appears to indicate that the uranium content of

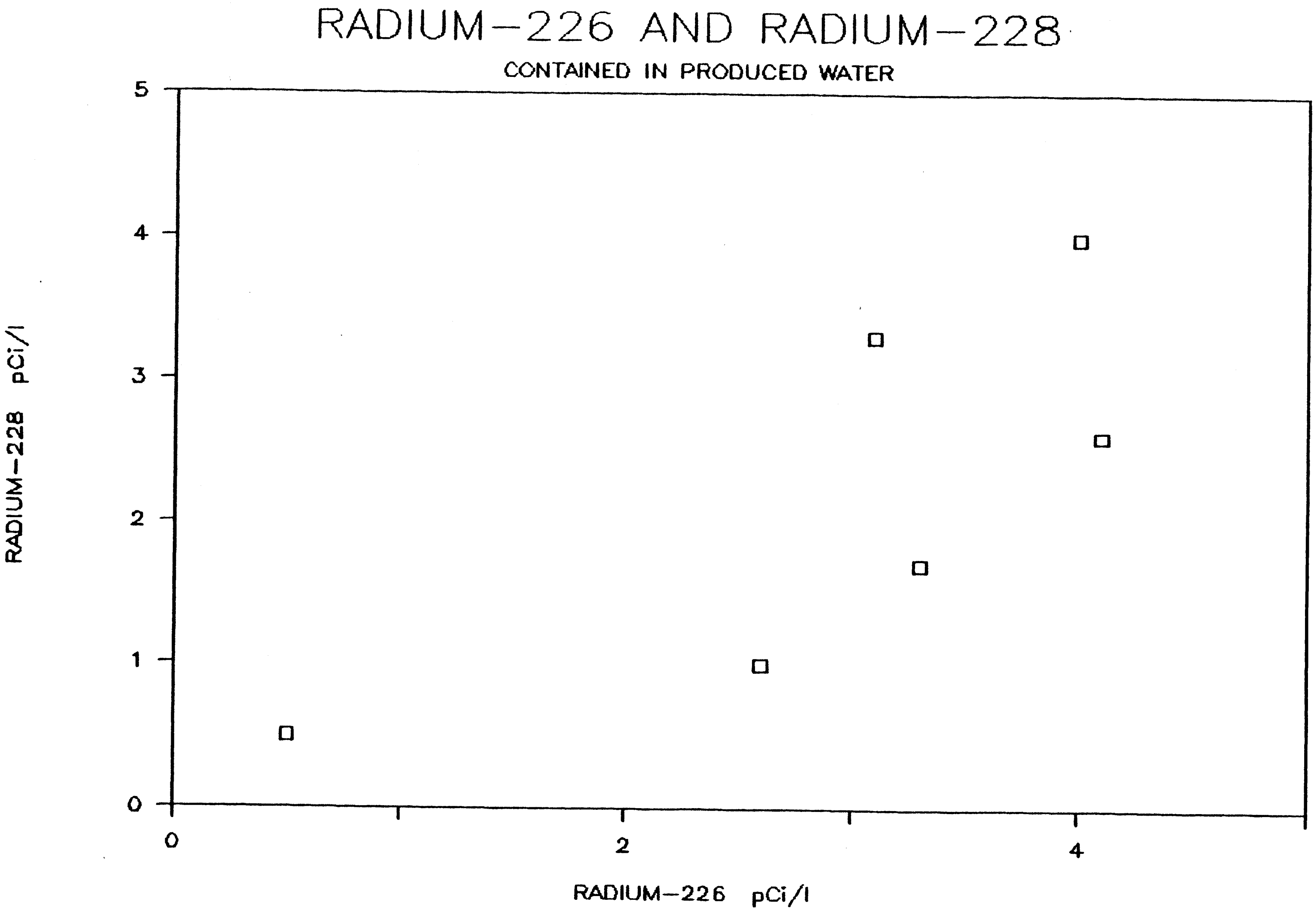

Figure 28. Radium-226 and radium-228 in produced water.

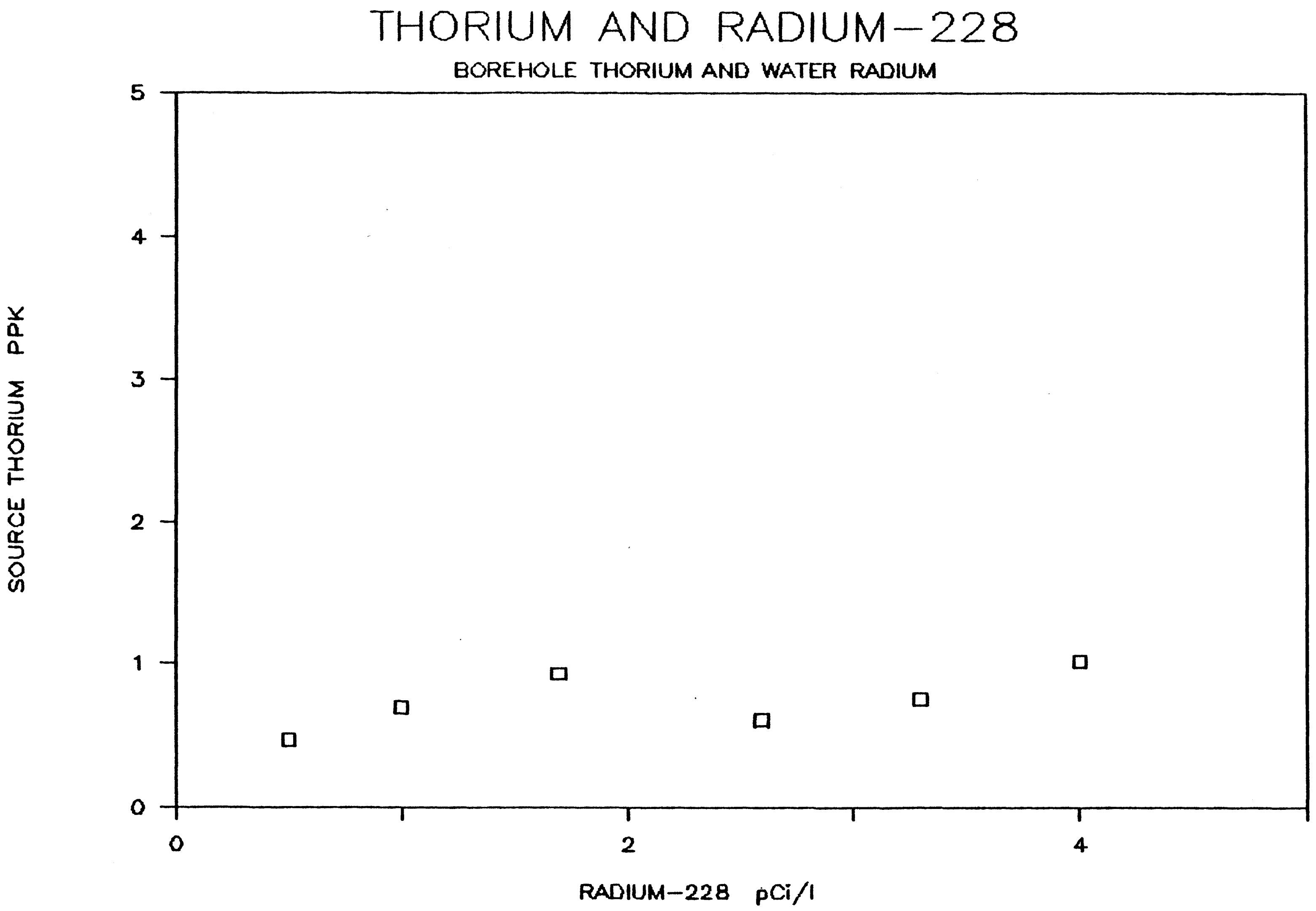

Figure 29. Borehole thorium and radium-228 in produced water.

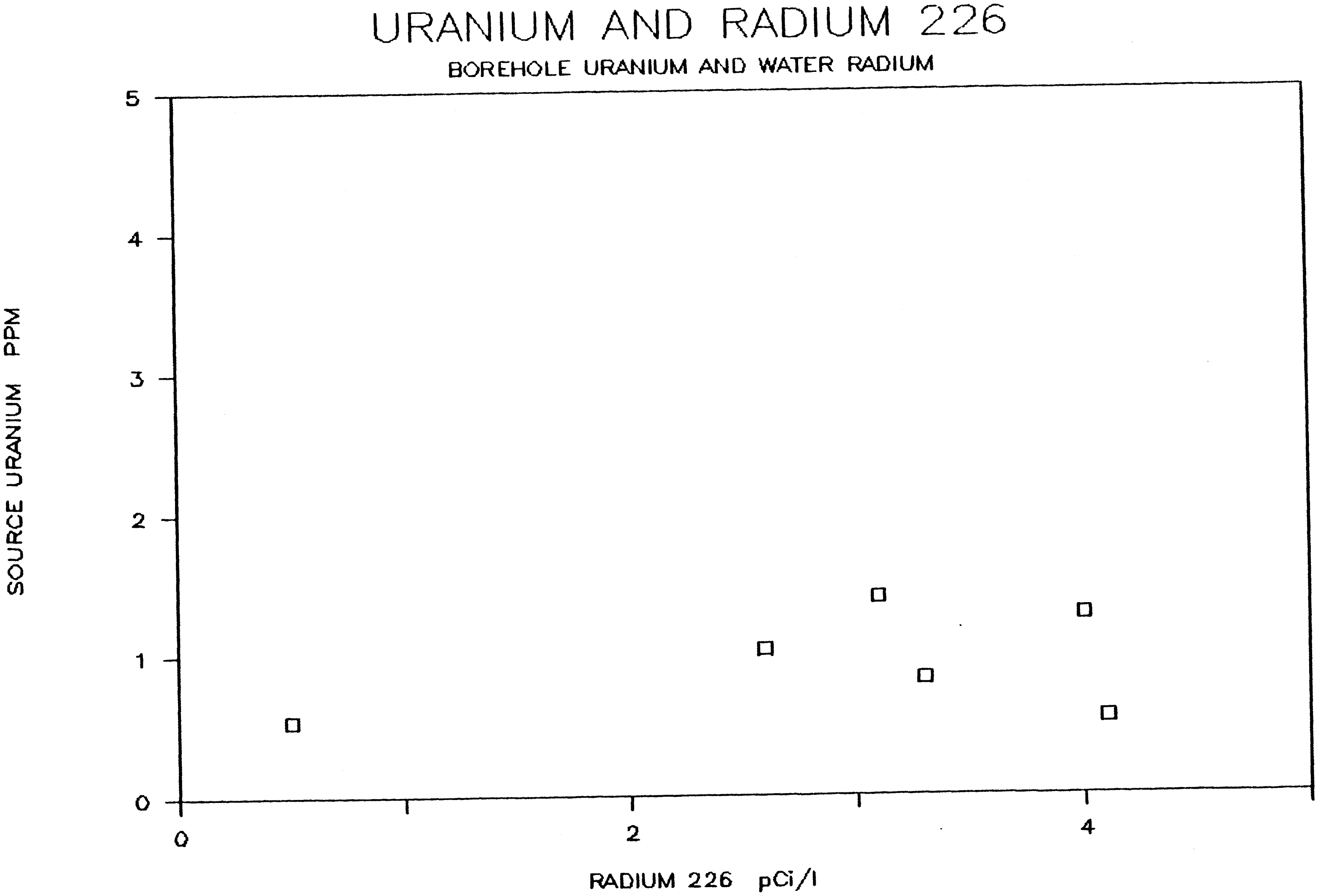

Figure 30. Borehole uranium and radium-228 in produced water.

wellbore rocks does not determine the radium-226 content of the water. It should be noted, however, that if one well, Parks, is removed from this data set, the correlation coefficient increases to 0.77 indicating the uranium content of the wellbore is a significant factor in determining the radium-226 levels in produced water. In the opinion of the author, the Park well should be discounted and the conclusion drawn that the borehole content of uranium is a significant factor in determining the radium-226 content of the produced water. However, the relationship is not as strong as the relationship between thorium and radium-228, which indicates that radium migration may be a factor.

BOREHOLE DISTRIBUTION OF URANIUM AND THORIUM

The potassium content of the rocks at any particular depth is a measure of the shale content of these rocks. The correlation of potassium with uranium for each borehole, Table V, demonstrates that the uranium is not strongly associated with clay minerals but is distributed throughout the borehole rather independently of the presence of shale. An exception to this rule is provided by the Burleigh Road well where the presence of uranium is linked to the presence of shale. Given this exception however, Table V demonstrates that mapping shale percentages could not be used to imply uranium content.

The presence of thorium within the borehole is generally coupled to the presence of shale, Table V. The single exception to this coupling is provided by the Franklin well. The fairly high correlation of thorium with shale and much lower correlation of uranium with shale requires

TABLE V The correlation of potassium, thorium and uranium within selected boreholes.

Well Name	Correlation Coefficients K - U	K - Th	U - Th
Parks	0.31	0.60	0.20
Burleigh	0.67	0.60	0.52
Imperial	0.41	0.55	0.10
North Fond du Lac	0.23	0.54	0.17
Franklin	0.20	0.34	0.17

a difference in the spatial location of the two elements. This spatial difference is clearly demonstrated by the correlation between uranium and thorium, Table V. With the exception of the Burleigh Road well, there is very little correlation between uranium and thorium. This is rather strange in view of Figure 29 which defines a very high correlation, .91, between average borehole thorium and average borehole uranium. The physical mechanism necessary to produce uncorrelated depth distributions with highly correlated averages is unclear.

THE COMPARISON OF WELL LOGS

It was previously noted that the six wells for which complete geophysical logs were available provided an interesting data set in that the logs appeared similar and yet the radiometric quality of produced waters were significantly different. Figure 31 displays the thorium content of the Mary Hill borehole as a function of bulk density. The bulk density axis may be taken as a lithology axis with densities above 2.7 representing the dolomite section and densities less than 2.5 representing the sandstone section. For the Mary Hill well approximately one half of the total thorium is contained within the carbonate section. This differs significantly from the North Fond du Lac well, Figure 32, where the thorium is primarily associated with low density, high porosity, sandstone. Uranium within the Mary Hill wellbore is also at high levels within the dolomite section, Figure 33, while the uranium in the Fond du Lac well is again associated with high porosity sandstone, Figure 34. These figures combined with the water quality data of Table IV suggest that the carbonate section may be a factor in determining the observed levels of radium-226 and radium-228.

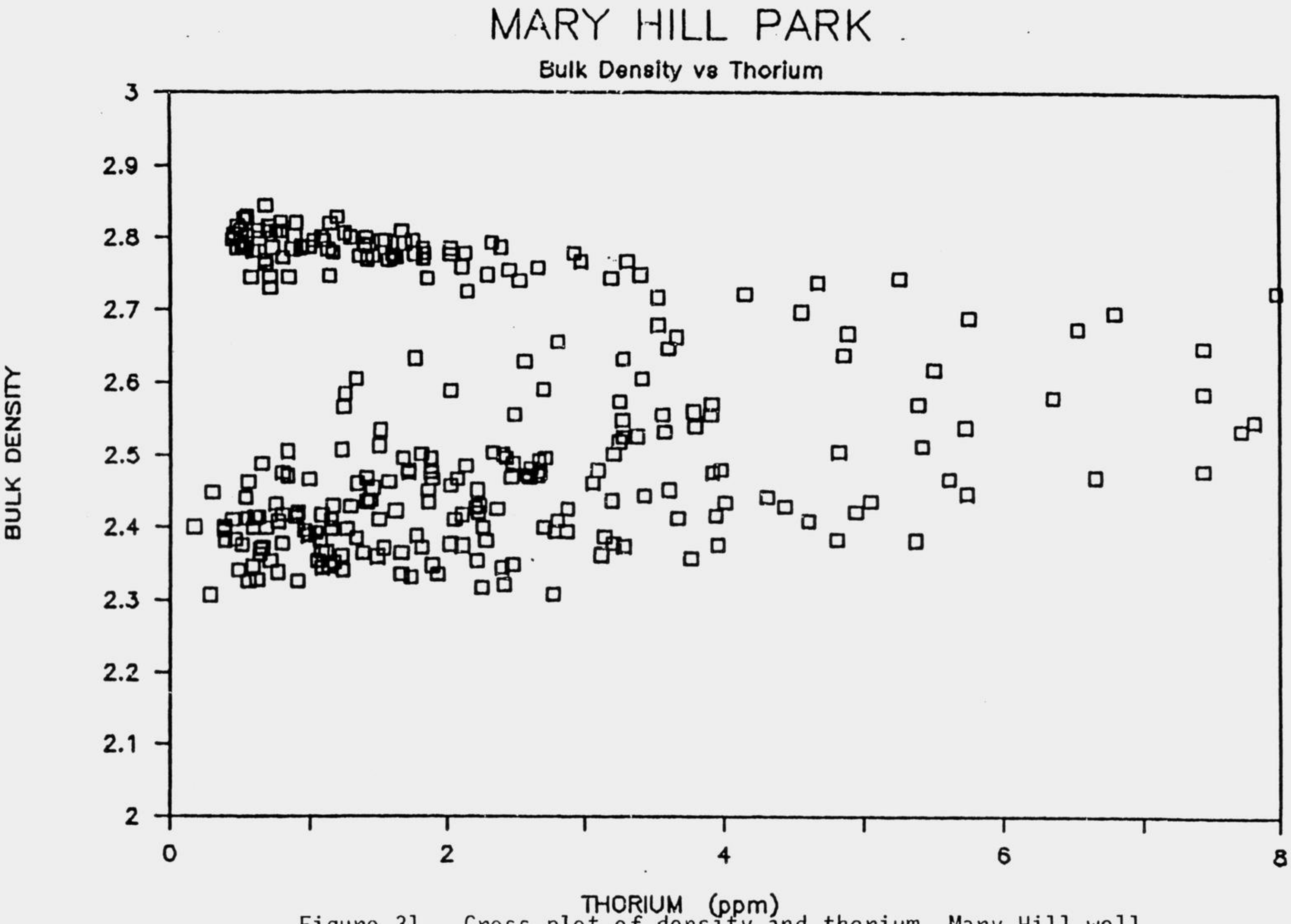

Figure 31. Cross plot of density and thorium, Mary Hill well.

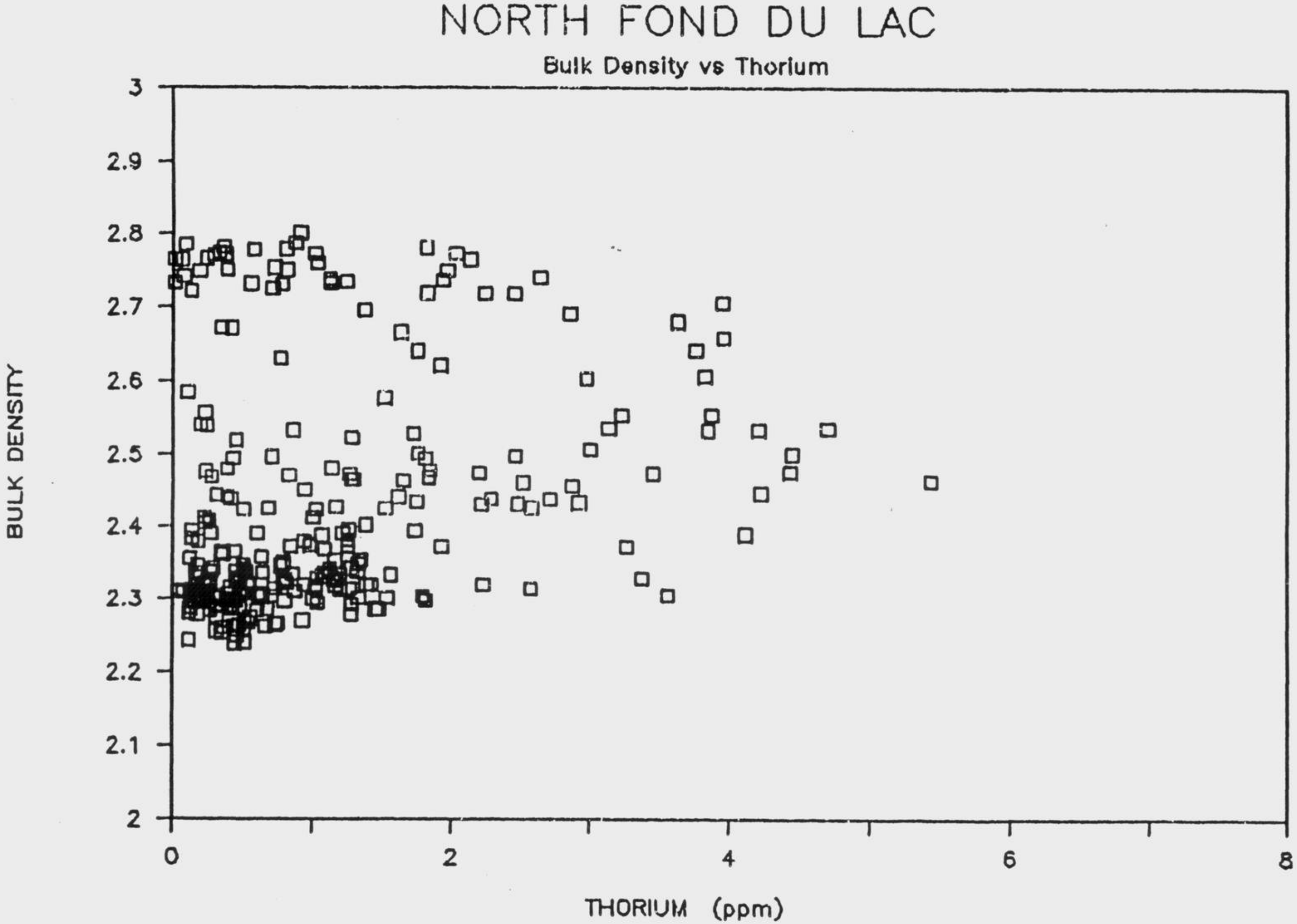

Figure 32. Cross plot of density and thorium, North Fond du Lac well.

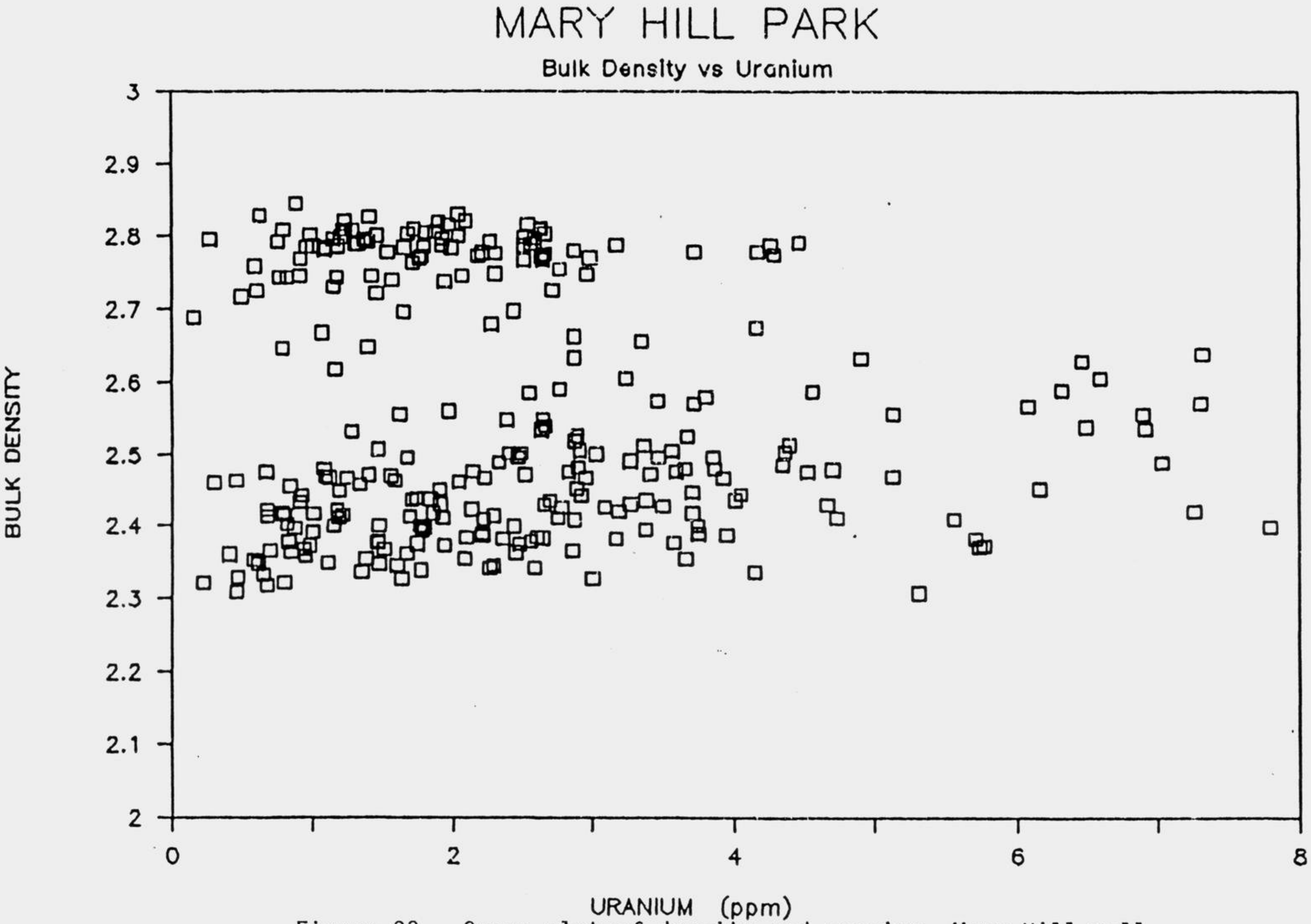

Figure 33. Cross plot of density and uranium, Mary Hill well.

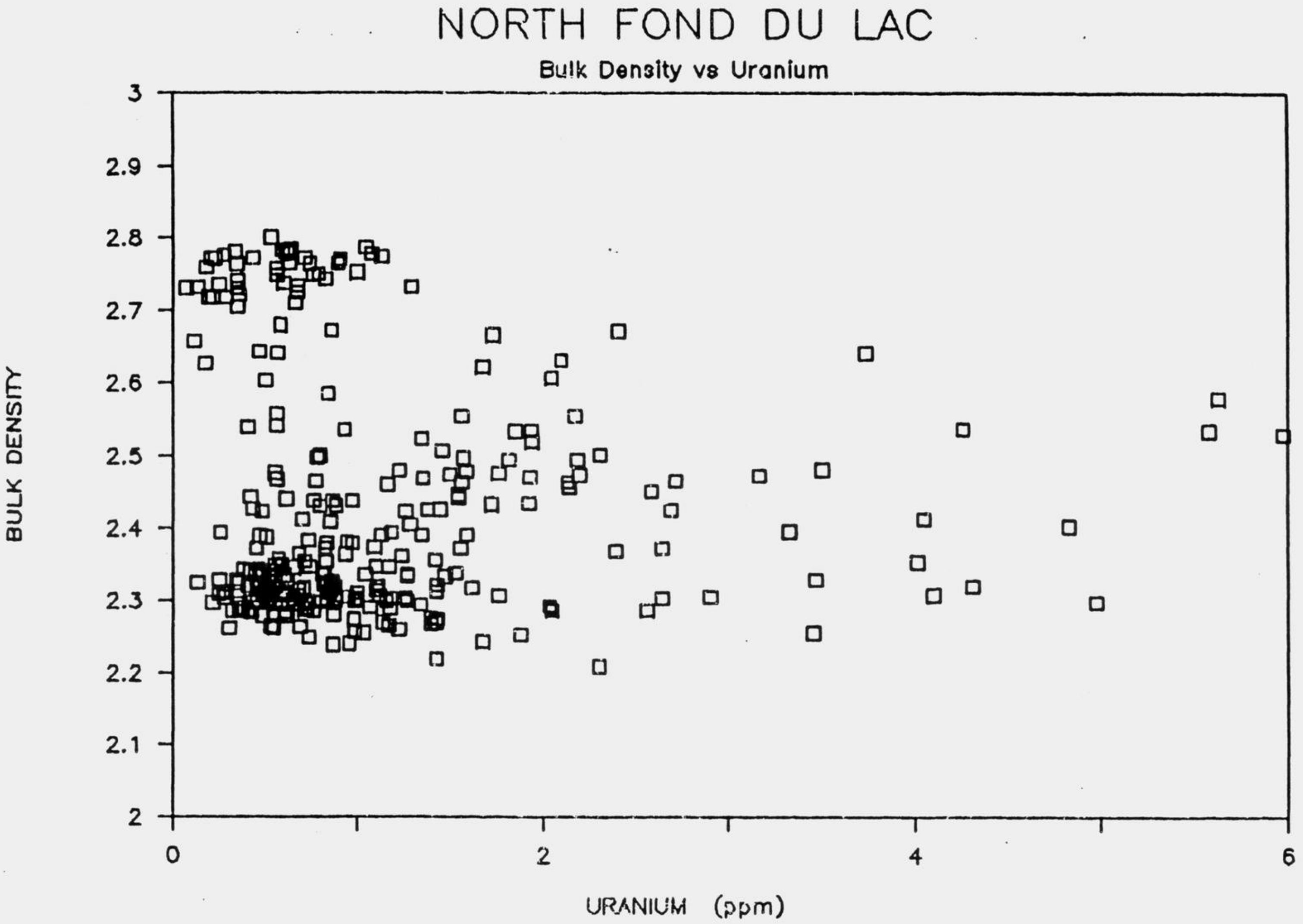

Figure 34. Cross plot of density and uranium, North Fond du Lac well.

The relationship of thorium to lithology for the Park well is presented in Figure 35. Approximately, one half of the thorium within the wellbore is again associated with the carbonate section. This differs somewhat from the Imperial Estate well wherein the majority of thorium is associated with the sandstone section, Figure 36. However, the Imperial Estate well does show an association of approximately one quarter of the thorium associated with the dolomite section although generally at levels less than 1ppm. The uranium within the two wellbore formations exhibits a similar distribution.

Uranium within the Park well is evenly distributed between the dolomite and sandstone sections, Figure 37, while uranium within the Imperial Estate well, Figure 38A, is biased towards the sandstone section. Combining these figures with the water quality data of Table IV again suggest that the carbonate section plays a significant role in determining the radium levels of the produced water.

The relationship of thorium to lithology for the Franklin well is presented in Figure 38B and for the Burleigh Road well in Figure 39. The Franklin well contains higher amounts of thorium within the dolomite and sandstone sections. The uranium distribution within the two wellbores, Figures 40 and 41, is again biased towards higher uranium values in both the sandstone and dolomite sections of the Franklin well. Combining the thorium results, Figures 38B and 39, with the water quality data of Table IV again suggest the Carbonate section as a major source of radium-228 although, in this case, the sandstone section may also be a significant source.

To quantitatively estimate the role of each formation in determining the resulting radiometric water quality, a formation figure of merit was defined for radium-226, FM 226, and for radium-228, FM 228, as,

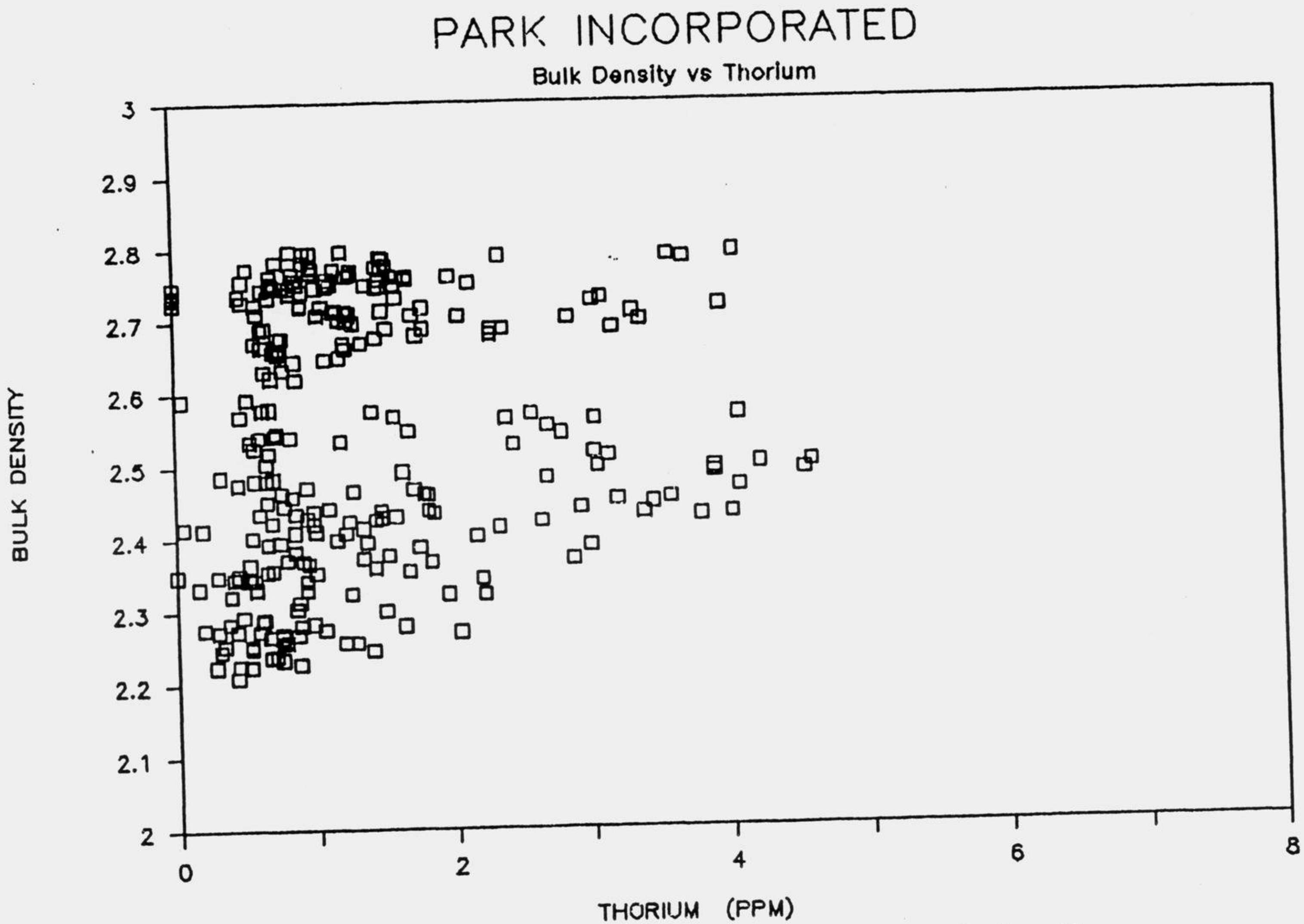

Figure 35. Cross plot of density and thorium, Park well.

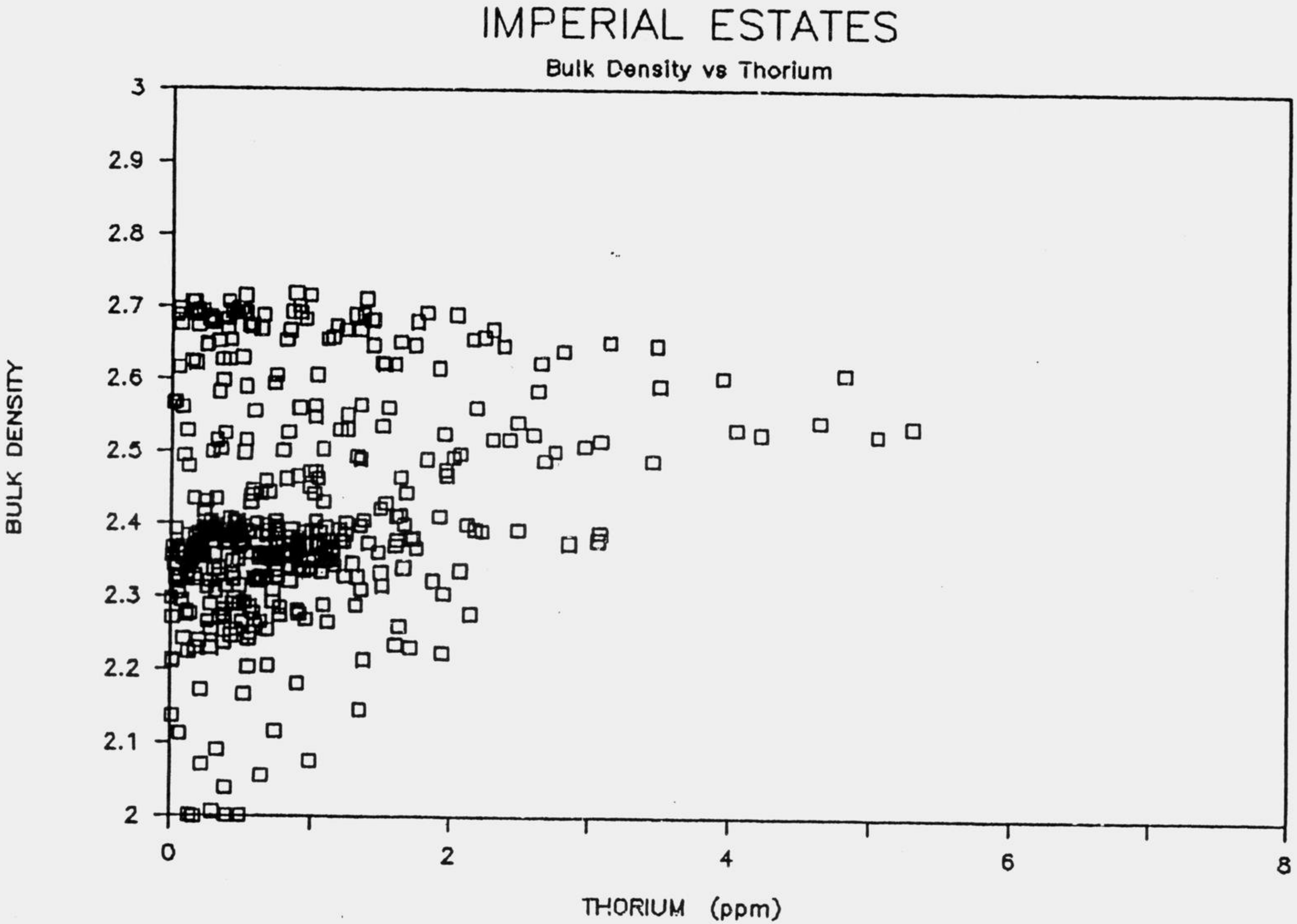

Figure 36. Cross plot of density and thorium, Imperial Estates well.

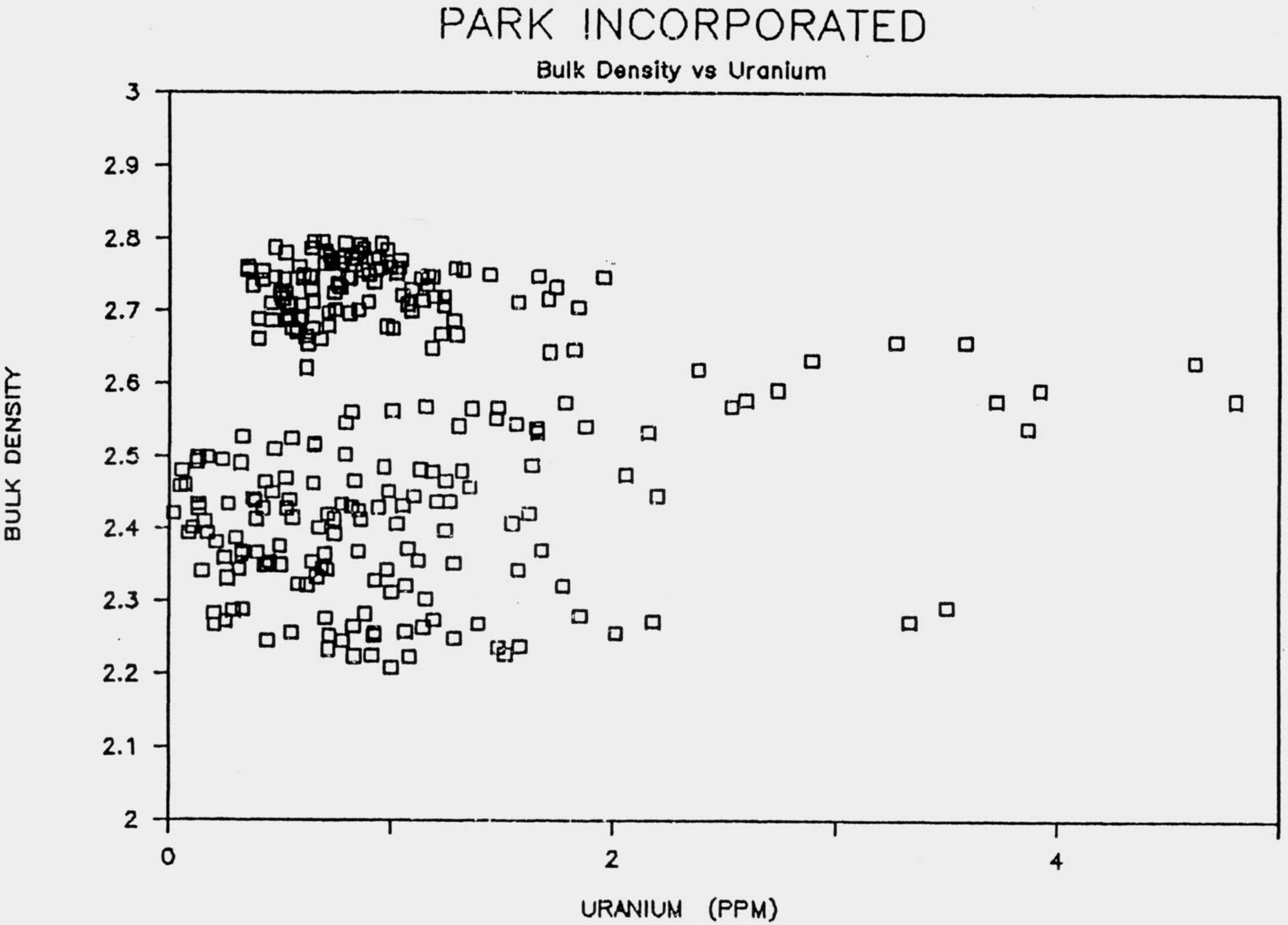

Figure 37. Cross plot of density and uranium, Park well.

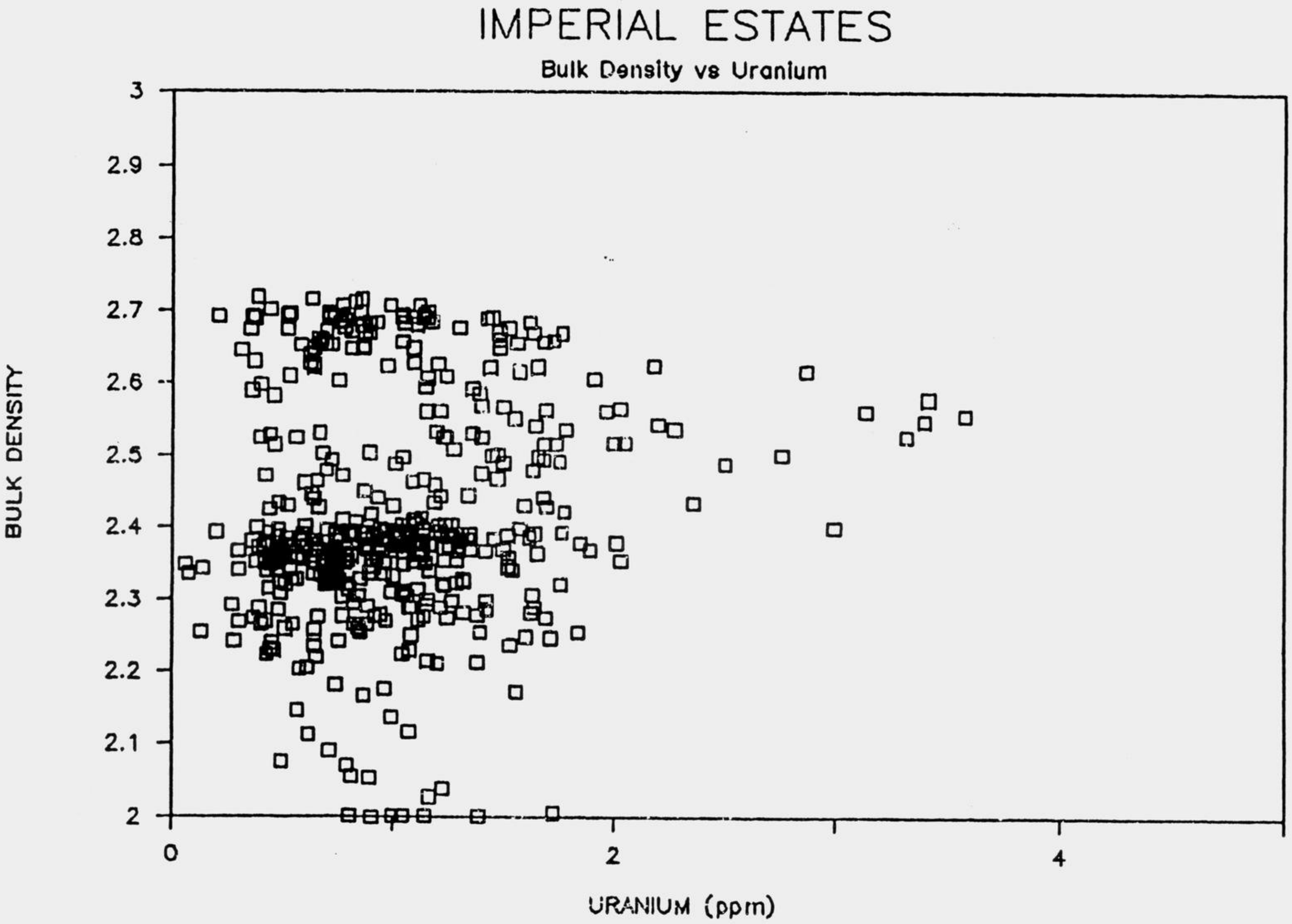

Figure 38A. Cross plot of density and uranium, Imperial Estates well.

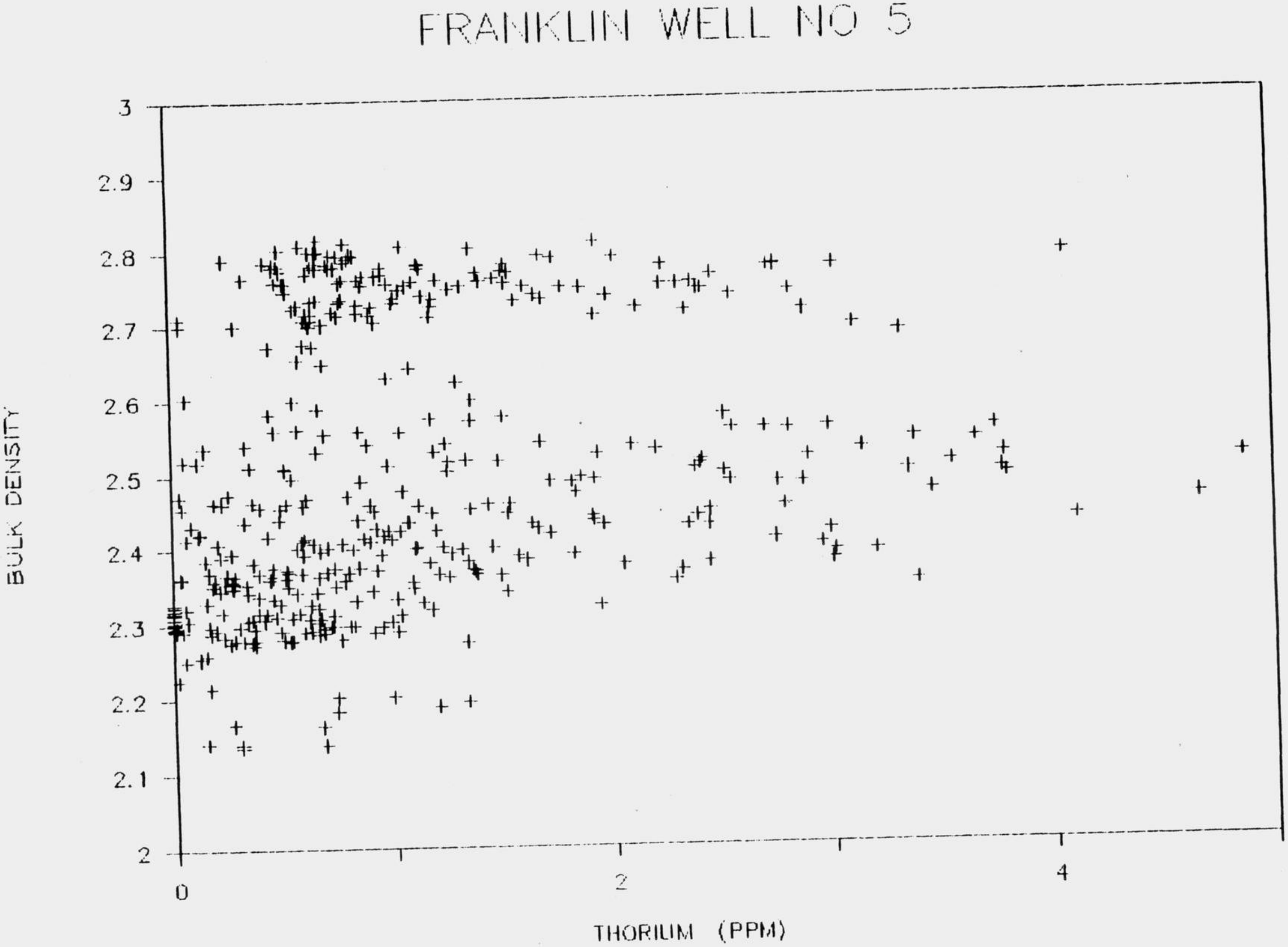

Figure 38B. Cross plot of density and thorium, Franklin well.

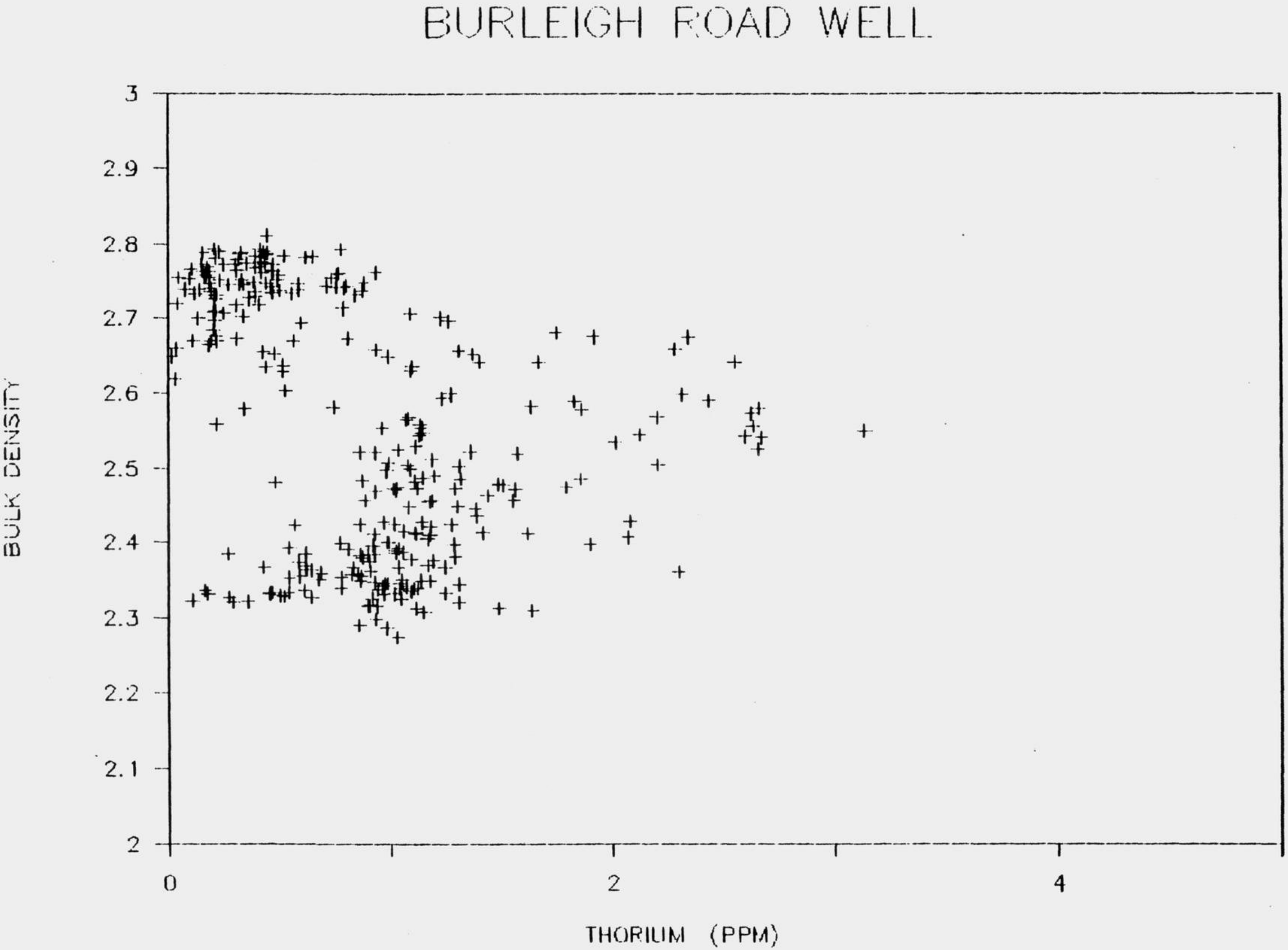

Figure 39. Cross plot of density and thorium, Burleigh well.

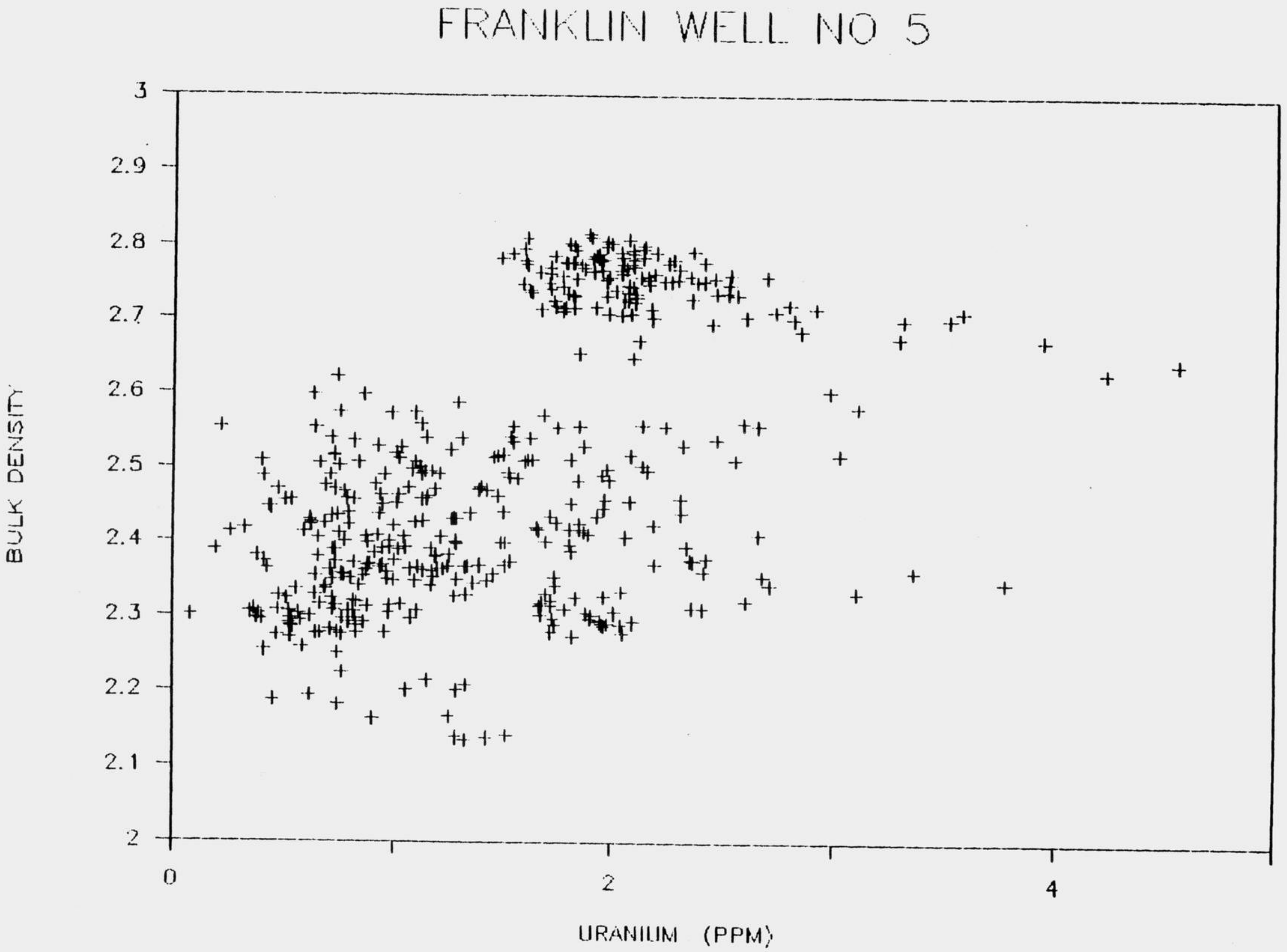

Figure 40. Cross plot of density and uranium, Franklin well.

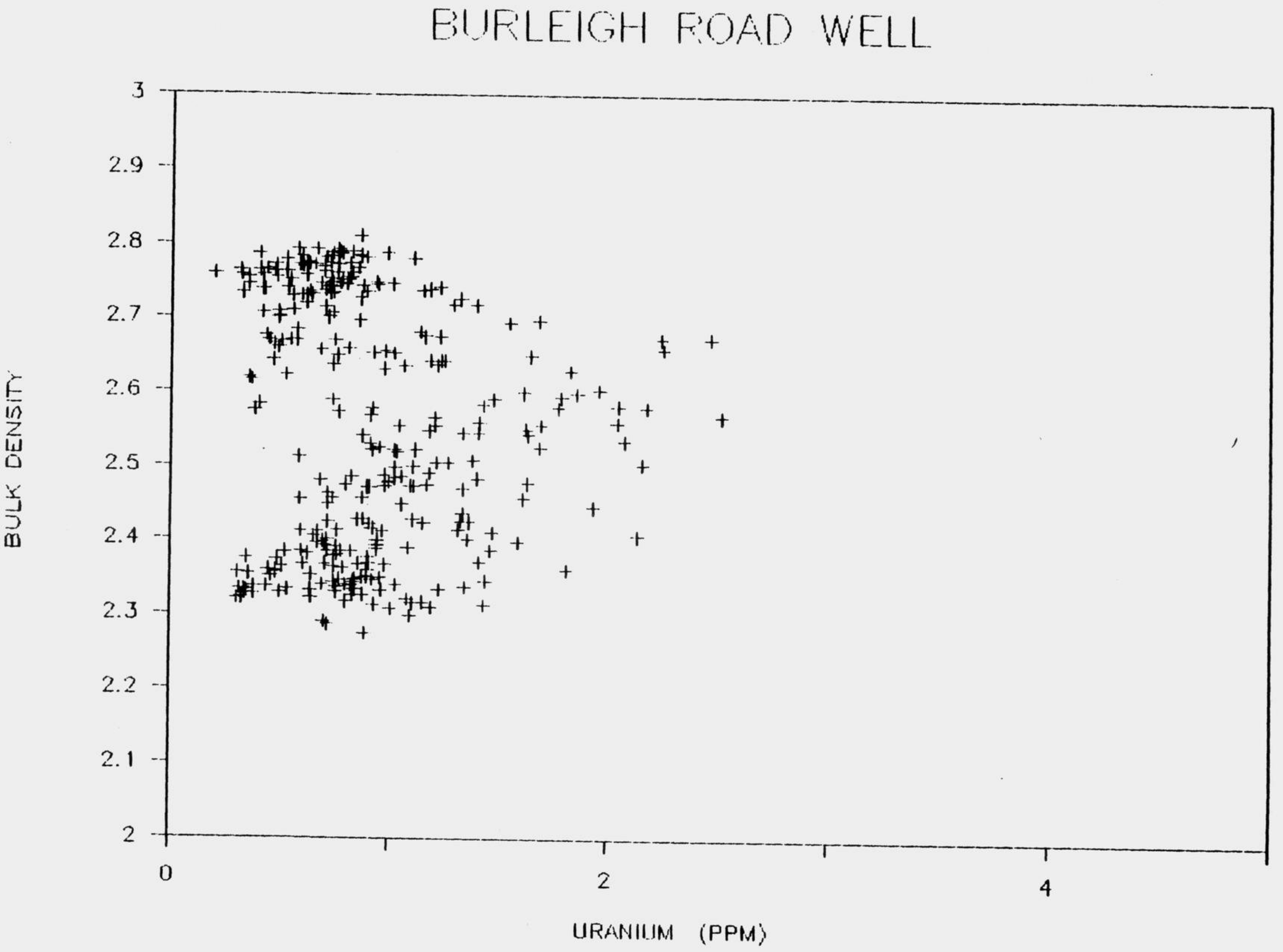

Figure 41. Cross plot of density and uranium, Burleigh well.

$$\text{FM-226} = U_i \frac{FT}{B} \qquad (3)$$

and

$$\text{FM-228} = Th_i \frac{FT}{B} \qquad (4)$$

where

U_i = Spectral gamma measured uranium content at one foot increments within the borehole in PPM,

Th_i = Spectral gamma measured thorium content at one foot increments within the borehole in PPM, the summation is over the formation thickness,

FT = the formation thickness,

B = the total length of open borehole.

Equations 3 and 4 assume that each formation contributes water to the wellbore in proportion to its percentage of the openhole length and that the radiometric quality of the contributed water is directly proportional to the total radiometric content of the formation. The figures of merit defined above were calculated for each formation encountered by each of the wells for which complete geophysical logs were available. It should be noted that, as defined, a high figure of merit should yield high radium water while a low figure of merit should yield low radium water.

The thorium figure of merit for the formations encountered within the study area are compared with the radium-228 content of wellbore water in Figure 42. Based on the data presented in Figure 42 there is no reasonable relationship between the figure of merit and the radium-228 content of produced water for the Mt. Simon, the Eau Claire, or the St. Peter sandstone. However, there is a very strong linear relationship between the radium-228

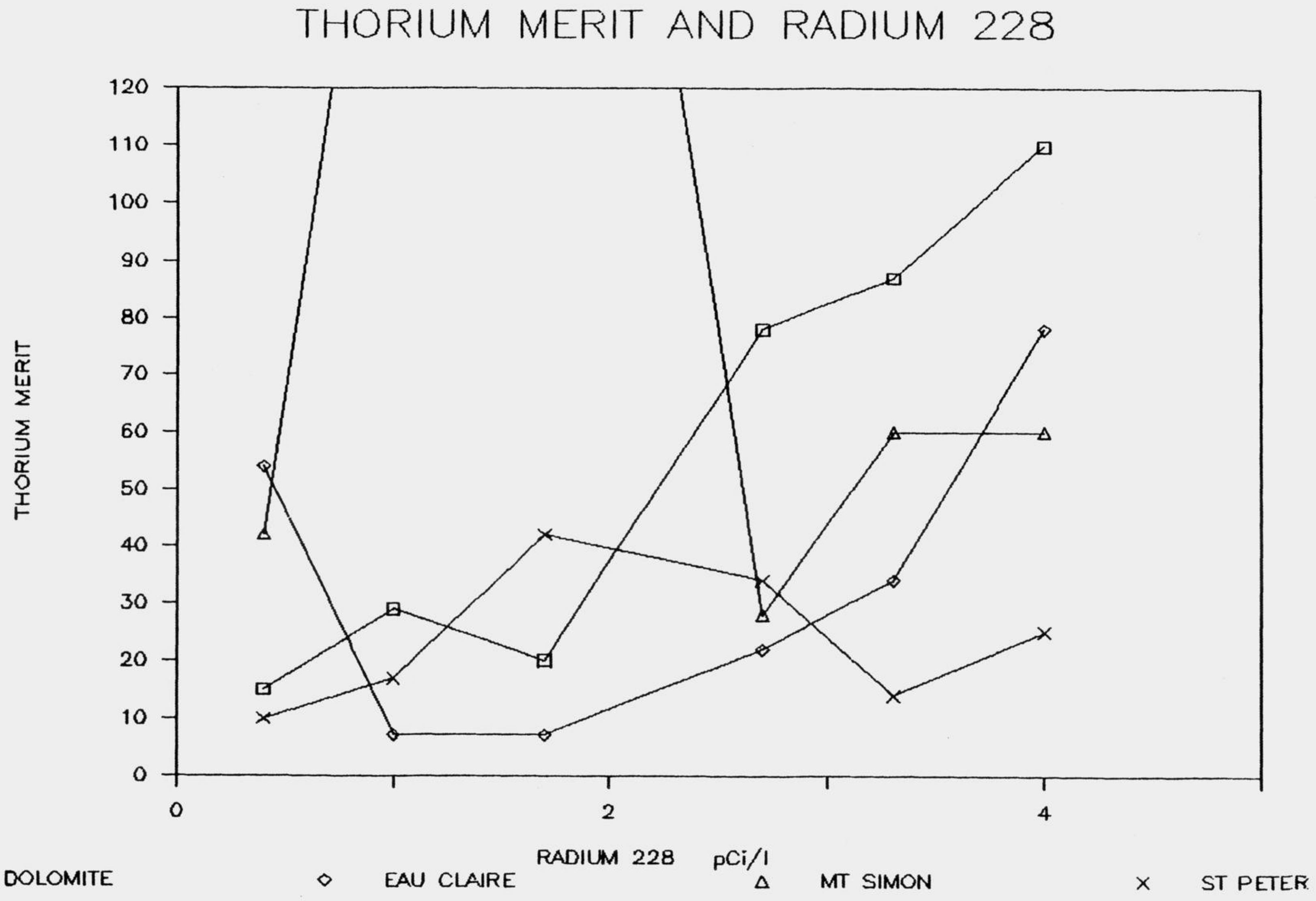

Figure 42. Formation figure of merit for thorium and radium-228 concentrations in borehole water.

water quality and the dolomite section of the wellbore consisting of the Galena and Platteville formations. Because of the complexity of the curves in Figure 42 the results for the Galena, Platteville are repeated alone in Figure 43. The correlation coefficient for these data is 0.93 which indicates a very strong connection between the thorium figure of merit for the dolomite section and the radium-228 content of the produced water. It is also interesting to note that the trend of these data includes zero radium-228 at a zero figure of merit. This implies that the dolomite section is the only source of radium-228 and no other formation influences the radiometric water quality.

The uranium figure of merit for each formation is compared to the levels of radium-226 in produced water in Figure 44. The results are similar to the thorium results in that there is no reasonable relationship between radium-226 and the uranium figure of merit for the Mt. Simon, the Eau Claire, or the Galena, Platteville formations. However, there is a very strong linear relationship for the St. Peter formation. The St. Peter data are replotted for clarity in Figure 45. The correlation coefficient for these data is 0.97. The trend of these data approaches a positive FM-228 as the radium-226 level approaches zero. This suggest that the St. Peter formation contains some uranium which does not contribute to radium-226 levels in the produced water and that no other formation effects the radiometric water quality.

Figures 43 and 45 are highly significant in that they strongly indicate the thorium source for radium-228 in produced water is contained entirely within the dolomite section of the wellbore and that the uranium source for radium-226 in the produced water is contained entirely within the St. Peter sandstone section of the wellbore.

These relationships are totally unexpected in that the actual uranium and thorium contents are much higher within the Eau Claire formation than within

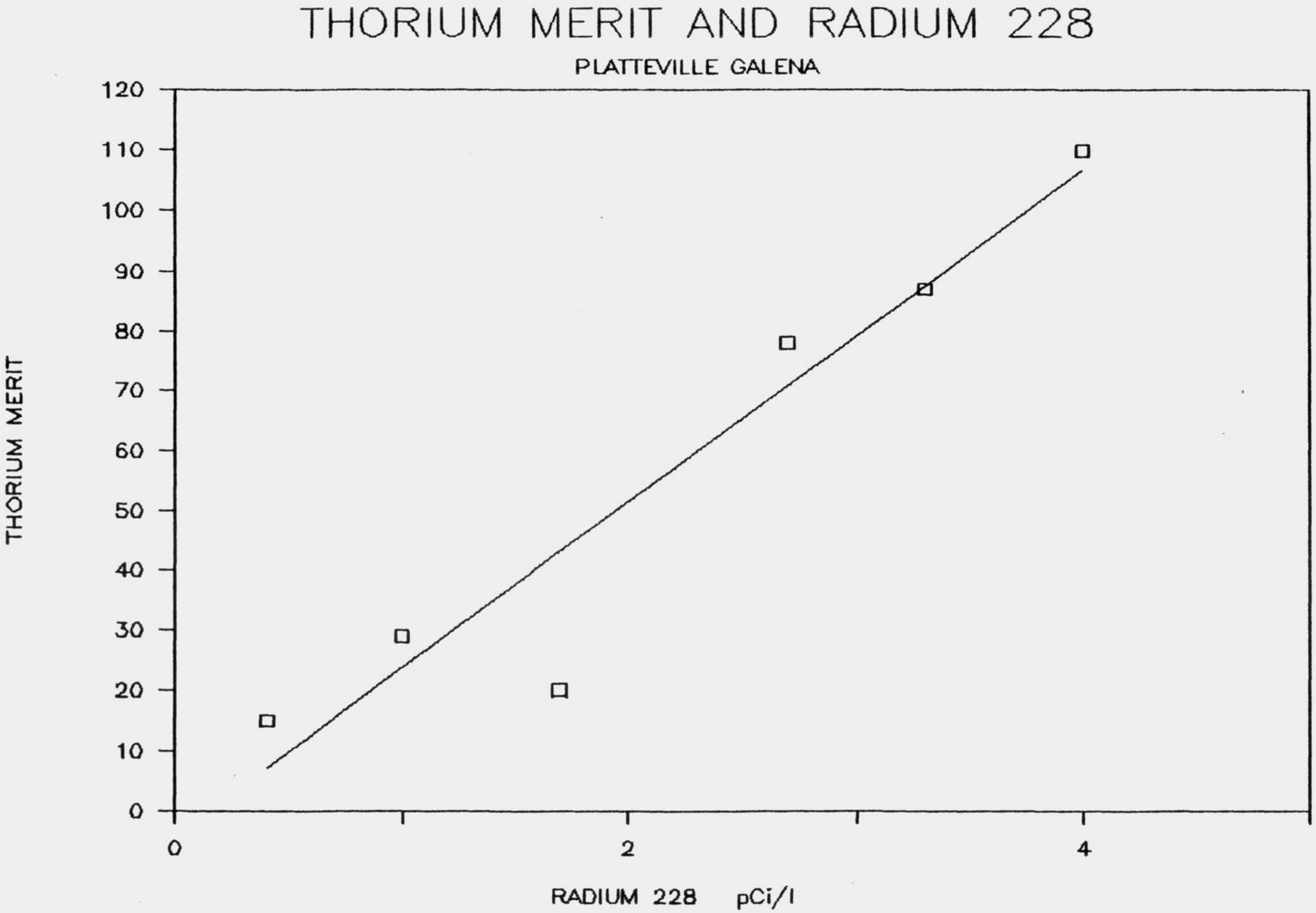

Figure 43. Figure of merit for the dolomite sections and radium-228 in borehole water.

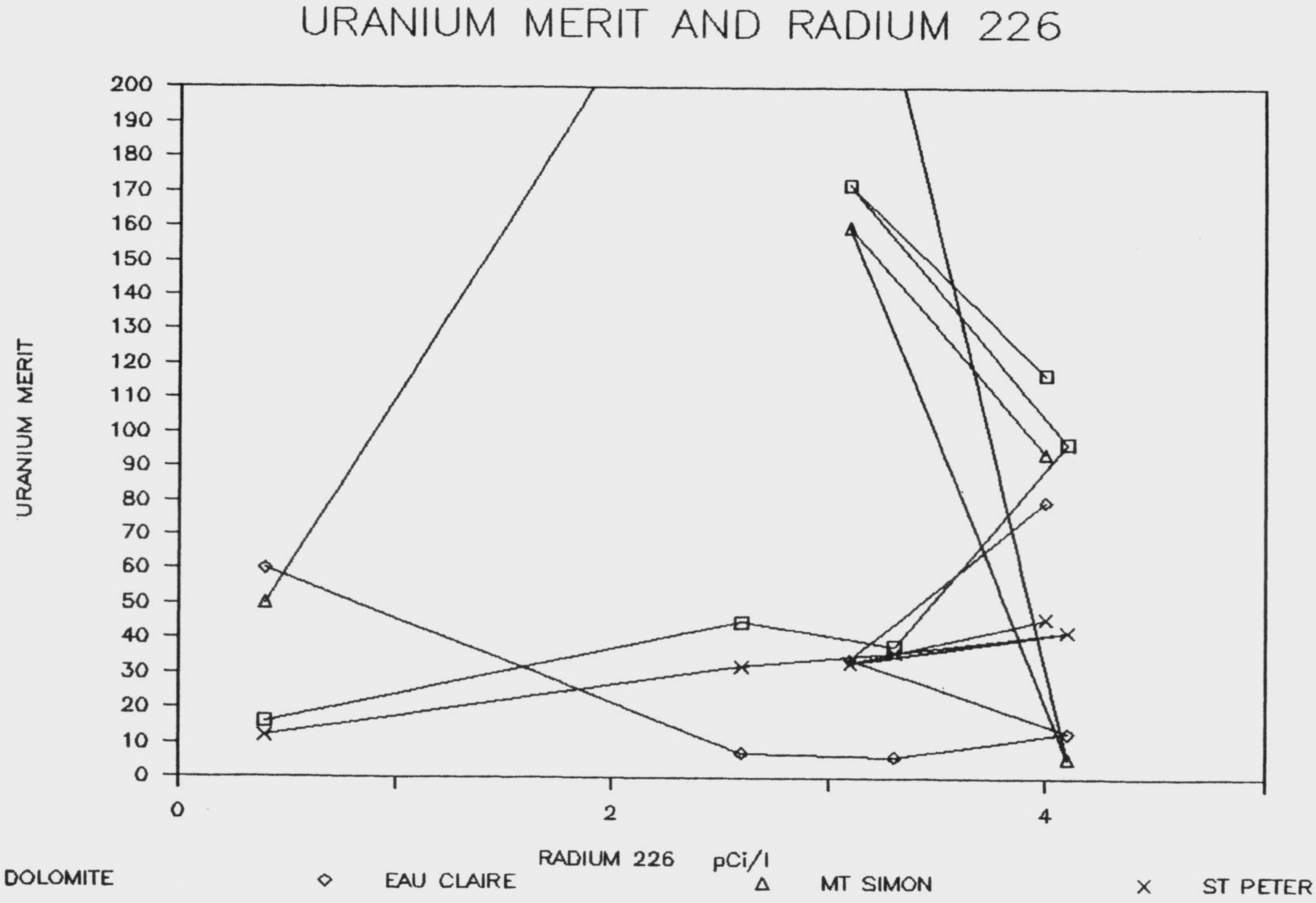

Figure 44. Uranium figure of merit and radium-226 in borehole water.

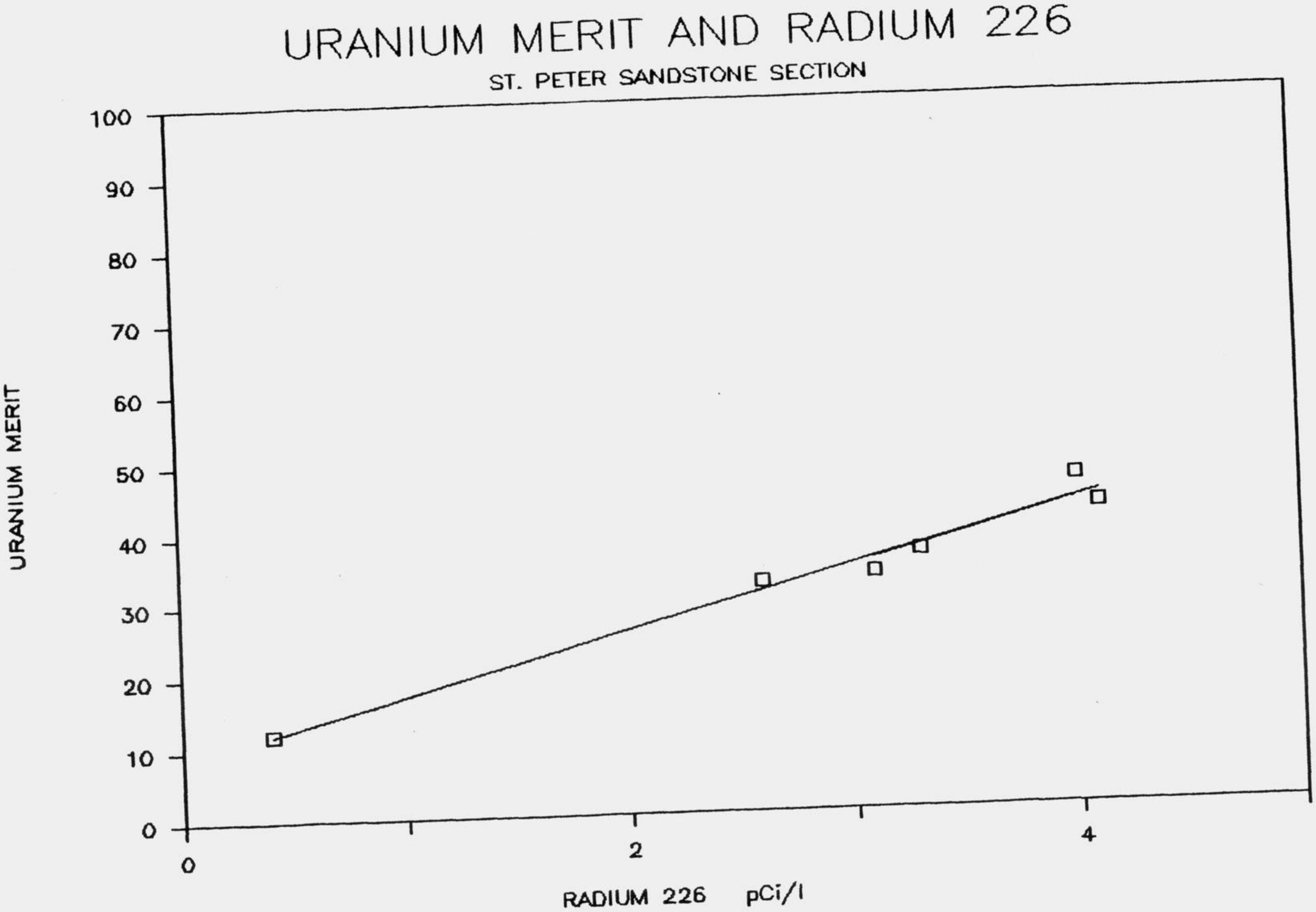

Figure 45. Uranium figure of merit for the St. Peter sandstone and radium-226 in produced water.

the other formations. The generally high levels of thorium and uranium within the Eau Claire in comparison to the other formations is demonstrated by the geophysical log sections presented in Figures 46, 47, and 48. While the levels within the Eau Claire are high, Figures 43 and 45 clearly indicate it is the lower radiometric levels of the dolomite and St. Peter sections which determines the radiometric quality of the produced water. For these sections to control the radiometric water quality it would appear necessary to require that the radium produced by uranium and thorium decay in the other formations is simply not available to the pore water. This in turn requires that either the water chemistry within the Galena, Platteville, St. Peter sections is different from the remainder of the wellbore or that the habitat of uranium and thorium within these sections differs from the habitat of these elements in the other portions of the wellbore.

Figures 43 and 45 also provide a possible explanation for the results of the casing experiments conducted at the Franklin and Burleigh Road wells. The Eau Claire section at the Franklin well is approximately 180 ft thick and this section was cased in an attempt to improve the radiometric water quality. Based on figures 42 through 45, casing the Eau Claire should have no effect on the radium content of the produced water and, in fact, no effect was observed. The Eau Claire section of the Burleigh Road well is approximately 70 ft thick and this section was also cased to improve the produced water. If the casing string was entirely within the Eau Claire formation, no reduction in radium levels should have resulted. However, if a portion of the lower St. Peter formation was also cased in the process, a reduction in the radium-226 levels would be expected along with no change in the radium-228 levels. This is in keeping with the direction, but not the magnitude, of the actual

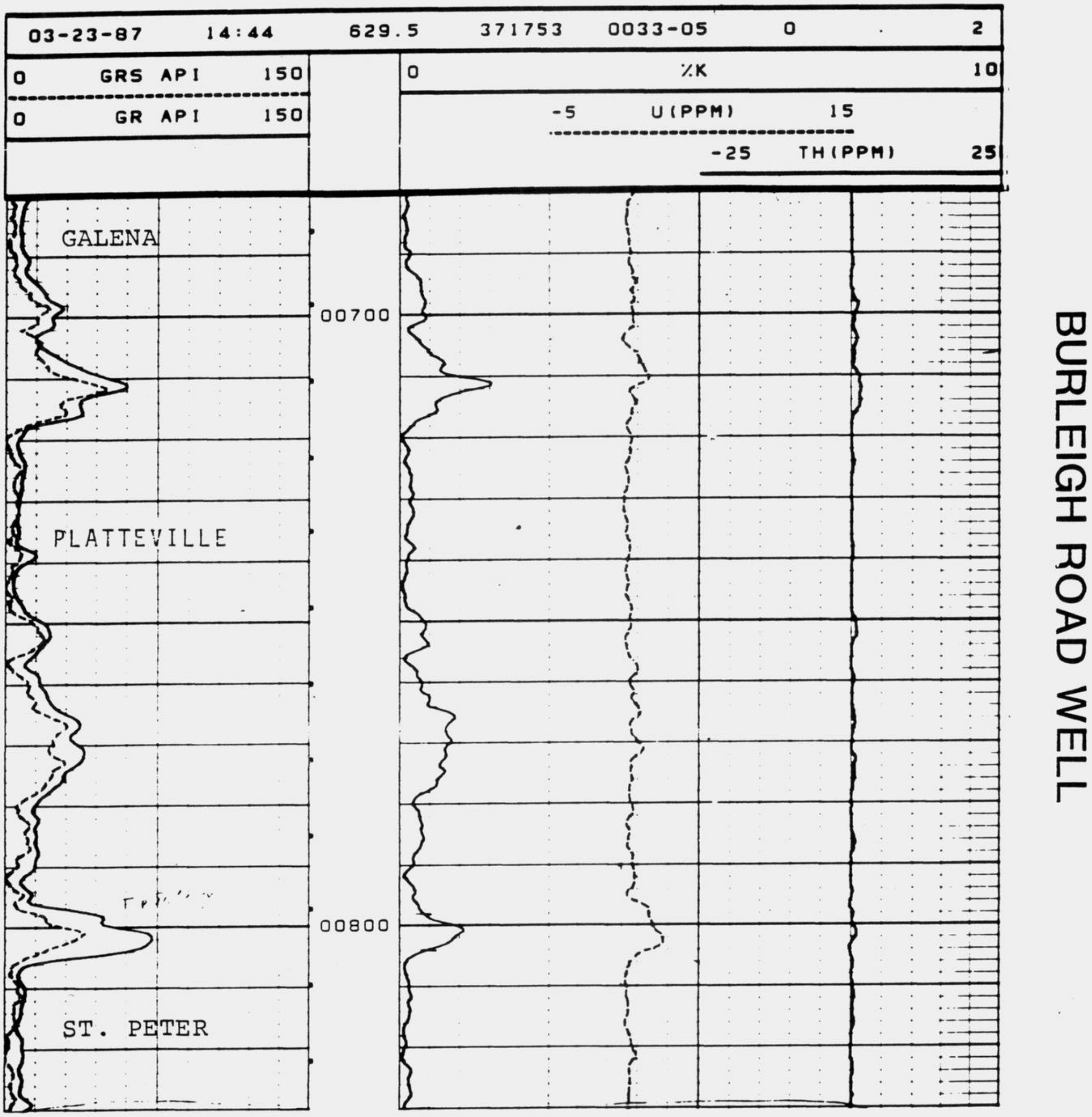

Figure 46. Sample spectral gamma log for the dolomite section.

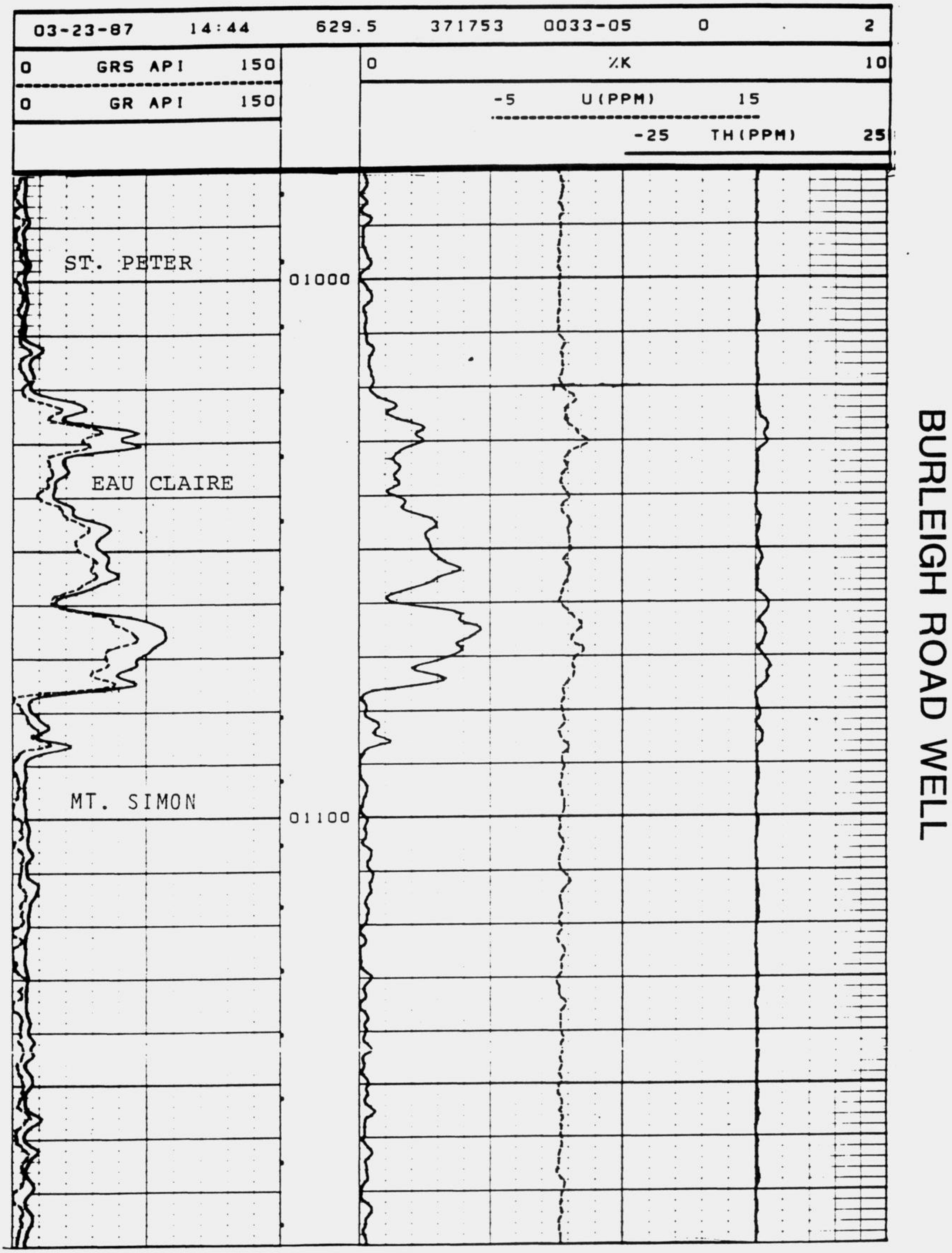

Figure 47. Sample spectral gamma log for the St. Peter, Eau Claire, and Mt. Simon sandstone.

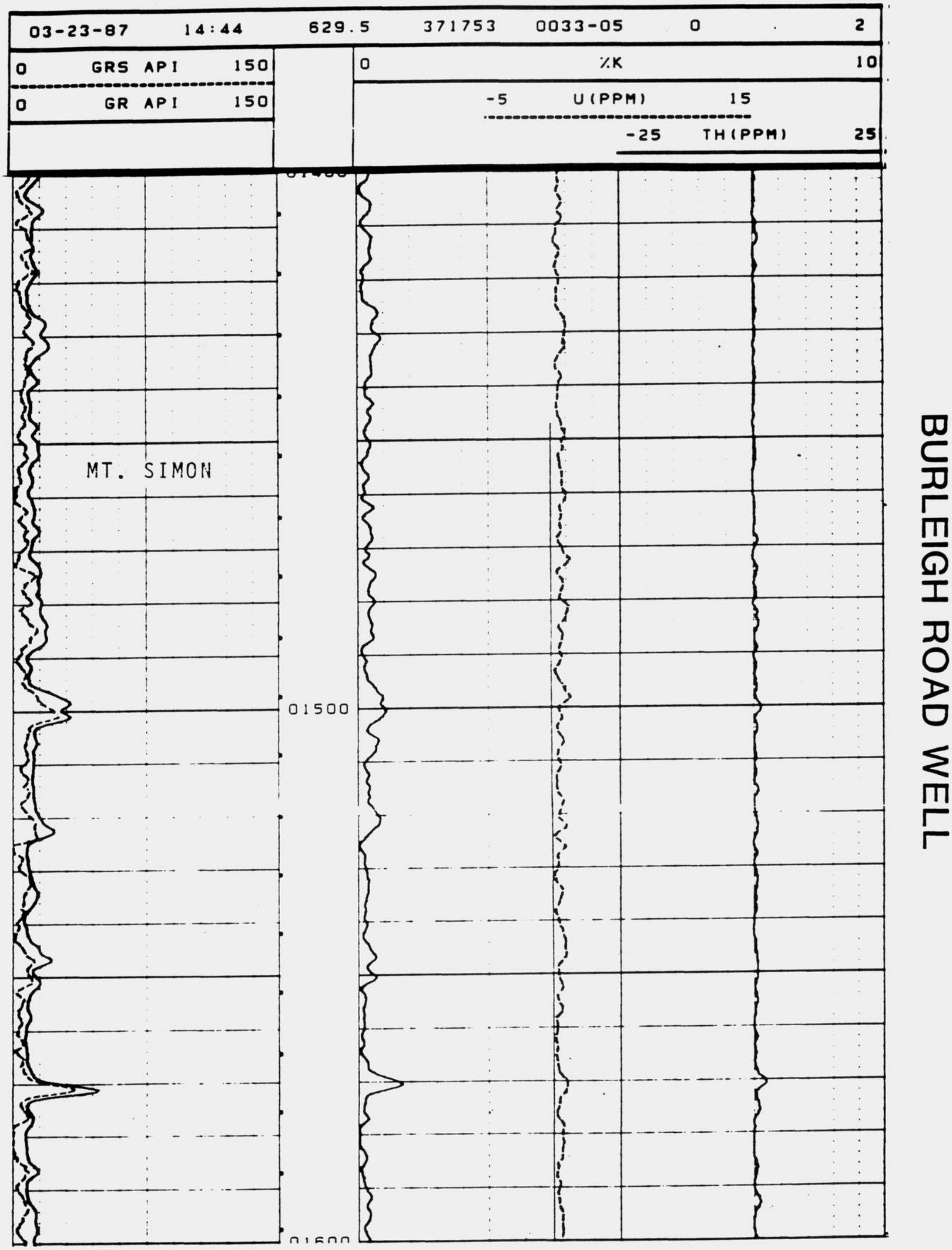

Figure 48. Sample spectral gamma log for the Mt. Simon sandstone.

results which apparently indicated an 80 percent decrease in radium-226 and a 27 percent decrease in radium-228.

COMPARISON OF SPECTRAL GAMMA LOGS WITH ANALYTICAL METHODS

In order to test the validity of spectral gamma logs in identifying the quantity of radioisotopes in enriched zones within the aquifer two analytical methods were used to test the values of spectral gamma logs: instrumental neutron activation analysis and gamma-ray spectroscopy. Both methods utilized well cuttings which were procured from the Wisconsin Geological and Natural History Survey core library. These samples were initially collected by drilling crews during water well construction. Instrumental neutron activation analyses for uranium and thorium were performed at the University of Wisconsin - Madison Nuclear Laboratory, while gamma-ray spectroscopy analyses, for the same two radioisotopes, were determined at Argonne National Laboratory.

Two wells were chosen to make the comparisons: Franklin City well #5 and Carriage Hills Subdivision well. Measured concentrations of uranium and thorium from the three methods (gamma-ray logs) were compared by cross-plotting the data. Cross-plots of gamma-ray spectroscopy and neutron activation data were initially plotted to check the consistency of analytical measurements made on well cuttings. Then, gamma-ray spectroscopy values were cross-plotted against spectra gamma log values to evaluate the measurements of equivalent sample intervals.

Theoretically sample points of uranium and thorium measured by any of the two methods should lie on the 1:1 line between the two methods. However, as Figures 49 to 56 illustrate there are departures, in some cases considerable, from the 1:1 line, in spite of the fact that correlation coefficients in most cases are quite high.

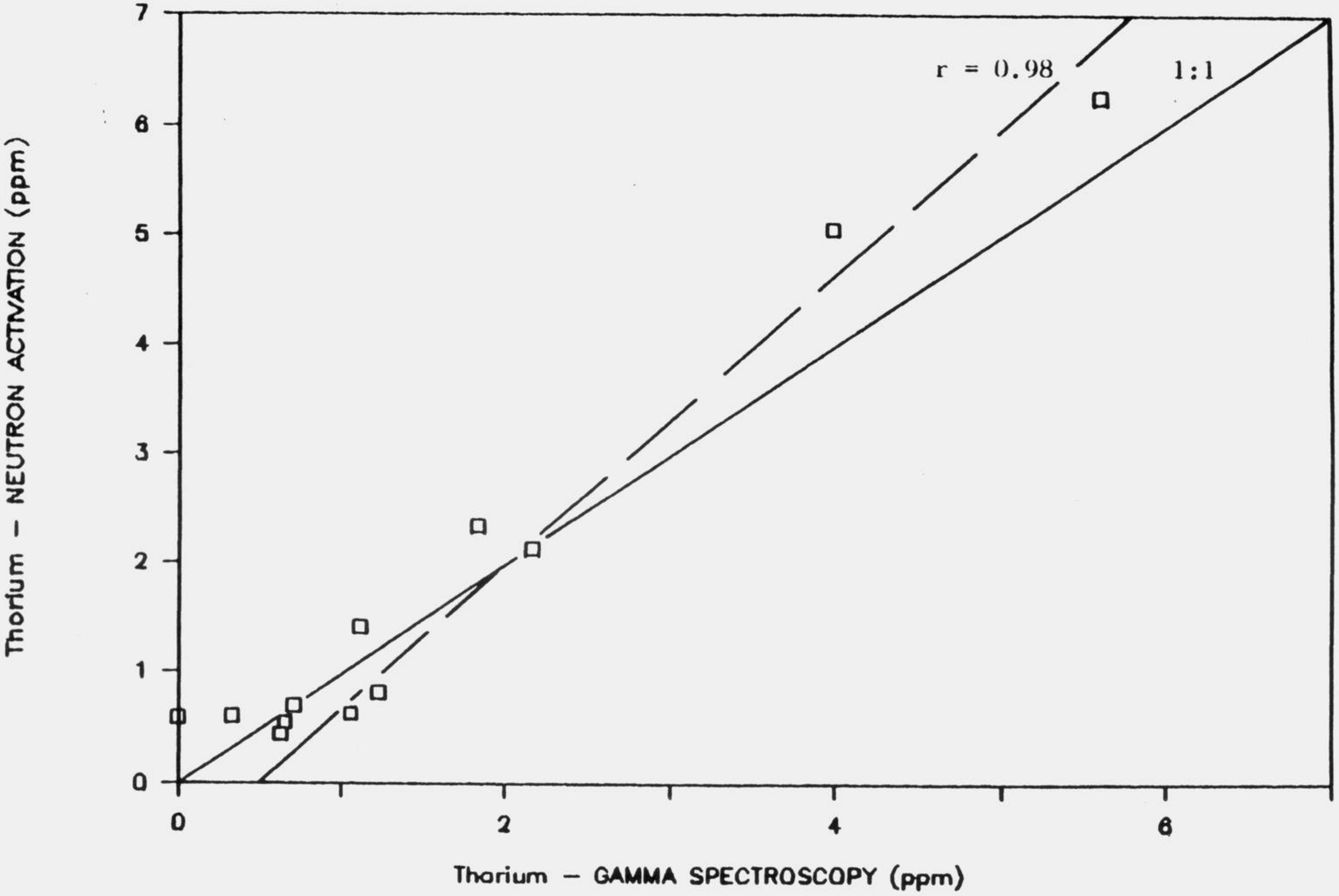

Figure 49. Franklin City Well #5. Cross-plot of Th-232 concentration in parts per million (ppm), Gamma Spectroscopy (GS) vs. Neutron Activation (NA). The slope of the best fit line (dashed) is 1.1.

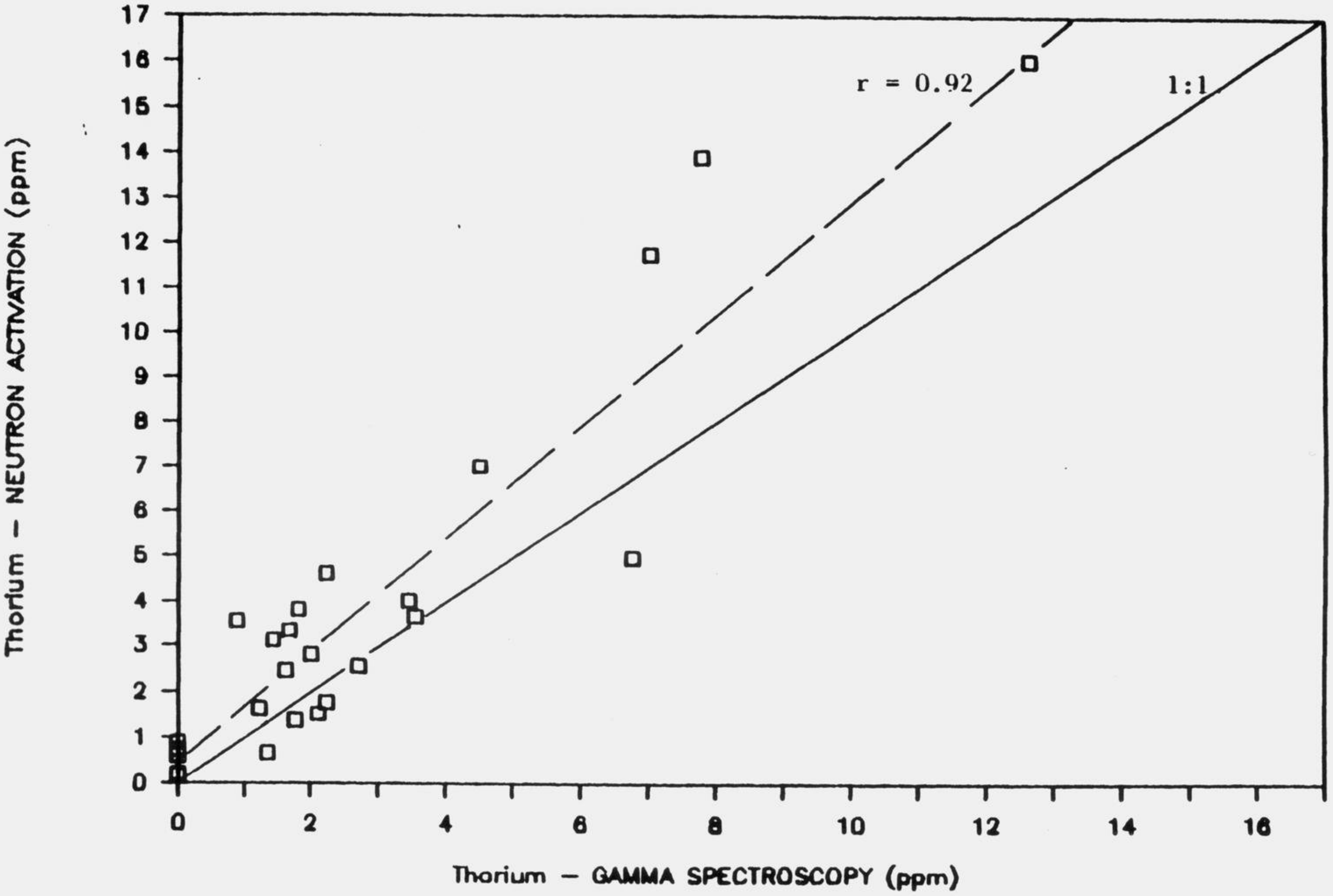

Figure 50 Carriage Hills Subdivision. Cross-plot of Th-232 concentration in parts per million (ppm), Gamma Spectroscopy (GS) vs. Neutron Activation (NA). The slope of the best fit line (dashed) is 1.3.

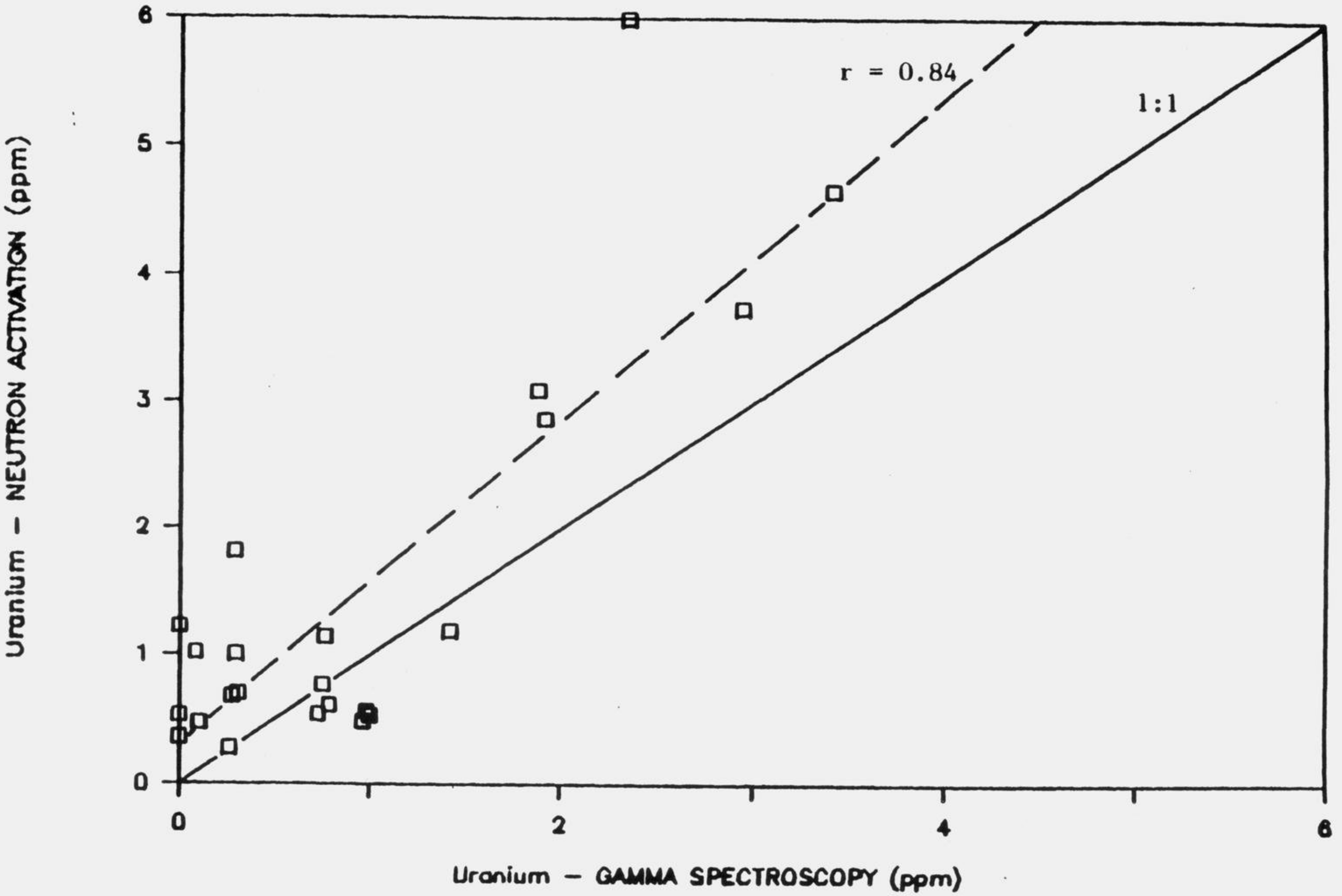

Figure 51 Carriage Hills Subdivision. Cross-plot of U-238 concentration in parts per million (ppm), Gamma Spectroscopy (GS) vs. Neutron Activation (NA). The slope of the best fit line (dashed) is 1.3.

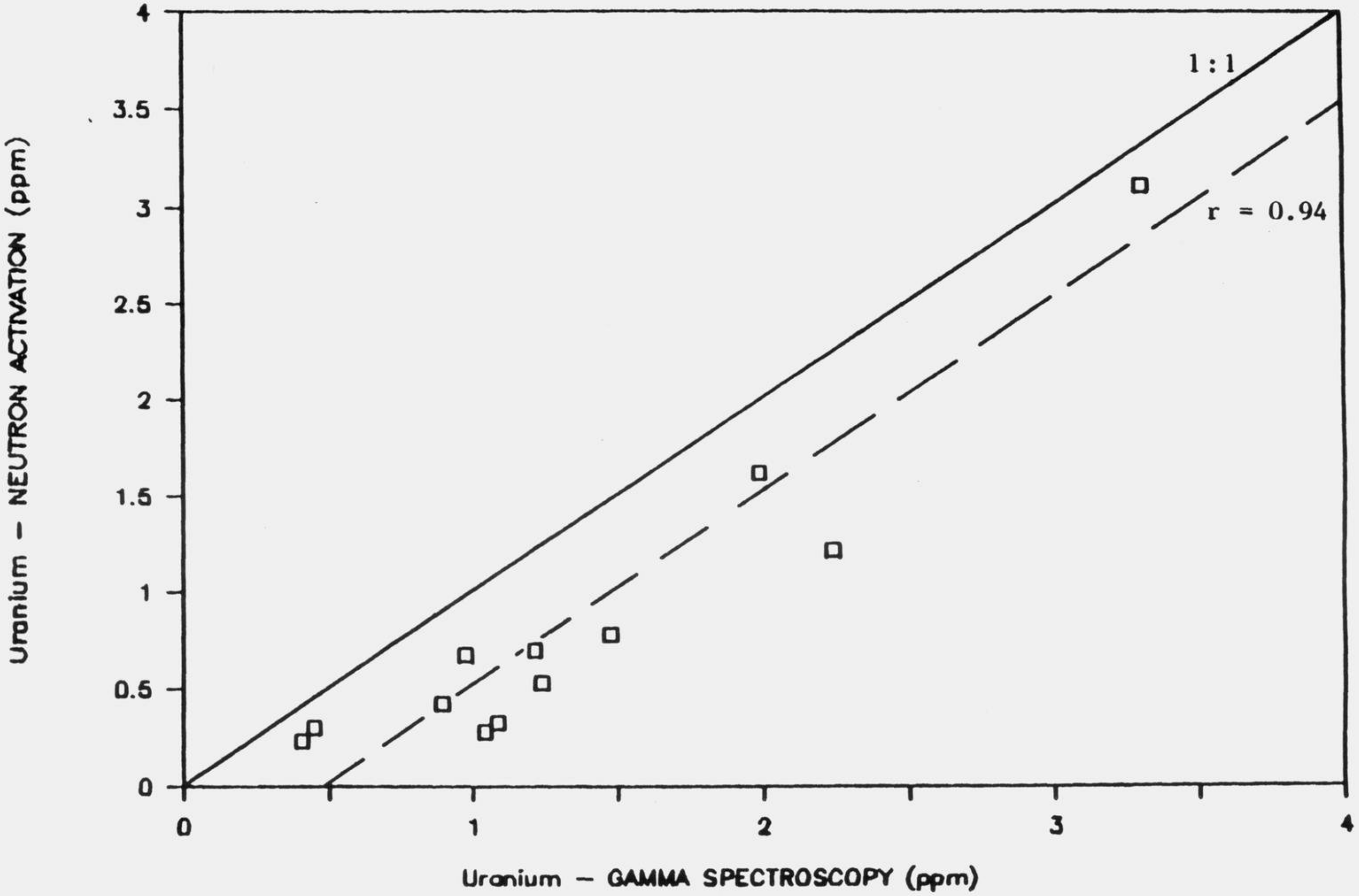

Figure 52 Franklin City Well #5. Cross-plot of U-238 concentration in parts per million (ppm), Gamma Spectroscopy (GS) vs. Neutron Activation (NA). The slope of the best fit line (dashed) is 0.95.

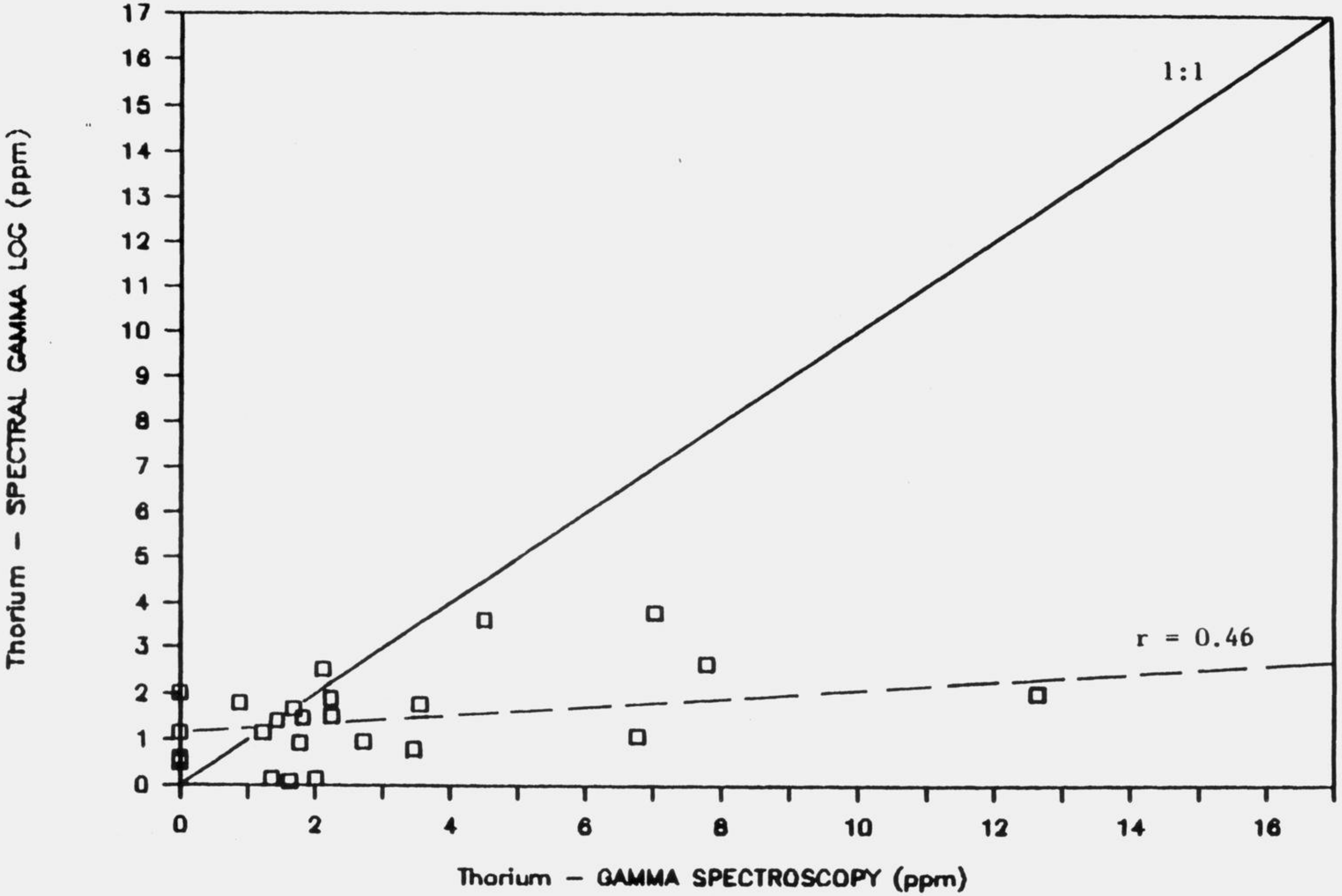

Figure 53 Carriage Hills Subdivision. Cross-plot of Th-232 concentration in parts per million (ppm), Gamma Spectroscopy (GS) vs. Spectral Gamma Log (SGL). The slope of the best fit line (dashed) is 0.15.

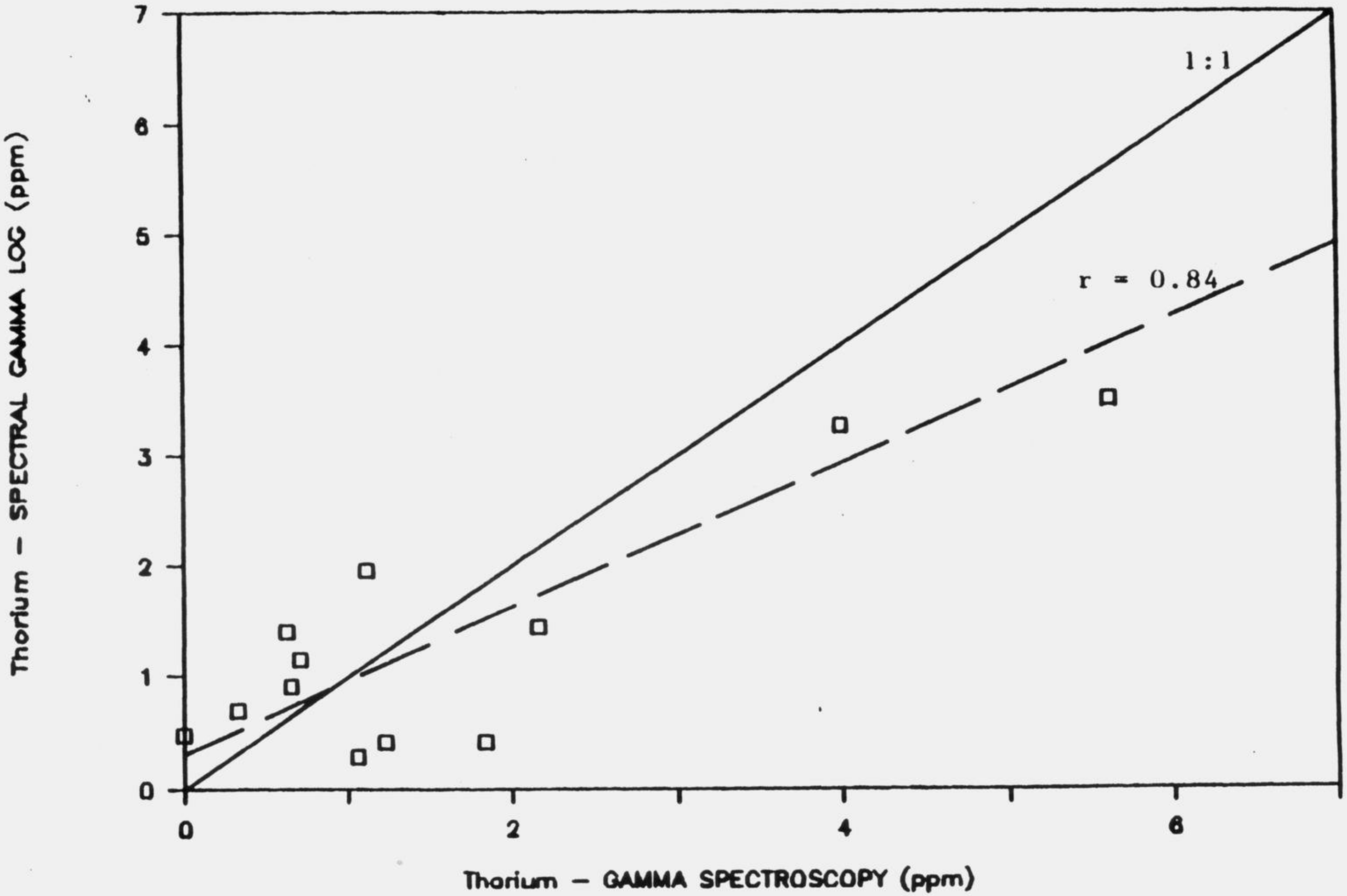

Figure 54 Franklin City Well #5. Cross-plot of Th-232 concentration in parts per million (ppm), Gamma Spectroscopy (GS) vs. Spectral Gamma Log (SGL). The slope of the best fit line (dashed) is 0.56.

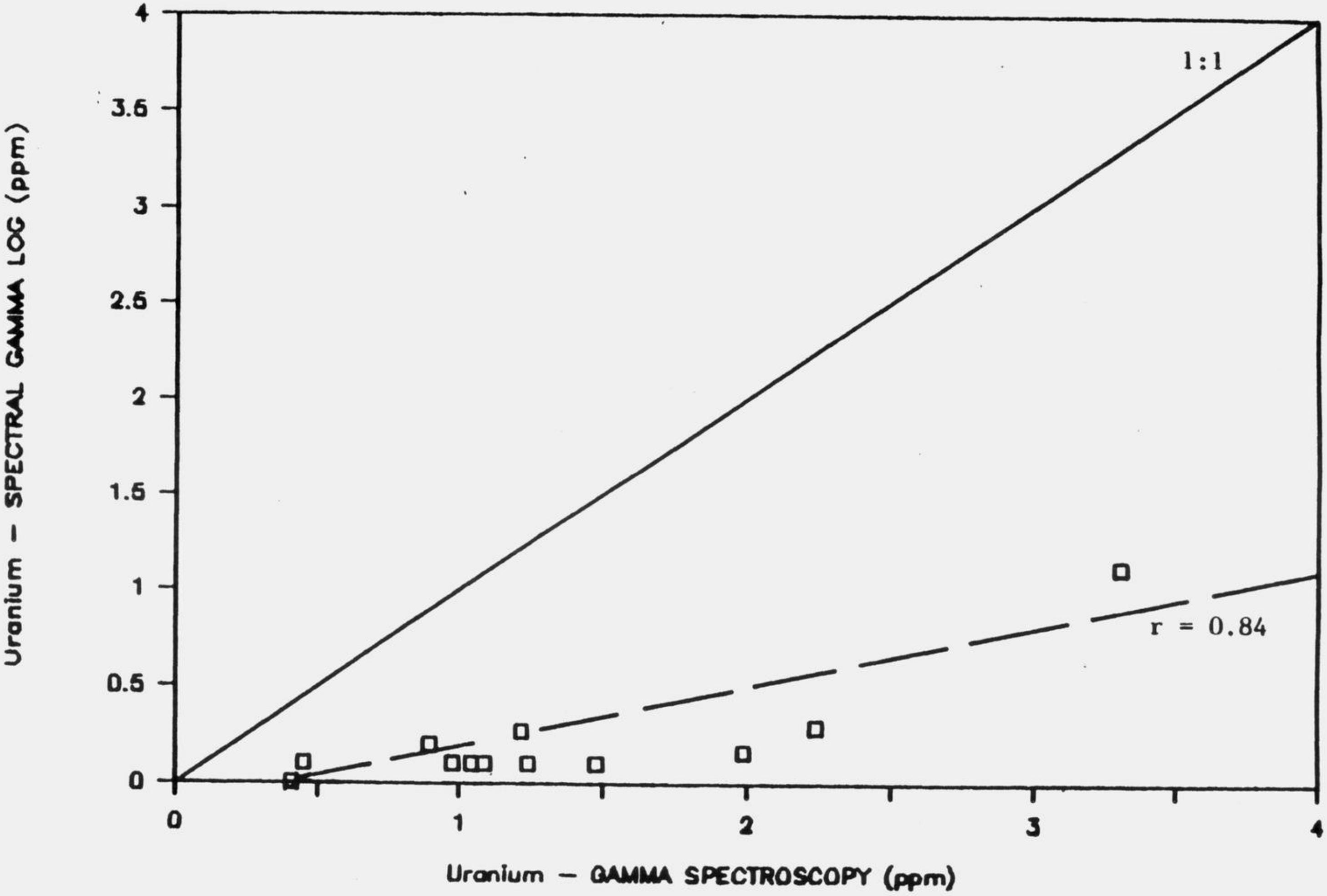

Figure 55 Franklin City Well #5. Cross-plot of U-238 concentration in parts per million (ppm), Gamma Spectroscopy (GS) vs. Spectral Gamma Log (SGL). The slope of the best fit line (dashed) is 0.30.

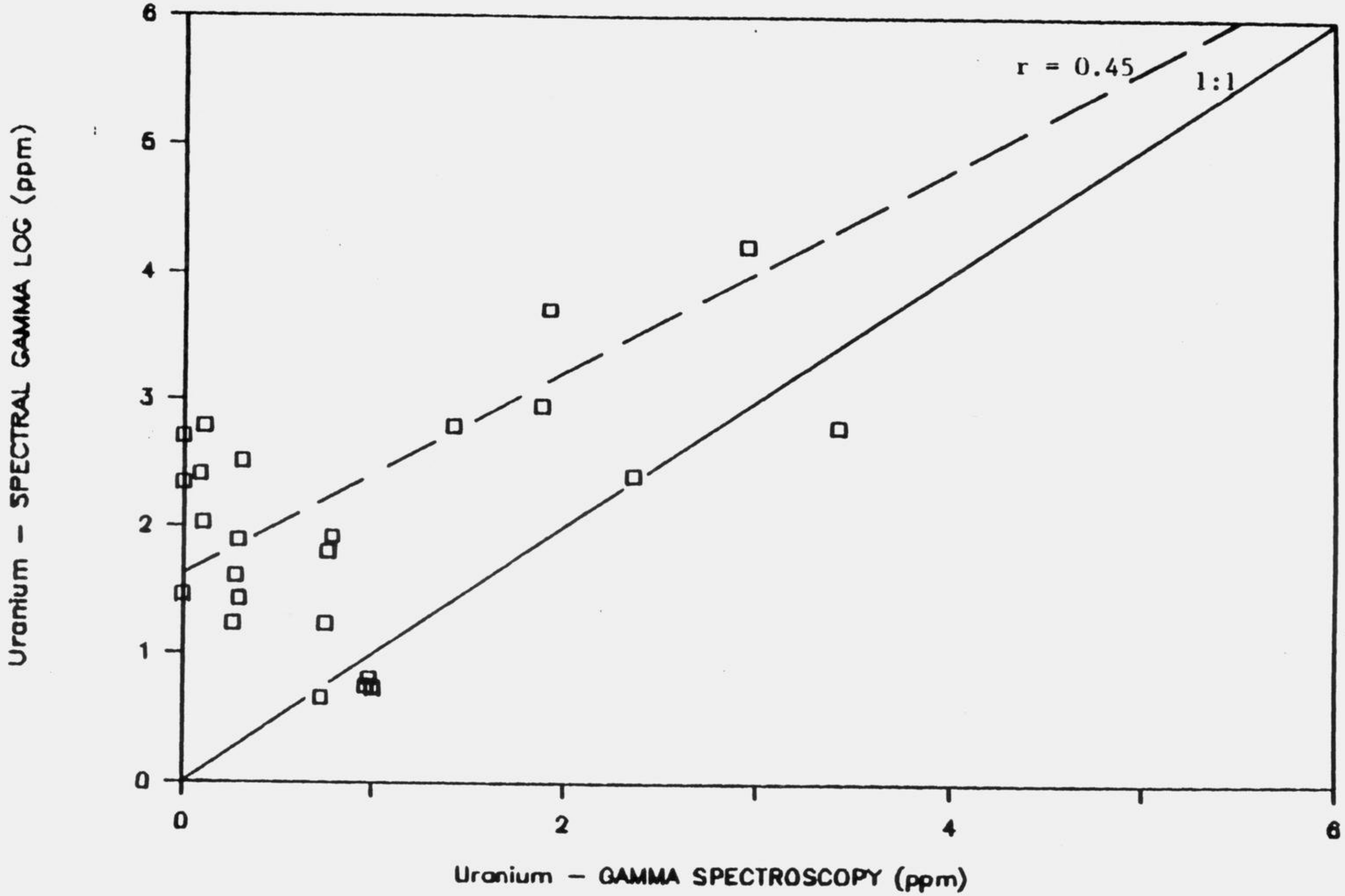

Figure 56 Carriage Hills Subdivision. Cross-plot of U-238 concentration in parts per million (ppm), Gamma Spectroscopy (GS) vs. Spectral Gamma Log (SGL). The slope of the best fit line (dashed) is 0.45.

Figure 49 and 50 illustrate that cross-plots of gamma-ray spectroscopy values for thorium versus neutron activation analyses depart from 1:1 line in such a way that neutron activation values tend to be higher than the gamma-ray spectroscopy values. This is especially true for samples where the concentration of thorium is in excess of about 4 ppm. Similar picture emerges from Figure 51 and 52 in which uranium values by neutron activation are higher than gamma-ray spectroscopy for Carriage Hills Subdivision well, but lower for Franklin City well #5. The reason for this inconsistency is not clear but may have to do with the preferential mobility of uranium-238 daughters (U-234, Ra-226 and Ra-222) in the Franklin City well #5.

Comparisons have been made between five - window interpretation of the spectral gamma log values with the standard three-window interpretation, and the results, illustrated in Figures 57 and 58, reveal that five-window interpretations for thorium and uranium provide a better correlation with gamma-ray spectroscopy values than three-window interpretation.

It is not clear why there are discrepancies in the thorium and uranium values between the three methods employed in this study. Generally the gamma-ray spectroscopy method is regarded to be more accurate and more representative than neutron activation method and it is for this reason that the former was used for comparison with the spectral gamma logs. However, the discrepancy between gamma-ray spectroscopy and spectral gamma logs is less certain but may be a reflection of bore hole sampling method. Because a cable-tool drilling method was used to advance each borehole, and well cuttings were removed from the borehole using a grab-type collection method they may not be truly representative of the subsurface stratigraphy and geochemical environment.

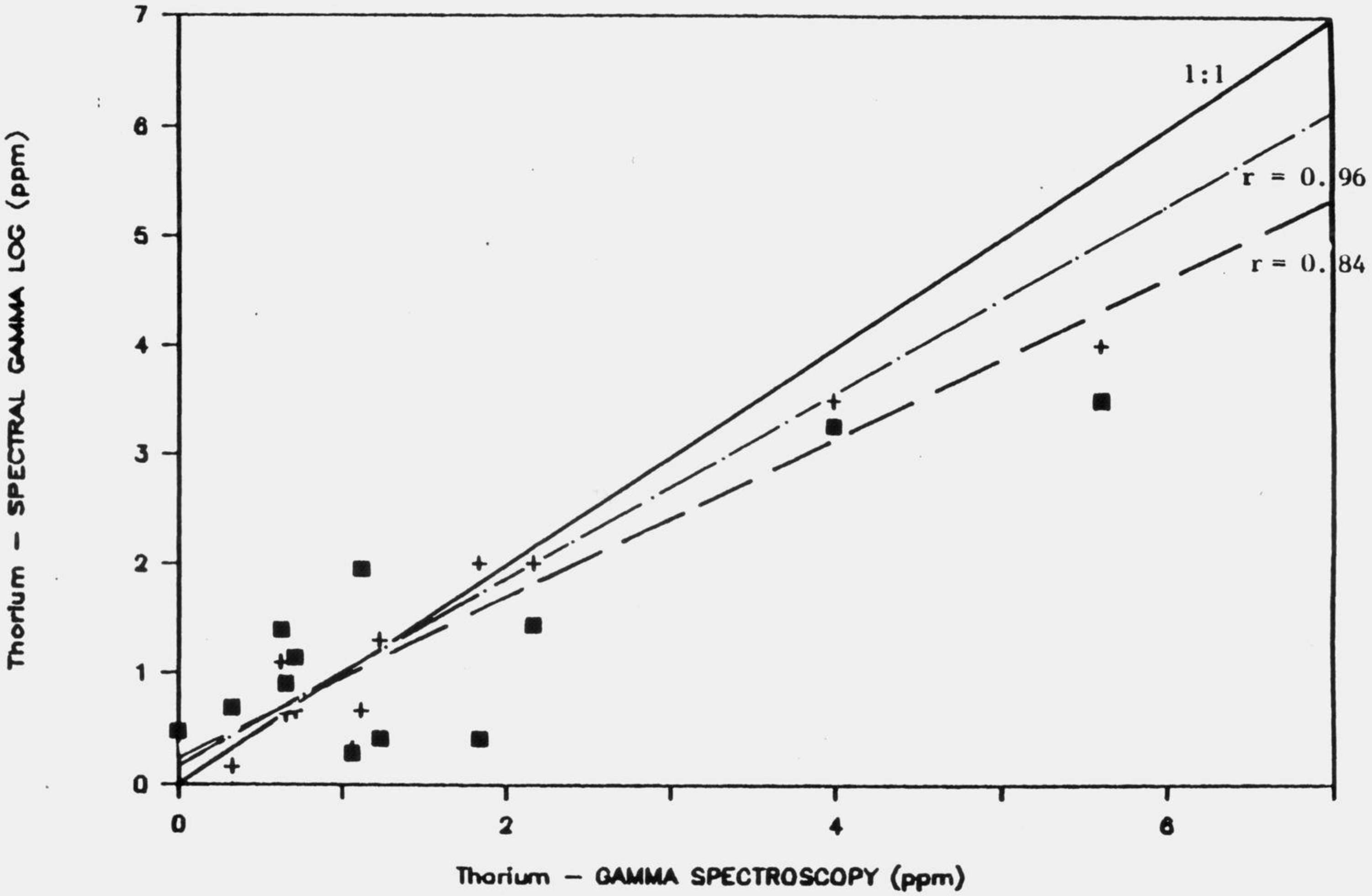

Figure 57 Franklin City Well #5. Cross-plot of Th-232 concentration in parts per million (ppm), Gamma Spectroscopy (GS) vs. Spectral Gamma Log (SGL) - ■ three-window interpretation, best fit line (dashed) slope = 0.56; + five-window interpretation, best fit line (dash-dot) slope = 0.73.

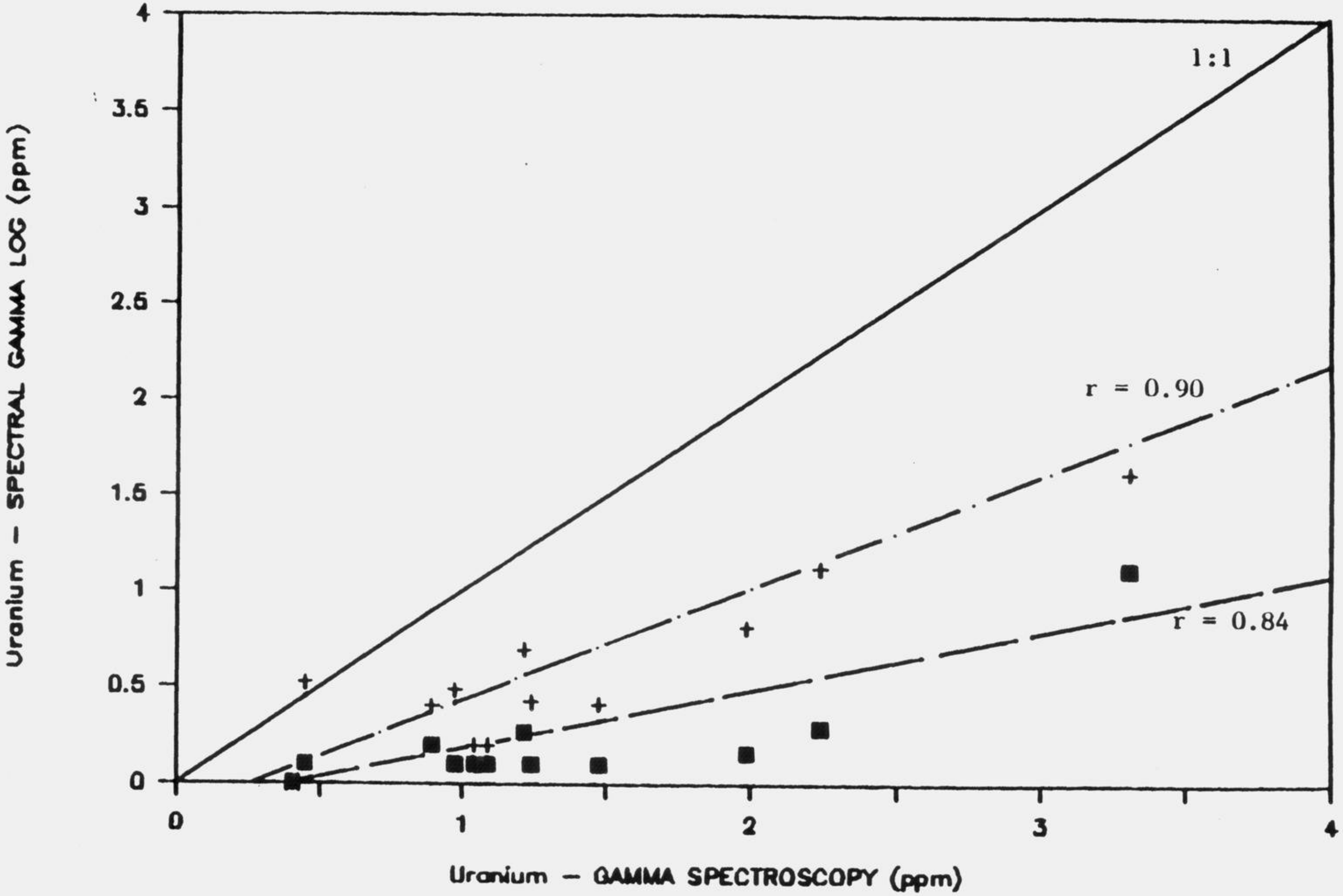

Figure 58 Franklin City Well #5. Cross-plot of U-238 concentration in parts per million (ppm), Gamma Spectroscopy (GS) vs. Spectral Gamma Log (SGL) - ■ three-window interpretation, best fit line (dashed) slope = 0.30; + five-window interpretation, best fit line (dash-dot) slope = 0.50.

THE COMPARISON OF LITHOLOGY WITH URANIUM AND THORIUM CONCENTRATIONS

The samples used for the analytical analyses were checked under polarized microscope for their mineralogy, sorting, and grain coatings and the results compared with uranium and thorium values. Generally an increase in the percent of shale is accompanied by an increase in uranium and thorium concentrations whereas an increase in the percent of quartz is accompanied by a decrease in uranium and thorium concentrations. On the other hand an increase in the percent of carbonate is not accompanied by an increase or decrease in the concentration of uranium and thorium. Similarly there is no obvious correlation between the percent of iron oxide grain coatings and the concentration of uranium and thorium. However, determination of isotopic concentrations of uranium-238 and thorium-232 concentrations associated with grain coatings in a small group of samples suggests otherwise.

Sample intervals selected for the isotopic determination of uranium and thorium are presented in Table IV. For this procedure, uranium and thorium were separated from leachate derived from surface grain coatings, and the activities of all uranium and thorium isotopes in the uranium-238 and thorium-232 decay series were determined. Comparing these data with whole sample concentrations of uranium-238 and thorium-232 measured by neutron activation, gives the percentage of total uranium and thorium present in the coatings. For the purposes of this discussion, uranium-238 and thorium-232 concentrations of Carriage Hills Subdivision samples determined using neutron activation were corrected by dividing reported values by 1.5, the approximate relationship noted in the cross-plots of these data (Figures 50 and 52). Due to the paucity of data points, it is not possible to make definitive

Table 6 Comparison of U-238 and Th-232 concentrations measured by Neutron Activation (NA) and Alpha Spectroscopy (AS)

Uranium-238

Sample	Lithology	Fm.[1]	NA (ppm)	AS (ppm)	$\frac{234}{238}$	Percent[2]
CH0920	arenaceous carbonate	SP	$6.0^{\pm.07}$	$0.05^{\pm.001}$	2.7	1
CH0950	sandstone	SP	$0.54^{\pm.03}$	$0.11^{\pm.03}$	1.4	31
CH1250	calc-argillaceous sandstone	EC	$0.67^{\pm.06}$	$0.14^{\pm.01}$	1.5	31
CH1515	shale	MS	$3.73^{\pm.14}$	$1.4^{\pm.06}$	ND[3]	56
CH1520	shale	MS	$4.67^{\pm.13}$	$1.2^{\pm.01}$	1.0	39
FR0920	sandstone	SP	-	ND[4]	-	-
FR1150	shale	EC	$1.21^{\pm.13}$	$0.05^{\pm.02}$	1.2	4
FR1425	sandstone	MS	$0.32^{\pm.04}$	$0.04^{\pm.01}$	1.6	7

Thorium-232

Sample	Lithology	Fm.[1]	NA (ppm)	AS (ppm)	$\frac{228}{232}$	Percent[2]
CH0920	arenaceous carbonate	SP	$2.82^{\pm.05}$	$0.07^{\pm.02}$	1.7	4
CH0950	sandstone	SP	$0.59^{\pm.02}$	$0.19^{\pm.03}$	0.670	48
CH1250	calc-argillaceous sandstone	EC	$2.55^{\pm.04}$	$1.04^{\pm.06}$	1.03	61
CH1515	shale	MS	$11.72^{\pm.09}$	$3.4^{\pm.11}$	1.0	44
CH1520	shale	MS	$7.01^{\pm.07}$	$4.8^{\pm.16}$	1.1	100
FR0920	sandstone	SP	$0.60^{\pm.02}$	$0.1^{\pm.01}$	1.4	2
FR1150	shale	EC	$6.26^{\pm.03}$	$5.2^{\pm.19}$	1.0	83
FR1425	sandstone	MS	$0.70^{\pm.02}$	$0.29^{\pm.03}$	1.2	41

Notes:

1. Fm. - formation: SP - Saint Peter, EC - Eau Claire, MS - Mount Simon
2. Percent of U-238 or Th-232 associated with surface grain coatings:

$$\frac{\text{Concentration of Isotope (Alpha Spectroscopy)}}{\text{Concentration of Isotope (Neutron Activation)}}$$

NA data for Carriage Hills Subdivision were corrected by dividing by 1.5. The uncorrected sample concentrations of U-238 and Th-232 are reported in this table.

3. U-234 activity not determined due to analytical error
4. Sample lost during plating process

statements regarding the relationship between uranium-238 and/or thorium-232 concentration and lithology.

In the case of uranium-238, the presence of shale (clay) interbeds appears to allow a greater percentage of uranium to exist in surface grain coatings. This effect seems to be more prevalent in the Mount Simon Formation (samples CH1515 and CH1520), than in the Eau Claire Formation (FR1150). Carbonates, such as CH0920, had very little uranium-238 associated with surface grain coatings.

Thorium-232 associated with surface grain coatings appears to vary considerably within both lithologic group and formation. Sample CH0950 and FR0920 are both sandstone intervals from the Saint Peter Formation, but have varying percentage of thorium-232 associated with the surface grain coatings. Shale interbeds within the Eau Claire Formation (samples CH1250 and FR1150) and the Mount Simon Formation (samples CH1515 and CH1520), appear to have as much as 100 percent of the thorium-232 in the sample associated with the surface grain coatings.

The occurrence of the parent radionuclides, uranium-232 and thorium-232, in the surface grain coatings, make both parent and daughters of these series more readily available to the ground water system. The results presented in Table IV imply that variable percentages of these radionuclides will be associated with surface grain coatings.

CONCLUSIONS

The following conclusions are a summary of the proceeding analyses and interpretations.

1. The radium-228 content of water produced from the Cambrian, Ordovician aquifer of Wisconsin is apparently determined by the thorium content and thickness of the Sinnipee group, Galena and Platteville formations.

2. The radium-226 content of water produced from the Cambrian, Ordovician aquifer is apparently determined by the uranium content and thickness of the St. Peter formation.

3. The Dresbach group, Eau Claire, and Mt. Simon formations, play little, if any, role in determining the radiometric water quality.

4. Due to mineralogy or water chemistry, radium-228 produced by the decay of thorium within the carbonate section of the aquifer is available to the porewater while thorium decay in other sections of the aquifer does not produce available radium-228.

5. Due to mineralogy or water chemistry, radium-226 produced by the decay of uranium within the St. Peter formation is available to the porewater while uranium decay within other sections of the aquifer does not produce available radium-226.

6. The source for both the radium-226 and radium-228 observed in produced water is contained within the immediate vicinity of the borehole.

7. Generally, increases in uranium and thorium concentrations are accompanied by increases in shale (clay) content and decreases in quartz content in the aquifer matrix.

8. The casing of selective borehole sections to reduce radium levels should not be attempted until the source of these elements is more fully defined.

9. Complete geophysical well logs, density, neutron, gamma, induction and spectral gamma were necessary for this study. The above conclusions would not have been possible without these logs. The conclusions are a demonstration of the value of the logs and the future logging of additional wells should be encouraged.

10. Structure maps of the St. Peter, Eau Claire, and Mt. Simon formations are of no value in selecting future well sites or in defining the radium levels of existing wells.

11. Percent shale maps for the Eau Claire and Mt. Simon formations are probably of no value in selecting future well sites.

12. Percent shale maps for the St. Peter sandstone, generated from older natural gamma logs as part of this study, are potentially of value in selecting well sites for low levels of radium-226.

13. Percent shale maps for the combined Galena, Platteville formations would be of some value in selecting well sites for low levels of radium-228.

14. Maps of the uranium and thorium figure of merit, as defined in this study, for the Galena, Platteville and St. Peter formations would be of great value in selecting future well sites. However, the generation of these maps would require a greatly expanded base of full log suites and is probably not possible based on existing natural gamma logs.

15. The source of short lived radium-228 is apparently the carbonate section of the aquifer which is immediately beneath the Maquoketa shale formation. The source of long lived radium-226 appears to be the St. Peter sandstone which is immediately below the carbonate section and separated from the Maquoketa shale by approximately 300 ft. The apparent relationship of half-life to distance from the shale may provide a vague suggestion that the ultimate source of both radium isotopes is the Maquoketa shale. This relationship is, at best, vague but is enhanced somewhat by the strong correlation between

the Maquoketa shale subcrop and wells with high radium levels (Figure 4.)

16. The five-window interpretation of the gamma spectra improves estimates of uranium-238 and thorium-232 concentrations determined using SGL.

17. Radium in ground water is a function of the availability of both parent and daughter radioisotopes to the ground water system. uranium-238 and thorium-232 occur in the structure of heavy minerals and/or as complexes associated with surface grain coatings. Of these two sources, complexed species associated with grain coatings in contact with the pore spaces in the aquifer are most readily available to the ground water system. Thus, the occurrence of radionuclides in ground water and the associated aquifer matrix must be sensitive to the following parameters:
    1. availability of parent radioisotope
    2. half-life of parent and daughter radioisotopes
    3. major-ion concentration in ground water
    4. oxidation-reduction potential (Eh) of ground water
    5. pH of ground water
    6. presence of colloidal materials and/or particle coatings (sorption sites for complexed U and Th)

LIMITATIONS AND RECOMMENDATIONS

1. Lack of control over sample collection, preservation and storage of the well cuttings, degrades the confidence in laboratory analyses using these samples. Future work should include a sample collection program which utilizes sample cores or well cuttings collected, described and prepared for analysis or storage by project personnel.

2. Inconsistency in the spectral-gamma well logging operation may limit the use of these data in determining the in situ concentrations of uranium and thorium. Logging procedures for water-well surveys need to be developed. The effect of hole size, tool position, degree of signal processing, and logging rate on uranium and thorium measurements should to be considered.

3. Ground-water chemistry needs to be determined for the intervals of potential contamination. A water sampling program which allows for sampling discrete intervals through the use of packers at known depth, should be employed. Water should be analyzed for inorganics as well as Ra-226, Ra-228, Th-234, U-238, and Rn-222.

4. Percent iron oxide in sample should be determined analytically, and isotopic uranium, thorium and radium associated with surface grain coatings should be determined for each sample interval, to gain an understanding of the relationship between uranium-238 and thorium-232, and surface grain coatings in the aquifer system.

5. Spectral gamma logs should be obtained for the wells used in this study to
   - determine the error associated with SGL estimates of uranium-238 and thorium-232
   - evaluate the potential of the SGL to estimate the concentration of the closest long-lived daughters of uranium-238 and thorium-232 (Ra-226 and Ra-228) decay series to Bi-214 and Th-208 respectively.

6. Additional spectral gamma logs which are now available but were not available at the time of this study should be analyzed to more fully establish the major role of the carbonate and St. Peter sandstone sections in the determination of radiometric water quality.

REFERENCES

Adams, J.A.S., and Gasparini, P., 1970. Methods in Geochemistry and Geophysics: Gamma Ray Spectrometry of Rocks. Elsevier Publishing Co., Amsterdam, 280 p.

Asquith, G., and Gibson, C., 1982. Basic Well Log Analysis for Geologists. AAPG Publication, Tulsa, 215 p.

Brownlow, Arthur H., 1979. Geochemistry. Prentice-Hall Inc., New Jersey, 477 p.

Code of Federal Regulations, 1987, National Primary drinking water standards: v. 40, pt. 141.

Dobrin, Milton B., 1976. Introduction to Geophysical Prospecting. McGraw-Hill, Inc., New York, 630 p.

Dott, R.H. Jr., and Mai, H., 1985. A subsurface study of the St. Peter sandstone in southern and eastern Wisconsin: Wisconsin Geologic and Natural History Survey Circular 47, 23 p.

Doveton, J.H., 1986. Log Analysis of Subsurface Geology: Concepts and Computer Models. John Wiley & Sons, New York, 273 p.

Ehlers, E.G., and Blatt, H., 1982. Petrology: Igneous, Sedimentary and Metamorphic. W.H. Freeman and Co., San Francisco, 707 p.

Eisenbud, M., 1973, Environmental Radioactivity: New York, Academic Press, 494 p.

Emrich, G.H., and Lucas, H.F. Jr., 1963. Geologic occurrence of natural radium-226 in groundwater in Illinois: Bulletin of the International Association of Scientific Hydrology, v. 8, no. 3, p. 5-19.

Fertl, W.H., "Gamma Ray Spectral Logging: A New Evaluation Frontier." World Oil (7 part series), Gulf Publishing Co., March 1983-November 1983.

Fleischer, R.L., 1980. Isotopic disequilibrium of uranium: alpha-recoil damage and preferential solution effects: Science, v. 207, p. 979-981.

Freeze, R.A., and Cherry, J.A., 1979, Groundwater. Prentice-Hall Inc., New Jersey, 604 p.

Gableman, J.W., 1977. "Migration of Uranium and Thorium." AAPG Publication, Tulsa, pp. 348-351.

Gearhart Industries Inc., Interpretation of the Spectral Gamma Ray.

Gilkeson, R.H., Perry, E.C. Jr., Cowart, J.B., and Holtzman, R.B., 1984. "Isotopic studies of the natural sources of radium in Illinois:" University of Illinois Water Resources Center Research Report Number 187, 46 p.

Hahn, N., Personal Communication, 1988. State of Wisconsin Department of Natural Resources.

Hahn, N., 1984. "Radium in Ground Water and Removal Methods for Community Water Systems." DNR water supply paper.

Hassan, M., Hosin, A., and Combaz, C., 1976. "Fundamentals of the Differential Spectral Gamma Ray Log." SPWLA 17th Annual Logging Symposium, June 9-12, 1976.

Langmuir, D., 1978. "Uranium Solution-Mineral Equilibra at Low Temperatures with Applications to Sedimentary Ore Deposits." Geochimica Et Cosmochimica Acta, v. 42, n. 6, pp. 547-569.

Lock, G.A., and Hoyer, W.A., 1971. "Natural Gamma Ray Spectral Logging." The Log Analyst, Sept.-Oct.

Markios, M., 1981. "Distribution and Possible Causes of Radionucleides in Ground Waters of Missouri." Conference on Trace Substances in Environmental Health, pp. 69-77.

Miller, I., and Freund, J.E. , 1985. Probability and Statistics for Engineers. Prentice-Hall, New Jersey, 530 p.

Ostrom, M. 1970. Sedimentation cycles in the Lower Paleozoic rocks of western Wisconsin in Fieldtrip gudiebook for Cambrian-Ordovician geology of western Wisconsin: Wisconsin Geologic and Natural History Survey, Madison, Information Circular No. 11, p. 10-34.

Rama, and Moore, W.S., 1984. Mechanisms of transport of U-Th series radioisotopes from solids into groundwater: Geochimica et Cosmochimica Acta, v. 48, p. 395-399.

Serra, O., Bal;dwin, J. and Quirein, J. , 1980, Theory, Interpretation, and Practical Application of Natural Gamma Rayu Spectroscopy. SPLWA 21st Annual Symposium, July 8-11.

Telford, W.M., Geldhart, L.P., Sheriff, R.E., and Keys, D.A. Applied Geophysics. Cambridge University Press, Cambridge, 860 p.

APPENDIX 1

WISCONSIN WATER WELLS WITH RADIUM VIOLATIONS

SYSTEM NAME - WITH RADIUM VIOLATION	COUNTY	SYSTEM COMPOSITE COMBINED RADIUM (pCi/l)
1. Holland Sanitary District No. 1	Brown	34.3
2. Bellevue Sanitary District No. 1	Brown	21.1
3. City of Waukesha	Waukesha	20.6
4. Dunn Sanitary District No.1-Downsville	Dunn	20.6
5. Taycheedah Correctional Institute-Fond du Lac	Fond du Lac	20.1
6. Sunset Well Co-op-Appleton	Outagamie	18.2
7. City of Princeton	Green Lake	14.6
8. Fairview Village	Portage	13.1
9. Pleasant Prairie San Dist. No. 1-Timber Ridge System	Kenosha	13.0
10. Monaco Heights Subdivision-Hales Corners	Milwaukee	11.8
11. City of New Berlin	Waukesha	10.6
12. Crestview Sanitary District-Racine	Racine	10.6
13. Village of Germantown	Washington	9.3
14. Southern Wisconsin Center-Union Grove	Racine	9.1
15. City of Peshtigo	Marinette	9.0
16. Village of Eagle	Waukesha	8.7
17. Village of Brownsville	Dodge	8.7
18. Pleasant Prairie San. Dist. No. 1-Industrial Park System	Kenosha	8.6
19. City of Fond du Lac	Fond du Lac	8.6
20. Town of Scott Sanitary District No. 1	Brown	8.6
21. City of Hustisford	Dodge	8.5
22. City of Mayville	Dodge	8.5
23. Town of Pewaukee San. Dist. No. 3	Waukesha	8.2
24. City of Franklin Water Utility	Milwaukee	8.1
25. Mary Hill Park San. Dist.-Fond du Lac	Fond du Lac	8.0
26. St. Coletta School No. 1-Jefferson	Jefferson	7.7
27. City of Berlin	Green Lake	7.6
28. Hyland Co-op-Pewaukee	Waukesha	7.6
29. Rustic Acres M.H.P.-Suamico	Oconto	7.6
30. Village of Waterford	Racine	7.4
31. Village of North Fond du Lac	Fond du Lac	7.2
32. Caddy Vista San. Dist.-Racine	Racine	7.1
33. Village of Lomira	Dodge	7.0
34. Edison Estates MHP-Oshkosh	Winnebago	6.8
35. City of Brookfield	Waukesha	6.7
36. City of Kaukauna	Outagamie	6.6
37. Security Acres Add. Subd.-Franklin	Milwaukee	6.2
38. City of Jefferson	Jefferson	6.1
39. Kilty's Kountry Kourt-Spencer	Marathon	6.0
40. Carol Beach Estates Subd.	Kenosha	5.9
41. City of Menomonie	Dunn	5.9
42. Bristol Utility District No. 1	Kenosha	5.8
43. Village of Union Grove	Racine	5.7
44. Village of Mukwonago	Waukesha	5.7

050878- Mineralogical and
Geophysical Monitoring
of Naturally Occurring
Radioactive Elements in
Selected Wisconsin
Aquifers